IEEE Access
Multidisciplinary ⋮ Rapid Review ⋮ Open Access Journal

Received 15 March 2024, accepted 3 April 2024, date of publication 8 April 2024, date of current version 18 April 2024.

Digital Object Identifier 10.1109/ACCESS.2024.3386430

RESEARCH ARTICLE

Application-Oriented Review of the LLC-Based Resonant Converters

JASEM SHAHSEVANI, (Student Member, IEEE), AND REZA BEIRANVAND, (Senior Member, IEEE)
Faculty of Electrical and Computer Engineering, Tarbiat Modares University, Tehran 14115-194, Iran
Corresponding author: Reza Beiranvand (beiranvand@modares.ac.ir)

ABSTRACT The LLC resonant converter is a widely utilized power electronics converter, due to its numerous industrial and domestic applications. This converter offers some advantages such as soft-switching operation of all switches, high efficiency, high power density, low voltage stress, minimal electromagnetic interference (EMI) noise, input/output isolation, wide input/output voltage range, and reliable and good performance under the wide load variation ranges, as well as good light-load operation. However, this converter has certain limitations, which can be addressed to enhance its operation and efficiency. This paper provides an in-depth review and comparison of various LLC-based resonant converter configurations, focusing on their operational principles, mathematical analysis, control methods, and some practical applications including electric vehicle chargers, TV power supplies, LED drivers, photovoltaic cells, HVDC production, fuel cells, and wireless power transfer applications. By examining the strengths and weaknesses of the different LLC resonant converter designs, this study aims to contribute to the ongoing research efforts in improving the performance and efficiency of this important power electronics converter.

INDEX TERMS DC–DC power conversion, LLC resonant converter, resonant power conversion.

I. INTRODUCTION

In recent years, there has been an increasing demand for high-efficiency and compact power supplies due to rising electric energy costs and the need for smaller circuit volumes [1], [2], [3]. Power supplies have widespread applications in computer systems, telecommunications, home appliances, LED lamps, and more, driven by advances in information technology. Various approaches have been proposed to reduce power losses in power supplies, including resonant converters, soft-switching techniques, bridgeless converters, and single-stage topology converters [4], [5], [6], [7].

Pulse-Width-Modulation (PWM) converters are widely used in power electronics converters. However, they are associated with high levels of electromagnetic interference (EMI) noise, due to their hard-switching conditions. Power losses in the PWM converters are directly proportional to the switching frequency. To address this issue, numerous methods have been proposed to reduce switching losses in the PWM converters. However, these methods may increase costs and introduce complexity to the converter design [8], [9], [10], [11].

Resonant converters have gained significant attention in recent years, due to their low EMI noise and reduced switching losses, which are achieved through the soft-switching techniques. Soft-switching operation allows for higher switching frequencies, resulting in decreased weight and volume of the converter. There are various configurations of resonant converters, with the LLC resonant converter being particularly well known. The LLC resonant converter offers advantages such as wide input/output voltage and load ranges, high efficiency, input to output isolation, and numerous applications [12], [13], [14], [15].

The LLC resonant converter features a simple structure and operational states. To further enhance its efficiency, particularly in light-load conditions, expand its input/output voltage range, and reduce voltage stress across switches, numerous configurations have been proposed based on the LLC resonant network. These improvements involve modifications in the switching network and algorithm, resonant

The associate editor coordinating the review of this manuscript and approving it for publication was Zhilei Yao.

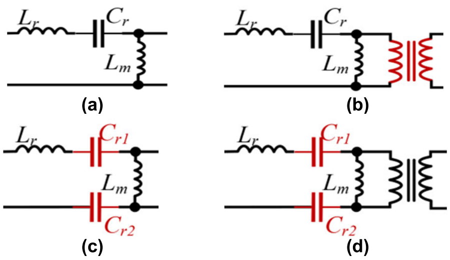

FIGURE 1. Four common LLC resonant networks, (a) basic, (b) inductive isolation, (c) capasitive isolation, and (d) capasitive-inductive isolation.

tank, transformer, and rectifier network. An effective way to improve the efficiency of the LLC resonant converter is through a proper control algorithm. Various control methods can be employed, including Pulse-Frequency-Modulation (PFM), PWM, Phase-Shift Modulation (PSM), Pulse-Width and Amplitude Modulation (PWAM) approaches, variations in the resonant tank, as well as combinations of these methods.

The LLC resonant converters find application in a wide range of fields, including electric vehicle chargers, TV power supplies, LED drivers, photovoltaic cells, HVDC production, fuel cells, and wireless power transfer, among others.

In this paper, a comprehensive review of the LLC resonant converter topologies is presented, by focusing on their applications. The discussion includes various structures of the LLC-based resonant converters. Section II examines the applications of different LLC resonant converter configurations, including multilevel converters, bidirectional converters, and voltage step-up/down converters. In Section III, various control methods such as PSM, PWM, PFM, and their combinations are explored. Section IV provides an analysis of the LLC resonant converter, covering power losses, mathematical analysis, design approaches, and operational states. Section V offers a fundamental comparison of the LLC converter with basic PWM and resonant converters. Section VI delves into the challenges and future opportunities for the LLC resonant converter. Finally, the discussions are summarized, and conclusions are drawn in Section VII.

II. LLC RESONANT CONVERTER DIFFERENT APPLICATIONS AND CONFIGURATIONS

LLC resonant converters can be implemented in various configurations to reduce power losses and improve efficiency and power density. One approach is to use finer components, although this increases cost. Another method is to explore new converter configurations, which can address issues such as power losses, cost, EMI noise, and component stresses. In this section, we will discuss some LLC-based resonant converters in detail, all of which are based on the LLC resonant network shown in Fig.1. In certain isolated applications, the transformer's primary-referred leakage inductance (L_r) can be utilized as the resonant inductor. This approach helps to further compact the resonant tank. For Wireless Power

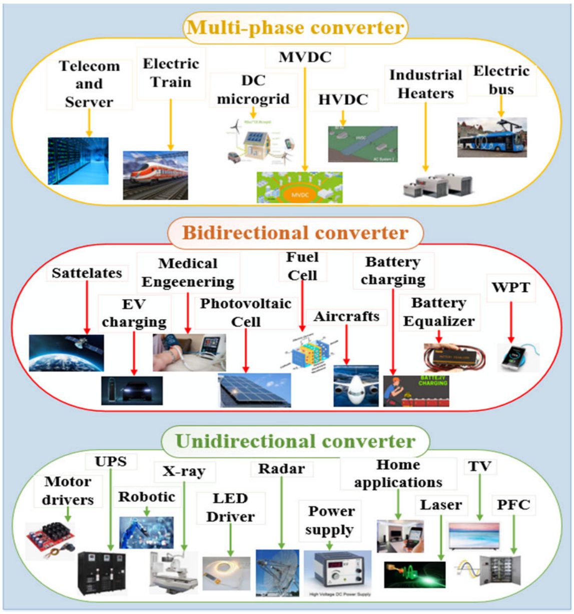

(a)

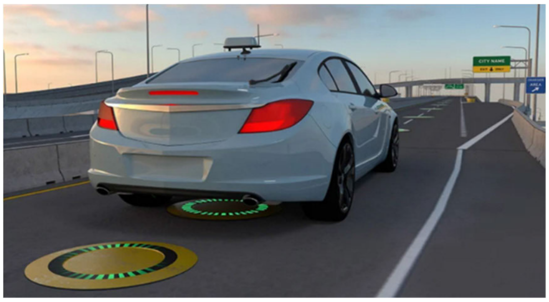

(b)

FIGURE 2. (a) LLC-based resonant converters applications and (b) Electric vehicle charging system based on the WPT approach.

TABLE 1. Some Well-Known WPT Approaches.

Technique	Power Range	Antenna	Application
Inductive Coupling	Medium	Winding	Battery charger
Inductive resonant Coupling	Medium	Integrated resonant winding	EV and laptop charger
Capacitive Coupling	Low	Electrode or metal sheets	WPT for massive devices

Transfer (WPT) applications, a core-less transformer may be employed, while ferrite core transformers can be used for high-density converters. By considering different configurations and design choices, these LLC resonant converters aim to optimize efficiency, power density, and other performance parameters. The specific characteristics and advantages of each configuration is discussed in the following sections.

A. LLC-BASED RESONANT CONVERTERS APPLICATIONS

LLC-based resonant converters have numerous applications in both home and industrial settings, thanks to their

TABLE 2. WPT-Based LLC Resonant Converters Comparison.

	Ref.	Input voltage (V)	Output voltage (V)	Output power (kW)	Efficiency (%)	Switching frequency (kHz)	L_r (μH)	C_r (nF)	L_m (μH)	Circuit and Control Complexity	Switch Voltage Stress	Number of components
ICWPT	[16]	100	24	0.033	95	~100	800	3	12	Low	V_{in}	Low
CCWPT	[17]	400	400	1.6	96	NM*	63	2×16	1.6	Low	V_{in}	High
	[18]	200	200	1	90	~250	16.2	25	81	Low	V_{in}	Low

*NM= Not Mentioned

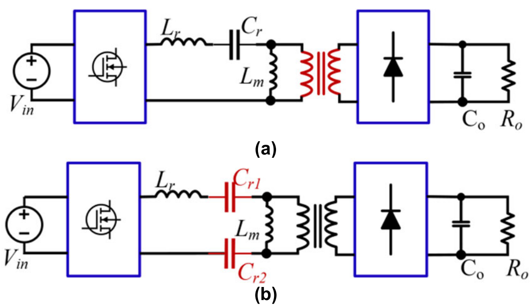

FIGURE 3. LLC resonant converter general configurations for wireless power transfer applications, (a) ICWPT-based and (b) CCWPT-based.

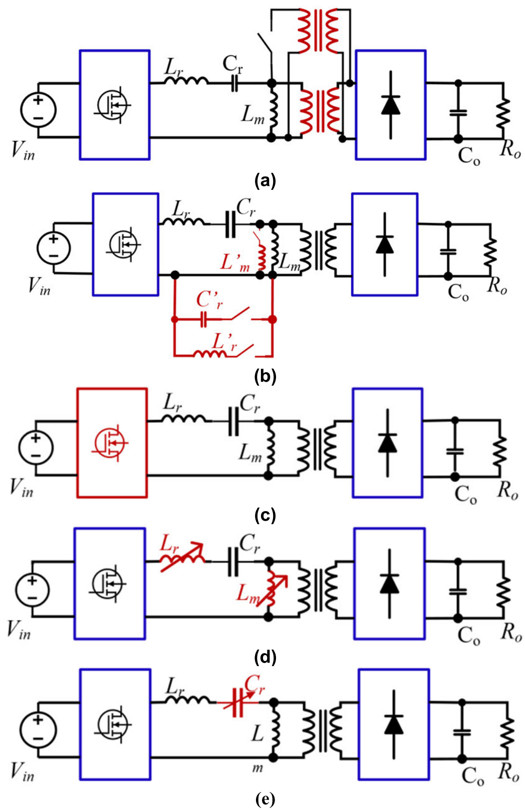

FIGURE 4. Some basic changeable LLC resonant structures. (a) Changeable transformer, (b) discrete changes in the resonant tank, (c) changeable switching network, (d) variable resonant inductors, and (e) variable resonant capacitor.

well-known benefits and advantages. Fig. 2(a) provides an overview of some of these applications. The versatility provided by the LLC resonant converter's ability to adapt to wide input and output voltage ranges benefits various applications in several ways:

1) POWER SYSTEMS

In renewable energy systems, electric vehicles, and grid-tied inverters, the LLC resonant converter's ability to handle wide voltage ranges enables efficient energy conversion from different input sources, such as solar panels, batteries, or the grid.

2) INDUSTRIAL EQUIPMENT

In industrial applications, where voltage levels may vary widely due to fluctuations in the power supply or different operating conditions, the LLC resonant converter ensures stable and reliable power delivery to sensitive equipment.

3) TELECOMMUNICATIONS

In telecommunications infrastructure, where voltage requirements can vary significantly between different components and operating environments, the LLC resonant converter offers a versatile solution for power management and distribution.

4) CONSUMER ELECTRONICS

In consumer electronics devices, such as laptops, televisions, and electric vehicles, the LLC resonant converter's ability to adapt to varying input voltage levels enhances energy efficiency and extends battery life.

Among LLC-based resonant converters applications, Wireless Power Transfer (WPT) is a prominent field in power electronics, encompassing devices such as electric vehicles (EVs), laptops, mobile devices, and battery chargers. Fig. 2(b) illustrates an example of an EV charging system based on WPT. The use of LLC resonant converters proves to be an efficient approach for WPT applications.

Due to their low electromagnetic interference (EMI), high switching frequency, and low power losses, resulting in enhanced efficiency and high power density. Table 1 outlines some of the approaches employed in WPT. The potential implications of the LLC resonant converter for future technology are significant. As WPT technology continues to evolve, the use of LLC resonant converters is expected to increase due to their efficiency, reliability, and cost-effectiveness. This could lead to advancements in areas such as electric vehicle charging infrastructure, consumer electronics, medical devices, and industrial automation. Additionally, the development of more efficient and compact LLC resonant converters could pave the way for new applications and innovations in the field of wireless power transfer. Although various converters have been proposed for inductive coupling WPT (ICWPT) applications [16], [19], [20], [21], the LLC resonant converter stands out for its simplicity and efficiency [16], This approach utilizes an air-core transformer instead of a conventional iron-core transformer, thereby reducing costs. The control of the LLC resonant converter in ICWPT applications can be achieved through pulse frequency modulation (PFM). However, it leads to increased circulating currents under light-load conditions. Similar topologies can be found in [19], [20], and [21]. The ICWPT-based LLC resonant converter shown in Fig. 3(a) is less efficient over long distances compared to the Capacitive Coupling Wireless Power Transfer (CCWPT) approach shown in Fig. 3(b), which offers improved safety, affordability, and reliability [22].

Furthermore, other converters based on the CCWPT technique have been proposed in [23], [24], [25], [26], [27], [28], [29], [30], and [31]. However, the LLC resonant converter outperforms these alternatives in terms of efficiency, reliability, and power density. In [17], a CCWPT-based LLC resonant converter with two transformers and two capacitors is presented, where the WPT capacitors sheets are connected to the car's windows to facilitate power transfer. This configuration, while suitable for EV charging in stationary conditions, exhibits high voltage stresses on primary stage switches and requires additional capacitors and a transformer, resulting in increased costs and lower efficiency under light-load conditions. To address these issues, a CCWPT-based converter proposed in [18], modifies the resonant capacitors for power transfer. However, circulating currents persist under light-load conditions, leading to reduced efficiency, and challenges related to high EMI noise and voltage stresses on components remain unresolved. A comparison of various WPT-based resonant converters is provided in Table 2. In practice, simpler structures with fewer components tend to be more efficient and reliable.

B. LLC RESONANT CONVERTER VARIABLE CONFIGURATIONS

DC voltage plays a pivotal role in a multitude of applications across various industries, spanning from low-power LED lights to high-power industrial motor drivers, battery chargers, and beyond. However, employing a one-size-fits-all approach in converter configurations for these diverse applications may prove inefficient or impractical. Recognizing this challenge, extensive research has been conducted into different converter structures that offer adaptability and modifiability to suit specific application requirements.

One such versatile converter structure is the LLC resonant converter, which has garnered significant attention and adoption due to its ability to operate over a wide range of input and output voltages while maintaining high efficiency. This adaptability makes it well suited for a range of applications, including but not limited to HVDC systems, fuel cells, WPT systems, and EV chargers.

In HVDC systems, where efficient power transmission over long distances is crucial, LLC resonant converters offer several advantages. Their ability to handle high input and output voltages while maintaining efficiency makes them ideal for voltage conversion and regulation in HVDC converters. Additionally, their inherent ability to operate in a resonant mode enables soft switching, reducing switching losses and enhancing overall efficiency in high-voltage applications.

Fuel cells, which are increasingly being used as clean energy sources, require efficient power conversion systems to convert the variable DC output voltage of the fuel cell stack into a stable output voltage suitable for various applications. LLC resonant converters excel in this regard, providing high efficiency and precise voltage regulation, thereby maximizing the utilization of fuel cell power and extending the operating range of fuel cell-based systems.

In wireless power transfer systems, where efficiency and reliability are paramount, LLC resonant converters offer significant advantages. By enabling efficient power transfer over large air gaps, LLC resonant converters facilitate the development of wireless charging systems for various applications, including consumer electronics, medical devices, and electric vehicles.

Furthermore, in the realm of electric vehicle charging, LLC resonant converters play a crucial role in providing efficient and fast charging solutions. Their ability to handle high input voltages, coupled with their high efficiency and compact size, makes them well-suited for on-board chargers and DC fast chargers, enabling rapid charging of electric vehicles while minimizing energy losses and maximizing charging efficiency.

In conclusion, the versatility, efficiency, and adaptability of LLC resonant converters make them indispensable in a wide range of applications, including HVDC systems, fuel cells, wireless power transfer systems, and electric vehicle chargers. Their ability to handle high voltages, coupled with their high efficiency and soft-switching capabilities, positions them as key enablers of efficient power conversion in various industries. In following section, some structures in this regard are debated and compared.

1) DIFERNET CHANGEABLE LLC RESOANT CONVERTER STRUCTURE

Discrete variation in converter topology involves making significant alterations, such as adding or removing components or integrating different networks within the converter.

TABLE 3. Comparison of Converters with Variation in Their Resonant Tank Structures.

		Ref.	Input voltage (V)	Output voltage (V)	Output power (W)	Efficiency (%)	Switching frequency (kHz)	Lr (µH)	Cr (nF)	Lm (µH)	Circuit and Control Complexity	Voltage stress on switches	Number of components	Application
Transformer		[44]	311	42	300	95	NM	33	23	510	Medium	NM	Low	Li-ion Battery charger
Transformer		[45]	100-400	NM	500	93	NM	NM	NM	NM	Medium	NM	Low	PV & fuel cell
Transformer		[48]	25-100	210	250	98	80-140	3.16	480	15.8 &5.49	Medium	NM	Low	NM
Resonant Tank Network	Discrete Variation	[49]	1000	48	2000	97.3	90	57.328	NM	NM	Low	V_{in}/2	Low	NM
Resonant Tank Network	Discrete Variation	[50]	300-400	12	2*300	96	200	12	36	87	Medium	V_{in}	Medium	NM
Resonant Tank Network	Discrete Variation	[51]	200	2000	20 k	92	20	5	4200	NM	Low	V_{in}	Low	MVDC grid
Resonant Tank Network	Continues Variation	[52]	50	NM	NM	NM	11.3	3.97	89.42	15.11	High	V_{in}	Low	Battery charger
Resonant Tank Network	Continues Variation	[53]	180-220	30-50	100	NM	90	31.5-66.5	47	85	High	V_{in}	Low	Light electric vehicles
Resonant Tank Network	Continues Variation	[54]	190-210	48	200	95	100	40.972	24	491.66	High	V_{in}	Low	NM
Switching Network		[55]	390	100-420	1100	97.6	50-150	62	32	382	Medium	NM	Medium	Battery Charger
Switching Network		[56]	220 ac	220 ac	1500	96.3	Output Freq. = 40 Hz	63	2 × 100	305	Medium	V_{in}	Medium	ac to ac converter
Switching Network		[57]	120	0-80	600	96	140	30	60	45	Medium	V_{in}	Low	EV Charger

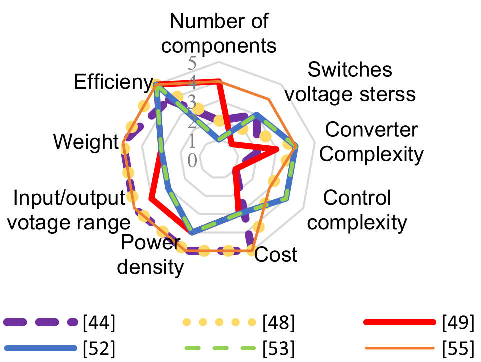

FIGURE 5. Comparison of some of the given converters in Table 3. 1: represents LOWEST and 5: HGHEST value.

Numerous approaches have been proposed to modify the structure of the LLC resonant converter, offering diverse benefits across various applications. In HVDC applications, discrete variation in converter topology presents an opportunity to increase voltage while maintaining efficiency. By optimizing the converter's structure, it becomes feasible to enhance voltage levels without compromising on overall system performance. For PV and fuel cell applications, where a wide range of input voltages is encountered, discrete variation enables converters to adapt effectively to varying input voltage conditions while preserving efficiency. This flexibility allows converters to operate optimally across a broad input voltage range, enhancing system versatility and performance. In battery and EV charging applications, discrete variation in converter topology offers additional advantages. By implementing changes in the converter's structure, it becomes possible to seamlessly switch between Constant Current (CC) and Constant Voltage (CV) charging approaches, facilitating efficient battery charging and accommodating diverse charging requirements. Moreover, in WPT applications, the converter can be divided into two parts connected through WPT approaches. This changeable structure

TABLE 4. Comparison of Some Step-Up and Step-Down Converters.

	Ref.	Input voltage (V)	Output voltage (V)	Output power (W)	Efficiency (%)	Switching frequency (kHz)	Lr (μH)	Cr (nF)	Lm (μH)	Converter and control complexity	Voltage stress on switches	Number of components	Application
Voltage Step-Down	[58]	48-85	3.3, 5, and 10	100	92	NM	2.2	47	9	High	NM	High	NM
	[59]	200-400	360	1440	95	100	21.7	94.4	120.6	High	$\frac{V_{in}}{2}$	High	Fuel cell
	[60]	120-240	24	600	96	100	50.7	50	370	Low	$> V_{in}$	Medium	Renewable energy
	[61, 62]	200-250	23-33.5	336	93	200	NM	NM	300	Low	V_{in}	High	Battery Equalizer
	[63]	400	50 and 200	420	96.5	70	30	166	435	High	V_{in}	Medium	TV power supply
Voltage Step-Up	[64]	390	500-840	1300	95	100	57	44	260	High	V_{in}	High	PEV battery charging
	[65]	25-50	760	300	96.1	75-110	4.1	620	13	High	V_{in}	High	Photovoltaic Systems
	[66]	165-200 and 65-115	360	500	~96	74-100	34.4	73.5	150	Low	$V_{Battery}$	Medium	PV & battery system
	[67]	240-440	2×2.5k	2×5k	98	37.5	211	NM	1500	High	V_{in}	High	MVDC
	[68]	24-48	400	1000	90.4	50, 300	NM	NM	5	High	V_{Bus}	Medium	Fuel cell

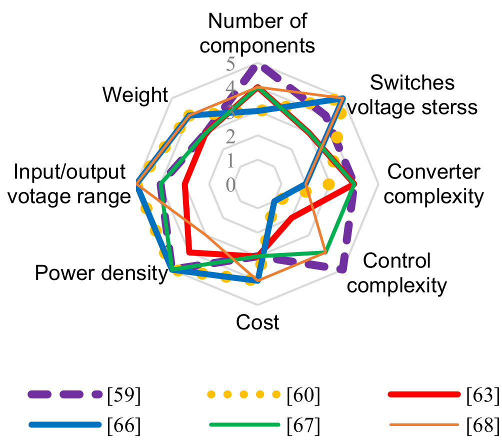

FIGURE 6. Comparison of some of the given converters in Table 4. 1: represents LOWEST and 5: HGHEST value.

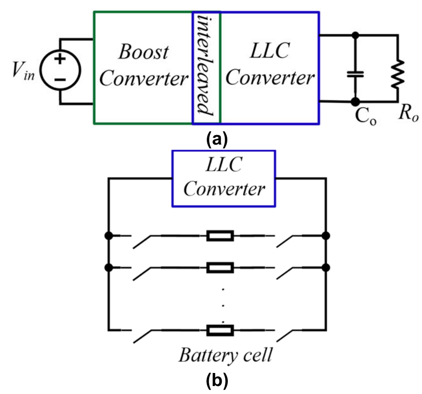

FIGURE 7. Two voltage step-down basic structures, (a) interleaved boost-LLC resonant converter and (b) battery equalizer circuit.

allows for effective power transfer, particularly considering variable distances and objects between the two parts of the converter. By adapting to changing environmental conditions and operating parameters, the converter can optimize power transfer efficiency and reliability in WPT systems. Overall, discrete variation in converter topology enhances the adaptability, efficiency, and functionality of LLC resonant converters across a range of applications, including HVDC, PV, fuel cell, battery charging, EV charging, and WPT. By leveraging this approach, converters can be tailored to meet specific performance requirements and operating conditions, driving innovation and advancements in power conversion technology.

a: VARIATION IN THE CONVERTER TRANSFORMER

The transformer is a significant component in LLC resonant converters as it provides input/output isolation, proper conversion ratio, and serves as both the series resonant and parallel inductors of the LLC resonant network.

Researchers have focused on improving the operation of the transformer to reduce power losses [32], [33], [34], [35], [36], [37], [38], [39], [40], [41], [42], [43]. For instance, a four-output transformer-controlled LLC resonant converter was proposed for Li-Ion battery charger applications in [44]. In this configuration, each output port is controlled by series-connected switches to enhance the converter's voltage gain and reduce switching frequency. Similar converters have been proposed in [45], [46], and [47], exhibiting comparable operations and topologies to the one presented in [44]. These converters, which operate within narrow switching frequency bands, can achieve better efficiencies compared to conventional LLC resonant converters. However, they suffer from high voltage stresses on components, high cost due to the specific transformer and extra output-controlled switches operating under hard switching conditions. Moreover, the full capacity of the multi-output transformer is not optimally utilized at all times due to its part-time usage in practical applications.

Another LLC resonant converter configuration was proposed in [48] to overcome the aforementioned drawbacks, by utilizing two transformers, which one of them is controlled through two series-connected switches. Although, this structure allows for control of the converter's resonant tank impedance near its resonance frequency, it is bulky and expensive for widespread practical use due to the two transformers and the additional two switches operating under hard-switching conditions. A detailed comparison of different converters can be found in Table 3. Fig. 4(a) illustrates the basic structure of the converter topologies where the transformer is changeable. In general, topologies with simpler transformer structures are more appealing, considering the cost and size implications as transformers are expensive and bulky components.

In summary, while the transformer is a crucial component offering galvanic isolation and voltage ratio, it is also a costly element in power converters. However, it is sensitive to harmonics and can lead to energy wastage and heating issues, potentially increasing the overall volume and cost of the converter. Despite various structures proposed to maximize the benefits of this component, there are several considerations to keep in mind. For instance, multi-input/output converters can increase the voltage ratio and power density, but they also exacerbate the aforementioned problems.

b: CONVERTERS WITH CHANGEABLE RESONANT TANK NETWORKS

The changeable transformer approach discussed earlier may lead to increased cost, power losses, and volume of the converter in practical applications.

To address these issues, an alternative approach utilizing changeable resonant tank components can be employed [49]. This approach is comparatively cheaper and helps to reduce voltage stresses on components while requiring fewer gate-drive circuits. However, it is important to note that using more switches than the conventional converter increases the cost and complexity of the circuit.

Another technique involves incorporating an additional resonant capacitor [50], along with the use of two additional switches, to control the converter's voltage gain characteristics. However, these additional switches do not operate under soft-switching conditions, which further increases the converter's cost and complexity.

In [51] a suggestion is made to add a capacitor in parallel with the magnetizing inductance of the transformer's secondary side. This configuration aims to reduce the voltage stress on the series resonant capacitor and improve the efficiency of the PWM-based LLC resonant converter under light-load conditions. However, this approach may increase the circulating currents in the converter and introduce input voltage harmonics to the transformer.

The basic configuration of a discrete variable resonant tank in an LLC resonant converter is depicted in Fig. 4(b), and a more detailed comparison of related converters can be found in Table 3 and Fig. 5.

In summary, a changeable resonant tank offers the advantage of adapting to various gain-frequency characteristics, which is beneficial for maintaining high efficiency. However, switching between modes can introduce harmonics, making it challenging to use these structures for applications with significant voltage variations.

c: CONVERTERS WITH CHANGEABLE SWITCHING NETWORKS

Modifying the switching network is another approach to controlling the output voltage of an LLC resonant converter. This method proves effective in achieving high efficiency across a wide range of input/output voltages and for various purposes.

In [55], a two-level LLC resonant converter is proposed for battery charging, utilizing a switching network consisting of five switches.

The converter operates in four different states, allowing for a wide output voltage range even with a narrow variation in switching frequency. Despite the advantages mentioned, discrete variation in the switching network introduces harmonics and imposes high voltage stresses on the switches. Additionally, the use of two resonant tanks, a transformer, and a rectifier network increases the cost.

Another converter in [56], introduces an ac/ac LLC resonant converter, wherein the secondary side switches do not operate under soft-switching conditions. As a result, the converter exhibits low efficiency in practical applications. A detailed comparison of changeable switching network converters can be found in Table 3. The basic structure of the changeable switching network topologies is illustrated in Fig. 4(c). However, it is important to note that these types of converters suffer from higher harmonics, increased cost, power losses, and the operation of some switches under hard-switching conditions, which adversely affect EMI performance.

d: CONVERTERS WITH VARIABLE RESONANT TANK COMPONENTS

In [52], [53], [54], [69], and [70], two LLC resonant converters with variable inductors are proposed, enabling variable quality factors and soft-switching operation. The output voltage is regulated by varying the inductor in applications with fixed switching frequency. The variable inductor operates in the knee zone of its B-H curve, providing a variable inductance. However, the full capacity of the inductor is not fully utilized, leading to sub-optimal cost-effectiveness, especially for high-power converters.

To increase the output power of variable inductor converters, multi-phase topologies can be employed [70], [71]. In [70], a battery charger is introduced for both Constant Current (CC) and Constant Voltage (CV) operation modes. It utilizes two resonant tanks, one of which includes a variable inductor for output voltage regulation, while the other operates near the resonant frequency to transfer the main portion of the output power. These two resonant tanks are connected in series at the output side. Similarly, in [72], two separate switching networks are used, but the single-phase converter issues persist, along with increased cost due to the two-phase structure.

Another approach involves using a variable capacitor instead of a variable inductor, leveraging the higher power densities, lower masses, volumes, and prices of capacitors. A fixed switching frequency LLC resonant converter based on a variable ceramic capacitor, whose capacitance depends on the applied voltage, is presented in [73] Although the converter regulates the output voltage by changing the quality factor, the variable capacitor employed has limited power density and variation range.

The basic configurations of LLC resonant converters with variable resonant tank components are depicted in Fig. 4(d) and (e). Further details and comparisons of related converters can be found in Table 3 and Fig. 5. It is worth noting that most of these converters are designed for fixed switching frequencies, resulting in lower efficiency under light-load conditions due to the presence of circulating currents.

In summary, the switch network provides the waveform that enters the resonant tank. As an active and impactful network, it is beneficial for controlling EMI noise and harmonics, as well as introducing new gain-frequency characteristics. While not as effective as the transformer and resonant tank in widening the gain range, it has the advantage of not introducing harmonics as large as the other two approaches. This is due to the waveforms entering the resonant tank from the switching network, which filters out harmonics as it is produced. Furthermore, changeable switching networks are advantageous in applications with limited variable input voltages, such as PV systems. Changeable transformers are useful for HVDC production, and changeable resonant tanks are beneficial for WPT and EV charging applications.

C. STEP-UP/DOWN LLC RESONANT CONVERTERS

In applications like battery chargers, converters play a critical role in stepping up or stepping down voltage as needed. This capability is essential due to factors such as the constant current (CC) and constant voltage (CV) characteristics of batteries, which require specific voltage levels for efficient charging. Additionally, the wide input voltage variations that converters must accommodate further highlight the importance of this functionality [74]. In this section, we delve into the intricacies of both voltage step-up and step-down LLC resonant converters. These converters are designed to efficiently regulate voltage levels, ensuring that batteries receive the appropriate charging voltage regardless of the input voltage fluctuations. This discussion will provide a comprehensive understanding of how these converters operate and their significance in battery charging applications.

1) VOLTAGE STEP-DOWN LLC RESONANT CONVERTER

Step-down LLC resonant converters are widely used in various industries and home applications where different voltage levels are required, such as 3V, 5V, 9V, 12V, 18V, 24V, 36V, 48V, and so on. The LLC resonant converter is a favorable choice for these applications due to its well-known advantages.

In one proposed design [58], a voltage step-down multi-output LLC resonant converter is utilized. Instead of a single output, this converter features multiple outputs, allowing for easy provision of different voltage levels. However, this converter lacks input-output isolation and can be expensive due to the large number of switches involved.

Another approach [60], a combination of resonant LLC and boost converters with PWM control is proposed. The voltage is first increased by the boost stage and then decreased by the LLC resonant converter. However, this approach increases losses and costs, and it is not highly efficient in practice. Similarly, an interleaved boost-LLC resonant converter is introduced in [75], Although the converter's input inductors are coupled with its output inductors in the rectifier stage, improving efficiency to some extent, the aforementioned drawbacks still exist. The basic structure of the interleaved boost-LLC resonant converter is shown in Fig. 7(a).

In [63], a two-output transformer is employed to supply two different loads. The first output is connected to a conventional LLC-based resonant converter, while the second output is connected to a forward converter. However, this topology suffers from low efficiency due to the hard switching operation of the forward converter.

To improve efficiency under light-load conditions, an LLC resonant converter design [76], proposes breaking the resonant inductor into two series-connected inductors by adding a resistor in parallel with one of them. While this approach enhances light-load efficiency, it increases cost and total power losses under full-load conditions due to the added resistor.

A soft-switching LLC resonant converter with reduced parasitic oscillation over a wide load range is introduced in [77], utilizing an additional transformer and inductor. However, this increases the weight, volume, and cost of the converter.

Another design [78], incorporates two resonant networks and transformers, along with a three-leg rectifier network. By using three switches in each leg, this topology reduces voltage stress on the switches to handle high-power values.

TABLE 5. Comparison of the Multi-Level Converters.

	Reference	Input voltage (V)	Output voltage (V)	Output power (W)	Efficiency (%)	Switching frequency (kHz)	Lr (μH)	Cr (nF)	Lm (μH)	Converter and its control complexity	Voltage stress on switches	Number of components	Application
Three-Level	[86]	120-240	24	480	94.1	100	25.3	100	170	Medium	V_{in}	Low	NM
	[87]	400	60-100	1000	NM	NM	25	100	NM	High	$\frac{V_{in}}{2}$ & V_{in} (Two legs)	High	Renewable energy systems
	[59]	200-400	360	1500	~95	100	21.7	94.4	120.6	High	$\frac{V_{in}}{2}$ & V_{in} (Two legs)	High	Fuel cell
	[88]	400-600	48	960	95	NM	16	2×260	80	Low	$V_{in}/2$	Low	NM
	[89]	400-600	48	480	~95	130-200	2×20	2×33	2×84	Low	$V_{in}/2$	High	NM
Five-Level	[90]	NM	90-220	100-135	NM	NM	NM	NM	NM	High	$V_{in}/2$	High	NM
	[91]	2×390	48	142.8	NM	~140	15	130	217	Medium	V_{in}	Medium	NM
Multilevel Multiphase	[92]	400	2500	7000	NM	35-45	200	70	300	High	V_{in}	High	HVDC
	[93]	380-420	250-420	3300	98	50	13.2	730	345	Low	V_{in}	Medium	EV battery charger
	[94]	500	6000	6000	99	21	308	22	1500	Low	V_{in}	High	MVDC renewable energy
	[95]	80-200	400	1000	97.5	80-160	4.6	282	17	Medium	NM	Medium	fuel cell
	[96]	380-420	320-420	3300	96.3	75-160	NM	134	74	Low	NM	Low	EV charger

However, its efficiency decreases under light-load conditions, and it results in higher volume and cost primarily due to the use of two transformers.

In the context of Li-ion battery equalization, a multi-output LLC-based resonant converter [61], [62], has been proposed. This converter generally outperforms conventional equalizer converters. However, it relocates the resonant capacitor to the transformer secondary side, leading to incomplete filtering of current switching harmonics and increased transformer losses.

These various step-down and up LLC resonant converter designs are compared in detail in Table 4, while the basic battery equalizer topology is illustrated in Fig. 7(b). It is important to consider the specific requirements and trade-offs associated with each design when selecting a converter for a particular application.

In summary, voltage step-down functionality is widely utilized in various industrial and commercial applications, with battery charging being a significant example. The ability to step down voltage efficiently is crucial in ensuring that batteries receive the correct charging voltage.

There are several factors that contribute to the versatility and effectiveness of voltage step-down converters. For instance, converters with multiple outputs can provide the flexibility to power different devices or components with varying voltage requirements. Additionally, incorporating Power Factor Correction (PFC) techniques in the converter design can improve efficiency and ensure that the converter operates at optimal performance levels.

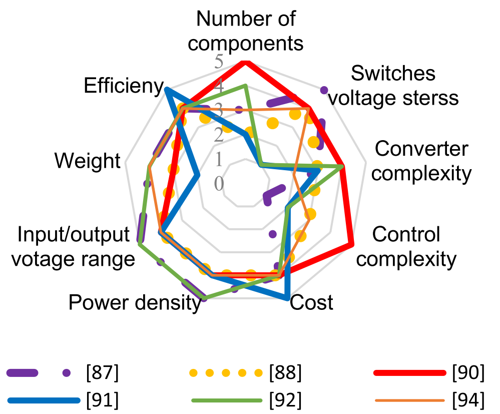

FIGURE 8. Comparison of some of the given converters in Table 5. 1: represents LOWEST and 5: HGHEST value.

Overall, voltage step-down converters play a vital role in numerous applications, including battery charging, where they contribute to the efficient and reliable operation of electronic systems.

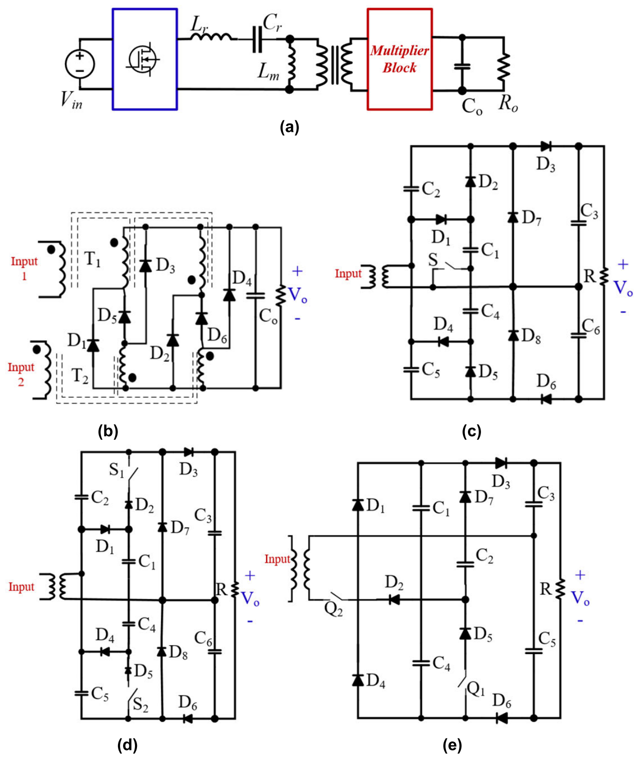

FIGURE 9. Multiplier rectifiers, (a) basic structure and (b)-(e) some multiplier rectifiers.

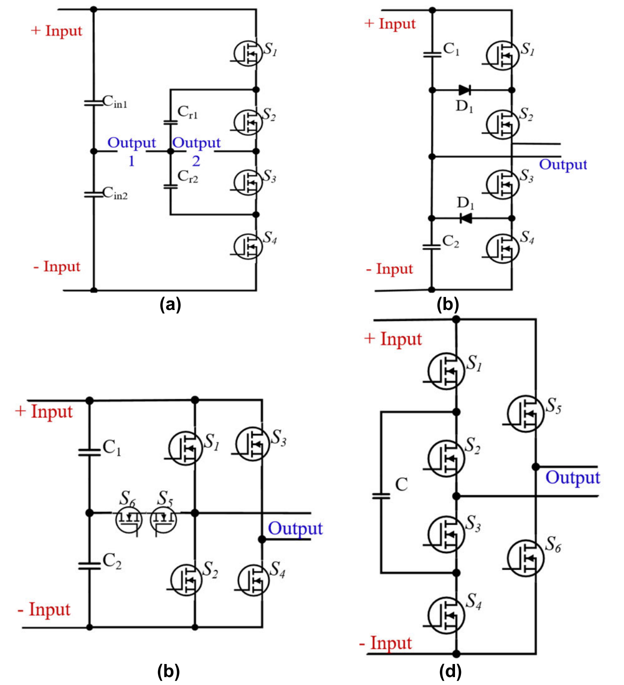

FIGURE 10. Some well-known three-level switching network structures.

2) VOLTAGE STEP-UP LLC RESONANT CONVERTER CONFIGURATION

Step-up LLC resonant converters play a crucial role in various applications, especially in scenarios where renewable energy sources, such as wind-powered turbines, generate distributed power with varying output voltage levels. These converters are essential for efficiently stepping up the voltage to match the requirements of the grid or other high-voltage systems.

One significant application of step-up LLC resonant converters is in HVDC (High Voltage Direct Current) systems. In HVDC applications, such as those involving photovoltaic cells and fuel cells, these converters are instrumental in converting the DC voltage from these sources to higher voltages required for efficient long-distance power transmission. The use of LLC resonant converters in HVDC systems is particularly advantageous due to their ability to operate at high efficiency and high power density levels, which are crucial for minimizing losses and maximizing the transmission capacity of the system.

The LLC resonant converter's suitability for step-up applications is attributed to its several advantages. Firstly, it offers low EMI (Electromagnetic Interference) noise, which is essential for maintaining the integrity of the power system and minimizing interference with other electronic devices. Additionally, LLC resonant converters are known for their low switching losses, which contribute to their high efficiency. Their ability to operate at high frequencies further enhances their efficiency and allows for the design of more compact and lightweight converters with high power density.

Overall, step-up LLC resonant converters play a critical role in enabling the efficient and reliable conversion of power from renewable energy sources and other distributed power generation systems to higher voltages suitable for transmission and distribution in modern power systems.

In [79], two voltage step-up topologies based on LLC resonant converters are presented, offering limited voltage gains. However, one of these topologies does not utilize transformer magnetizing and leakage inductances, making it suboptimal with regards to volume and cost.

A complex structure involving a two-resonant tank converter with a voltage multiplier cell at the secondary side is proposed in [80], This design achieves an 8-fold amplification of the input voltage, even with narrow switching frequency variations. However, this complex structure requires a significant number of components and a complex control approach.

Other approaches, such as multiplexer rectifier networks, have been used in [81] and [82], to multiply the output voltage by factors of 2, 3, and 5. Additional voltage multiplier cells can be found in [64], [65], [67], [83], [84], and [85], all are suffering from the similar issues as the given one in [80]. Despite their advantages, these converters exhibit low efficiency under light-load conditions, high voltage stress, and require numerous switches. Furthermore, the topologies presented in [64], [65], [67], [81], [82], [83], [84], and [85]. Furthermore [64], [65], [67], [81], [82], [84], and [85] feature complex structures, leading to increased costs in practical implementation. Fig. 9 illustrates a basic structure and some multiplier rectifier configurations.

In [66], an interleaved dual-input boost-LLC resonant converter is proposed, utilizing a full-bridge switching network for the battery and a boost converter for the photovoltaic cell input ports. While this design performs well in renewable energy applications, however it's charging path experiences high conduction losses, which negatively impacts battery charging operation. Interleaved boost-LLC resonant converters are found in [97], [98], and [99], all employing voltage-doubler rectifier networks.

In [97], the boost section provides only a voltage gain of two, and its volume and cost are high due to the numerous components in this structure. In [68], a series-connected boost-LLC resonant converter is proposed for fuel cell applications. While it shares the drawbacks of interleaved converters mentioned earlier, its efficiency is significantly reduced due to the series-connected stages. Additionally, current switching harmonics pass through the transformer in the topology presented in [100], increasing power losses. The presence of an extra primary diode in this structure also has a negative impact on efficiency.

To achieve high voltage gains, an interleaved Boost-LLC based resonant converter is proposed in [101] and [102]. This design incorporates series-connected capacitors at the output side to reduce voltage stresses when higher voltage values are desired. Although it achieves soft-switching operation over wide input voltage and load variation ranges, it lacks input/output isolation, which may be necessary high-voltage applications.

Table 4 provides a comparison of some related converters. Step-up converters are valuable in many applications where achieving a high step-up voltage gain is crucial. While combined converters with voltage multiplier cells typically offer voltage gains of 1-10, other structures can provide higher voltage gain values.

Voltage step-up converters, including LLC resonant converters, play a vital role in various applications where boosting the voltage level is necessary. One such application is voltage regulation in photovoltaic (PV) systems, especially during adverse weather conditions. When sunlight is low, the output voltage of PV panels decreases, affecting the overall efficiency of the system. By using a voltage step-up converter, the PV system can maintain a stable output voltage, ensuring optimal performance even in challenging conditions.

Another important application of voltage step-up converters is in providing High Voltage Direct Current (HVDC) in low input voltage applications. In scenarios where the input voltage is insufficient for HVDC transmission, a step-up converter can increase the voltage level to meet the requirements of the HVDC system, enabling efficient long-distance power transmission.

Battery charging is another area where voltage step-up converters are widely used. Modern battery charging schemes, such as Constant Current (CC) followed by Constant Voltage (CV), require a converter that can efficiently step up the voltage to provide the necessary charging profile. Step-up converters enable the charging of batteries with varying voltage requirements, ensuring safe and efficient charging.

Wireless Power Transfer (WPT) is another application where voltage step-up converters are essential, especially in scenarios where power needs to be transmitted over long distances. By stepping up the voltage, WPT systems can efficiently transfer power over greater distances, making them ideal for applications such as electric vehicle charging and wireless charging of electronic devices.

Among the various approaches used in voltage step-up converters, interleaved converters stand out for their flexibility in handling variable voltages and power levels. By interleaving multiple converters, these systems can achieve higher efficiency and better performance compared to traditional converters.

Rectifier networks with voltage multiplier circuits are another innovative approach to increasing voltage levels with lower complexity and cost. By using voltage multiplier circuits, these converters can efficiently boost the output voltage while keeping the overall system complexity and cost in check, making them attractive for various applications.

In conclusion, voltage step-up converters play a crucial role in a wide range of applications, from renewable energy systems to electric vehicle charging. Their ability to efficiently boost voltage levels while maintaining high reliability and performance makes them indispensable in modern power systems.

D. MULTI-LEVEL LLC-BASED RESONANT CONVERTERS

Multilevel converters have gained significant attention due to their ability to mitigate issues such as high voltage stress, noise, and current switching harmonics. These converters offer several advantages over traditional two-level converters, including reduced Total Harmonic Distortion (THD), lower EMI noise, and improved efficiency.

One key feature of multilevel converters is their ability to synthesize a sinusoidal output voltage waveform with reduced harmonic content. This is achieved by using multiple levels of voltage instead of just two levels (as in traditional converters), which allows for finer control over the output voltage waveform. By using more levels, the converter can approximate a sine wave more closely, resulting in lower harmonic content and reduced EMI noise.

In addition to lower EMI noise, multilevel converters also offer other advantages such as lower dv/dt stress on the switching devices, reduced common-mode voltage, and improved output waveform quality. These factors contribute to a more efficient and reliable power conversion process, making multilevel converters ideal for a wide range of applications including renewable energy systems, motor drives, and power distribution systems.

Overall, the use of multilevel converters in LLC-based resonant converters can significantly reduce EMI noise and improve overall system performance. Their ability to synthesize high-quality output waveforms makes them a preferred choice for applications where low harmonic distortion and reduced noise are critical.

1) THREE LEVEL LLC CONVERTERS

In [86], a three-level LLC resonant converter has been proposed, utilizing two series connected capacitors across the input voltage source. Two back-to-back connected switches are connected between these capacitors and the resonant tank.

Another topology for fuel cell voltage regulation has been proposed in [59], capable of operating in both two and three-level configurations by changing the pulse width. However, this converter suffers from disadvantages such as the complexity of control algorithms, different voltage stresses on the switches, and the presence of too many switches. In another manner [87], replaces the input source with a PV panel and includes a battery pack as a backup source. The converters in [103], [104], [105], and [106], employ two-leg switching networks for high voltage gain applications but suffer from high conduction losses and expensive components due to the use of multiple switches and gate-drives.

In [107] a three-level LLC resonant converter is proposed with the addition of two diodes, resulting in low EMI noise and reduced voltage stress on the components. However, the lack of soft-switching operation increases power losses and limits the switching frequency. Reference [88] reduces voltage stress on the resonant capacitor by using two resonant capacitors, but the implementation of PFM control complicates the converter design.

Although, using two transformers in [89] increases the cost and volume of the converter, but it enables operation under a wide input voltage range. Reference [90] employs two isolated three-level switching networks, operating as a three-level configuration for low input voltage and as a five-level converter for high-voltage applications. However, this topology becomes suboptimal, as one of the switching networks remains unused under light-load conditions. Connecting two full-bridge converters in series can generate a five-level output voltage, as proposed in [91], but this approach leads to high voltage stresses on the switches and increased converter cost.

In summary, three-level LLC-based resonant converters offer several advantages over their two-level counterparts, primarily in terms of reduced current harmonics. However, these converters face challenges such as increased voltage stress, greater complexity, and higher conduction losses. It is crucial to carefully consider these trade-offs when selecting a specific converter topology.

The additional voltage levels in three-level converters allow for the synthesis of a more sinusoidal current waveform, leading to improved performance in terms of harmonic content in the output current compared to traditional two-level converters. This feature makes them well suited for applications where low harmonic distortion is critical, such as in power supplies for sensitive equipment or in renewable energy systems.

Despite their advantages, the use of additional voltage levels in three-level converters can result in higher voltage stresses on components like switches and transformers. This increased stress can lead to higher losses and reduced efficiency, especially at higher power levels. Additionally, the control and modulation schemes for three-level converters are more complex compared to two-level converters, which can pose challenges during design and implementation.

Nevertheless, three-level LLC-based resonant converters remain popular in various applications due to their ability to reduce current harmonics and improve overall system performance. They are particularly favored in HVDC applications to reduce voltage stress on switches, lower EMI noise in other applications, and provide a wider voltage range in certain controlling schemes. Careful consideration of the trade-offs and selecting the appropriate converter design can help achieve a balance between performance, efficiency, and complexity in power conversion systems.

2) MULTIPHASE MULTILEVEL LLC-BASED RESOANT CONVERTERS

Multilevel configurations in LLC-based resonant converters are known for their complexity in control algorithms and increased conduction losses due to the higher number of components and gate-drive circuits required. Despite these challenges, they offer several advantages that make them well suited for converting higher power values.

One key advantage of multilevel converters is their ability to reduce voltage stresses on power switches. This is achieved by distributing the voltage across multiple levels, which helps in improving the overall efficiency and reliability of the converter. Additionally, multilevel converters help mitigate EMI noise and switching losses, leading to a more stable and efficient operation.

In DC-DC applications, increasing the number of phases and voltage levels in multilevel converters can enhance output power and reduce stresses. This is particularly beneficial in applications where high power conversion is required, such as in renewable energy systems or electric vehicles.

Moreover, multilevel converters with a high number of voltage levels are also used to minimize total harmonic distortion in AC applications. By synthesizing a more sinusoidal output waveform, these converters can improve the quality of the output voltage and reduce the impact of harmonics on the connected loads.

Overall, while multilevel configurations in LLC-based resonant converters come with their challenges, they offer significant advantages in terms of efficiency, reliability, and harmonic mitigation, making them a preferred choice for high-power and high-quality power conversion applications.

In [108], a multiphase multilevel converter is proposed with low current and voltage stresses on each switch. However, the increased number of power switches and gate-drives complicates the control circuit. Reference [109] utilizes a multi-LLC resonant converter connected in series at the output stage for HVDC and PV panels applications, aiming to supply a common load from different input voltage sources. While it offers reliability, any error in the output stage capacitors results in a complete shutdown, making it an expensive approach.

In [108], two interleaved LLC resonant converters are proposed for voltage step-up purposes, with one using a half-bridge switching network and the other using a full-bridge switching network without a resonant tank. The shared leg in their switching networks leads to high conduction losses, and the absence of a resonant tank in one phase increases core and winding power losses in the transformer, affecting efficiency.

In [108], two interleaved LLC resonant converters are proposed for voltage step-up purposes, with one using a half-bridge switching network and the other using a full-bridge switching network without a resonant tank. The shared leg in their switching networks leads to high conduction losses, and the absence of a resonant tank in one phase increases core and winding power losses in the transformer, affecting efficiency.

Several two and three-phase converters with common load and input voltage source have been proposed in [109], [110], [111], [112], [113], [114], [115], [116], [117], [118], [119], [120], and [121], to increase output power. Although the power is equally divided among the phases, the voltage stresses on switches remain high. In some cases, moving the resonant network to the secondary side [112], causes switching current harmonics to pass through the transformer, affecting its efficiency. In [114], one phase utilizes an LLC resonant converter while the other employs a Dual-Active-Bridge (DAB) converter, resulting in similar issues as [112]. Some proposed converters show improved performance with fewer gate-drive circuits and power switches, along with two resonant tank networks for power division [117], [118]. Multiphase LLC resonant converters with common load, input voltage, and rectifier network have also been developed for wide output voltage range applications [122], [123], [124], [125]. However, filtering out current switching harmonics completely using phase-shift control [122] affects transformer efficiency, and the common leg switches in [124] and [125] experience higher currents, degrading converter performance and efficiency.

In [93], [94], [126], [127], [128], and [129], multiphase LLC resonant converters with a common load and input voltage source are proposed for wide output voltage range and battery charger applications. Reference [94] uses coupled resonant inductors to balance the output voltage. Reference [126], three switches in half-bridge switching network has been used, converter has two transformer and resonant tank, the converter has few component but it has low efficiency.

In [130], a three-phase LLC converter featuring two resonant networks for high-power transfer is presented in [131], a three-phase converter is introduced, employing a three-leg switching and rectifier network alongside three resonant networks. Notably, this structure involves relatively few components, but it results in the second leg of the switching network handling higher power compared to the other legs. Reference [132], explores the connection of the resonant networks in a delta-delta configuration, while [133], puts forward a semi-active rectifier network designed to operate under hard switching conditions.

Reference [95] utilizes two resonant tanks and transformers without additional switches but suffers from increased cost and low efficiency at light-load conditions. Reference [134] proposes the use of two transformers to increase the output voltage, but it raises circulating currents, volume, and cost. Similar approaches with multiple transformers are employed in [135] and [136] to increase the output current. In [137], a double input/output transformer is used to increase efficiency compared to dual-LLC and full-bridge LLC resonant converters under high-load conditions. However, it comes with increased volume, cost, and design complexity [138] suggests a two-phase interleaved LLC resonant converter with few components and high efficiency, but each switch requires its own LLC resonant tank. Reference [139] utilizes a dual-transformer and an auxiliary LC resonant tank to increase efficiency, which increases the converter's cost, volume, and complexity. Reference [140] suggests the use of a resonant capacitor between the primary side of a dual-transformer and the input voltage source, with a combination of two parallel half-bridge switching networks. Although suitable for high-power battery charger applications, it is a massive and expensive solution.

In [141], an expandable LLC resonant converter with a multi-input/output transformer is proposed. However, the use of several switches without soft-switching operation reduces efficiency and increases volume and cost. Reference [142], introduces a two-phase interleaved LLC resonant converter with few components and high efficiency, but each switch requires its own LLC resonant tank. Additionally, some switches do not operate under soft-switching conditions, and the use of two transformers can increase cost and volume.

In [143], a three-level LLC resonant converter with four transformers is proposed, operating under soft-switching conditions and low voltage stress. However, the use of multiple transformers increases cost, power loss, and volume. References [144] and [145], propose LLC resonant converters with a matrix transformer to increase efficiency. These converters have high power density and are suitable for HVDC and MVDC applications, but they can suffer from high voltage stress, EMI noise, high cost, and low efficiency at light loads.

Table 5 provides a detailed comparison of the different converters, highlighting their performance characteristics. Interleaved converters with proper power division among components tend to offer better performance and compactness. Overall, the choice of the most suitable converter depends on the specific requirements of the application, balancing factors such as efficiency, cost, volume, voltage stress, and complexity. The basic multiphase-multilevel LLC resonant converter is shown in Fig. 13 (a).

Despite the usefulness of multilevel converters in various applications, the optimal configuration depends on the specific application requirements. For example, in wireless power transfer (WPT) systems, where cost is a significant factor, a single resonant network may be more suitable. This simplifies the design approach and reduces costs associated with multiple components. However, for charging stations requiring high power levels, using multiple resonant tanks can be advantageous. This allows for better distribution of power and reduces the stress on the individual components, improving overall reliability.

In applications where reducing electromagnetic interference (EMI) noise is crucial, employing multiple switch networks can be beneficial. By distributing the switching activity across the multiple networks, the overall EMI noise can be reduced, leading to improved performance and reliability of the converter.

For high voltage direct current (HVDC) applications, multilevel converters offer the advantage of being able to increase the number of voltage-sensitive components. This allows the voltage to be divided across these components, reducing the voltage stress on individual components and improving the overall efficiency and reliability of the converter.

In electric vehicle (EV) charging applications, multilevel converters offer several benefits. They can provide the capability to handle the high power levels required for fast charging while also maintaining efficiency. Additionally, the modular nature of the multilevel converters makes them well-suitable for EV charging stations, as they can easily be scaled up to meet increasing power demands.

Overall, the multilevel converters offer a high degree of flexibility and adaptability, making them suitable for a wide range of applications. By carefully selecting the configuration based on the specific requirements of the application, it is possible to achieve optimal performance and efficiency.

E. BIDIRECTIONAL LLC RESONANT CONVERTERS

Nowadays, batteries and power storage components play a crucial role in our daily lives, especially for DC energy storage. As a result, bidirectional converters that can simultaneously charge and use batteries as input sources have become essential for these applications. While unidirectional converters are suitable for certain scenarios, bidirectional multi-input converters are preferred in many cases. Unfortunately, the previously mentioned converters are primarily single-input unidirectional solutions and may not be suitable for bidirectional applications, in practice.

For bidirectional applications such as electric vehicle (EV) battery charging, various bidirectional converters based on the LLC resonant topologies have been proposed. These resonant converters, known for their soft-switching capability and high power density, are well suited for these applications. In the following sections, the bidirectional two-level LLC converters are reviewed and some of the proposed designs are well highlighted.

Bidirectional converters offer significant benefits for EV charging. They allow for efficient energy transfer in both directions, enabling vehicles to charge from the grid as well as return excess energy back to the grid, a process known as vehicle-to-grid (V2G) operation. This bidirectional capability is essential for maximizing the utility and efficiency of EVs, as it enables them to not only consume energy but also contribute to grid stability and energy management.

Additionally, bidirectional converters can help manage the power flow between the EV battery and other energy sources or loads, such as renewable energy systems or residential or commercial buildings. This flexibility allows for more efficient use of renewable energy and helps reduce the overall energy consumption and carbon footprint of the transportation sector.

Furthermore, bidirectional converters can help optimize the charging process for EV batteries, ensuring fast and efficient charging while minimizing stress on the battery cells. This can help extend the lifespan of the batteries and improve overall reliability and performance of the EVs.

Overall, bidirectional converters play a critical role in enabling the widespread adoption of electric vehicles and the integration of renewable energy sources into the grid. Their flexibility, efficiency, and reliability make them essential components in the evolving energy landscape.

1) BIDIRECTIONAL TWO-LEVEL LLC CONVERTERS

In [146] and [147], two However, challenges associated converters have been proposed. In [146], the converter is specifically designed for battery charging applications and features an LLC resonant tank on the primary side of the transformer. However, it utilizes a series LC resonant network on the secondary side, which is not symmetric in the forward and backward directions. Reference [148] incorporates a parallel inductor in the resonant tank to expand the voltage gain range, allowing for energy interface between energy storage systems and DC microgrid applications. However, the addition of the inductor introduces two parallel components in the L-LLC structure increase the circulating current. Furthermore, there is no resonant tank on the secondary side of the transformer, which allows switching harmonics to pass through the transformer, leading to heat generation and inefficiencies. Additionally, the presence of the added inductor adds complexity to the converter and its equations.

Another bidirectional LLC resonant converter is proposed in [149], which utilizes two switching networks on the primary side and a three-leg interleaved switching network on the secondary side. While this converter offers high power density, it also suffers from a high number of switches, gate-drives, and resonant components, which can negatively affect cost, conduction losses, and overall efficiency.

Other bidirectional LLC resonant converters have been proposed in [150], [151], [152], [153], [154], [155], and

[156], each with its own advantages and drawbacks. For instance, [150], introduces additional switches for parallel inductor control, but this object increases the converter complexity and its circulating current. In [154], the resonant network employed did not yield favorable results in terms of minimizing harmonics entering the transformer and reducing waste. In [155], the converter incorporates an LLC resonant network only in the forward conduction mode, Furthermore, full-bridge bidirectional LLC-based resonant converters have been explored in [157], [158], [159], and [160]. These converters aim to address some of the drawbacks, mentioned earlier. For example, the specifically designed converter for battery charging applications requires a wide output power range, which needs a wide switching frequency variation, in practice. However, one of the disadvantages of this topology is the high circulating current and associated power losses.

Additionally, several multilevel converters have been proposed in [161], [162], [163], and [164]. For instance [163] and [164] introduce several three-leg LLC resonant converters that offer high conversion efficiency values. These converters incorporate multiple transformers, which result in larger sizes and high volumes. However, most of these converters achieve peak efficiency above 90% and exhibit good performance overall.

In summary, bidirectional LLC resonant converters are particularly advantageous for battery charging and energy storage applications due to their ability to efficiently handle power flow in both directions. These converters play a crucial role in applications where energy needs to be stored and retrieved from batteries or other storage devices.

Despite their advantages, ongoing research is focused on further improving the efficiency and reducing the complexity of bidirectional LLC resonant converters. One key area is minimizing circulating currents, which can lead to increased losses and reduced efficiency. Researchers are exploring various control strategies and circuit designs to mitigate these circulating currents and improve overall converter performance.

Another area of research is reducing switching harmonics, which can contribute to increased EMI noise and reduced efficiency. Advanced modulation techniques and filter designs are being investigated to minimize these harmonics and improve the overall quality of the output waveform.

Additionally, efforts are being made to enhance the reliability and robustness of bidirectional LLC resonant converters, particularly in high-power applications. This includes improving the thermal management of the converter and optimizing the design to handle high voltage and current levels more effectively.

Overall, while bidirectional LLC resonant converters offer significant advantages for battery charging and energy storage applications, ongoing research is essential to address remaining challenges and further enhance their performance and efficiency. The bidirectional two level LLC resonant converters common structure is shown in Fig. 14(b).

2) BIDIRECTIONAL THREE-LEVEL LLC RESONANT CONVERTERS

Three-level LLC converters have emerged as a solution to address several key challenges encountered in two-level converters. One of the primary issues with two-level converters is the generation of electromagnetic interference (EMI) noise, which can lead to performance degradation and reliability issues in electronic systems. By employing three-level configurations, these converters can effectively reduce EMI noise, thereby improving overall system performance.

Another critical challenge in two-level converters is the high voltage stress experienced by the switches. This high stress can lead to increased losses and reduced efficiency. Three-level LLC converters help mitigate this issue by distributing the voltage stress across multiple levels, reducing the stress on individual components and improving overall system reliability.

Additionally, three-level LLC converters offer improved waveform quality, leading to reduced total harmonic distortion (THD) in the output voltage and current. This improvement is crucial in applications where clean power delivery is essential, such as in renewable energy systems and sensitive electronic equipment.

Despite these advantages, three-level LLC converters also present some challenges, including increased complexity in control algorithms and gate-drive circuits. Moreover, they may have higher conduction losses due to the increased number of components. However, ongoing research is focused on addressing these challenges to further enhance the performance and efficiency of three-level LLC converters. In [165] a bidirectional three-level LLC-based resonant converter is introduced, which incorporates two diodes in the switching network that unfortunately increase the power loss and components count and cost. Based on this work, [166] proposes another three-level LLC-based converter that improves upon the drawbacks of [165]. It offers three different operational modes based on the required voltage gain.

The bidirectional three level LLC resonant converters common structure is shown in 14(b) and Table 6 provides a comparison of some related converters, in more detail. The converters with proper filter networks demonstrate better performance as switching harmonics are effectively filtered in both forward and backward operation modes. Furthermore, the three-level structures exhibit lower voltage stress across the power switches.

F. USING THE LLC RESONANT CONVERTER FOR POWER FACTOR CORRECTION

The combined structure of interleaved boost and LLC resonant converters offers high efficiency, improved power factor correction, and reduced losses, making it an attractive choice for PFC applications because of following reasons.

1) REDUCED CURRENT RIPPLE

Interleaving multiple boost converters reduces the input current ripple seen by each individual converter. This reduction in ripple current leads to lower conduction losses in the input stage, improving efficiency.

2) BALANCED OPERATION

Interleaving ensures that the load is shared evenly among the converters, which helps in balancing the power distribution. This balanced operation minimizes losses and improves overall efficiency.

3) HIGHER VOLTAGE CONVERSION RATIO

Boost converters are used to step up the input voltage to a desired level. By interleaving multiple boost converters, higher voltage conversion ratios can be achieved without excessively high duty cycles, which improves efficiency.

4) SOFT-SWITCHING CAPABILITY

LLC resonant converters are known for their soft-switching operation, which reduces switching losses. When combined with interleaved boost converters, the overall system can maintain soft-switching characteristics, further enhancing efficiency.

5) IMPROVED POWER FACTOR CORRECTION

The combined structure ensures effective power factor correction by shaping the input current waveform to be in phase with the input voltage. This reduces losses and improves the overall power factor of the system.

6) OPTIMIZED CONTROL

Advanced control algorithms can be implemented in interleaved boost and LLC converters to further enhance efficiency. These algorithms can dynamically adjust the operation of the converters based on load and input voltage conditions.

A bridgeless converter for LED driver applications was proposed in [167], by combining an interleaved bridgeless

boost Power Factor Correction (PFC) rectifier with an LLC resonant converter. This configuration uses an additional capacitor and a series switch in the resonant tank, which complicate the circuit, increase its cost and power loss. A single-stage interleaved LLC resonant converter with a variable inductor for PFC application was introduced in [174] and [175], too. However, challenges associated with variable inductors are remained.

Also, a single-stage interleaved boost and LLC resonant converter was proposed in [168], which employs the PWM modulation approach to regulate the output voltage and to correct the power factor, simultaneously. An interleaved boost and LLC resonant converter was proposed in [169] and [170], where the AC input voltage is connected to a full-bridge LLC resonant converter through the two intermediate inductors and diodes. This configuration reduces the number of switches, as compared to the other PFC converters. However, these converters are typically designed for low-power applications and exhibit lower efficiency at low loads due to the employed PFM control and uncontrolled circulating currents.

A single-stage LLC-boost converter for PFC is also suggested in [176], where the AC input voltage is rectified and applies to the LLC resonant converter. However, this converter exhibits low efficiency under the light-loads. A three-level structure similar to [176] is given in [177], with a reconfigured rectifier network. The AC input voltage is directly applied to the LLC resonant and switching networks, reducing voltage stress, EMI noise, and incorporating PWM control for the three level as an additional control approach.

Also, the interleaved boost and LLC resonant converters utilizing PWM and PFM control approaches are proposed in [171] and [178], to enhance efficiency. However, these converters still face challenges under the light-load conditions.

A Cuk-LLC resonant converter is introduced [172] for PFC application in LED drivers, which involves a separate rectifier network to rectify the AC input voltage, whereas the previously mentioned converters incorporate interleaved rectifier networks. A three-phase LLC-based converter is also introduced in [173] for high-power PFC, consisting of three parallel converters sharing a common load and rectifier network. However, the aforementioned drawbacks persist.

Fig. 14 illustrates the basic PFC converter structure based on the LLC and boost topologies and Table 7 provides a comparison of some related converters. The interleaved LLC-boost structure, where the rectifier network is interleaved with the converter, offers a compact design with a simple structure and control approach. These converters provide higher efficiency compared to other PFC converters, primarily due to the lower conduction losses resulting from their compactness.

Some elite converters from each groups are simulated and compared as Table 8 to introduce more specifics.

In order to conduct a comprehensive analysis of the reviewed converters, a set of simulations has been performed, allowing for a comparative evaluation based on criteria such as relative cost, energy stored in resonant capacitors, voltage stress on Power MOSFETs, energy stored in resonant inductors and voltage stress on diodes. The results of this comparative study are presented in Fig. 15 (a, b, c), Fig. 16 (a, b, c), Fig. 17 (a, b, c), Fig. 18 (a, b), and Fig. 20(a, b) respectively. These characteristics are obtained based on (92) and (93), given later.

III. LLC RESONANTCONVERTER DIFFERENT CONTROL APPROACHES

As mentioned before, the LLC resonant converter is a useful power electronics converter, which is commonly controlled and regulated for various purposes such as output voltage or current regulation applications. Pulse Frequency Modulation (PFM) control technique is a popular control approach for this converter, due to its gain-frequency characteristics. By using this approach, when the converter operates at frequencies far from the resonant frequency, the circulating currents and

TABLE 6. Comparison of the Bidirectional Converters.

Ref.	Input Voltage (V)	Output Voltage (V)	Output power (W)	Efficiency (%)	Switching frequency (kHz)	Lr (µH)	Cr (nF)	Lm (µH)	Converter and its control complexity	Voltage stress across switches	Number of components	Application
[160]	400	250-450	1000	97	NM	23.34, 21.17	110, 120	128.37	Low	$V_{in\_(DC)}$	Low	Battery charger
[162]	200-280	400	800	97.2	71-140	NM	68, 101	NM	High	$V_{in\_(DC)}$	High	PV
[151]	400	160-220	1000	98	NM	115	22	2*460	Low	$V_{in\_(DC)}$	Low	Energy storage
[153]	3 k	1.5 k	30000	96	3-5	250	2000	4000	Low	$V_{in\_(DC)}$	Low	NM
[147]	380	NM	5000	97.8	NM	30	200	130	Low	$V_{in\_(DC)}$	Low	DC Power Distributi on System
[166]	400	50-450	300	94.3	32.5-50 & 65-100 Two control scheme	34.45	69.7	108	High	$V_{in\_(DC)}$ /2	Medium	NM

TABLE 7. Comparison of the LLC-Based PFC Converters.

Ref.	Input Voltage (V)	Output Voltage (V)	Output Power (W)	Efficiency (%)	Switching Frequency (kHz)	Cbus (µF)	Lin (µH)	Lr (µH)	Cr (nF)	Lm (µH)	Converter and its control complexity	Number of components	Power factor
[167]	220 ac	70 DC	100	95	200	NM	NM	NM	NM	NM	Medium	Medium	0.92
[168]	85-265 ac	48	300	93	NM	120	NM	177	13	NM	Low	Medium	0.98
[169]	100-130 ac	48	350	92	140	400	2×110	70	16.4	120	Low	Medium	0.997
[170]	110-220 ac	400	1 K	96	100	17	2×1000	37	68	NM	Medium	Medium	THD=3.9%
[171]	200	100	100	94	370-403	NM	170	90	1.98	324	Low	Low	0.95 THD=12%
[172]	277-380 RMS	50	100	91.65	NM	440	NM	58	47	275	High	High	0.97 THD=25.5%
[173]	380	300	10 k	98.1	34-39	NM	2×800	120	141	470	Medium	High	NM

related conduction losses are increasing, rapidly [179] Different control approaches, such as PFM, have varying effects on the performance and efficiency of LLC resonant converters. PFM control is known for its simplicity and ability to regulate the converter's output voltage or current by adjusting the switching frequency. However, the impact of PFM control on efficiency and performance depends on the operating conditions, particularly the proximity to the resonant frequency.

At frequencies close to the resonant frequency, PFM control can be highly efficient. The converter operates in a soft-switching mode, where switching losses are minimized, leading to higher efficiency. In this region, PFM control allows the converter to maintain stable operation while minimizing losses.

However, as the converter operates farther away from the resonant frequency, the effectiveness of PFM control diminishes. The control mechanism may increase the switching frequency to regulate the output, leading to suboptimal operation. This deviation from resonance can result in higher circulating currents within the converter circuit, increasing conduction losses and reducing overall efficiency. Additionally, operating at frequencies far from resonance can introduce additional challenges, such as increased stress on components and potential EMI issues.

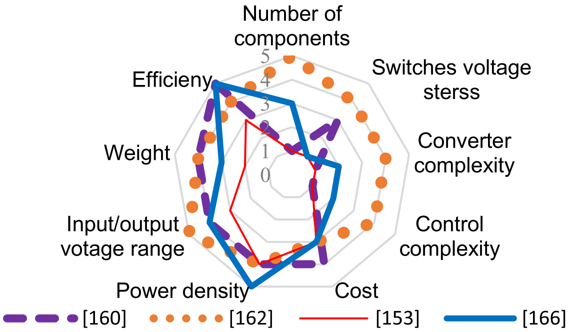

FIGURE 11. Comparison of some of the given converters in Table 6. 1: represents LOWEST and 5: HGHEST value.

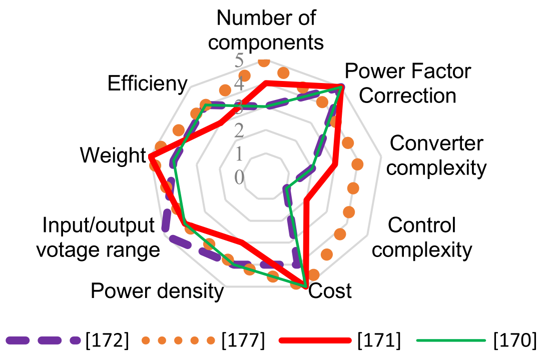

FIGURE 12. Comparison of some of the given converters in Table 7. 1: represents LOWEST and 5: HGHEST value.

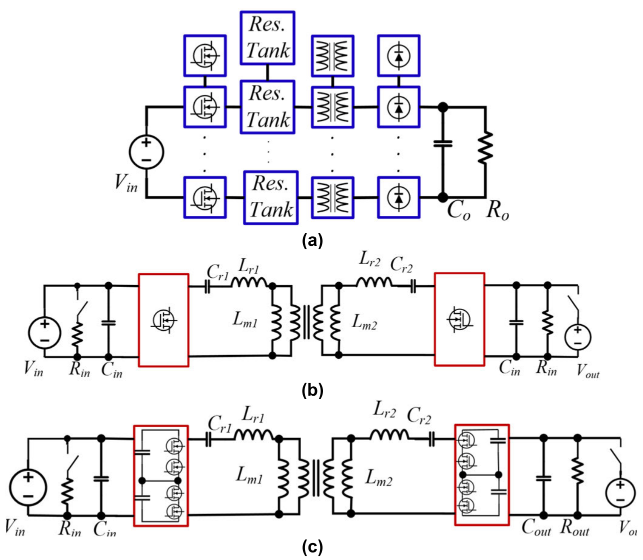

FIGURE 13. (a) Basic multi-phase and multi-level converter, (b) basic bidirectional LLC-based two-level converter, and three-level converter.

Overall, while PFM control offers simplicity and adaptability, its efficiency and performance in LLC resonant converters are highly dependent on the operating conditions. Careful consideration of the operating frequency range and control strategy is essential to ensure optimal performance and efficiency in LLC resonant converters.

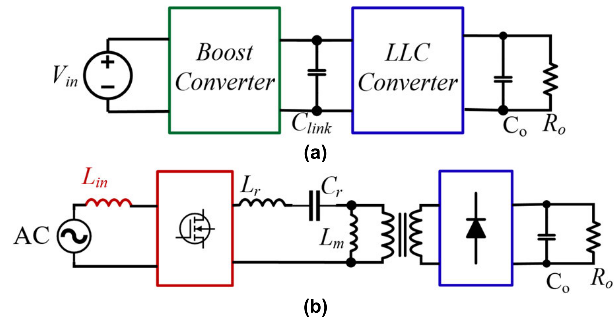

FIGURE 14. (a) Basic structure of the series connected Boost and LLC converters and (b) a single-stage interleaved boost and LLC resonant converter.

It should be mentioned that, there are several other approaches for fixed-switching frequency and converter control purposes, including Pulse Width Modulation (PWM), Phase Shift Modulation (PSM), Pulse Width Amplitude Modulation (PWAM), continuous and discontinuous variation in converter components, as well as combinations of these various approaches.

In the case of continuous and discontinuous variation of the converter components, a variable quality factor is obtained at a fixed switching frequency. So, the output voltage can be regulated by varying the quality factor parameter, because of the quality factor dependence voltage gain characteristics. Some of the variations include variable resonant series or parallel inductors, variable series capacitors, variation in the switching or rectifier network, variable transformers, and using the multipliers in the rectifier network.

In the PWM based approach, the output voltage is regulated by varying the converter duty cycle at a fixed switching frequency. This approach has been applied widely to the LLC resonant converters by many researches [60], [86], [127], [180], [181], and [182]. However, when the duty cycle deviates significantly from 50% value, the circulating currents are increasing. In addition, the variable duty cycle affects the transformer input current waveform, which increases the harmonics and power losses.

When PSM technique is used, all switches operates at 50% duty cycle value, but there is a phase difference between the converter's legs gate-drive signals, which controls the converter output signal. This approach has been applied to the LLC resonant converters, widely [122], [183], and [184]. Using this approach at a fixed frequency can provide soft switching conditions for the power switches. However, similar to the PWM method, when the transformer input signal deviates from the 180 degrees, higher harmonics degrade the converter efficiency, in practice.

By using the PWAM approach, a multilevel voltage waveform with the ability to control the highest and lowest voltage levels is obtained by varying the input voltage amplitude of the resonant tank. The output voltage regulation is achieved by controlling the pulse width of the highest voltage amplitude. This approach has lower harmonics, as compared to other approaches due to its multilevel structure, which also

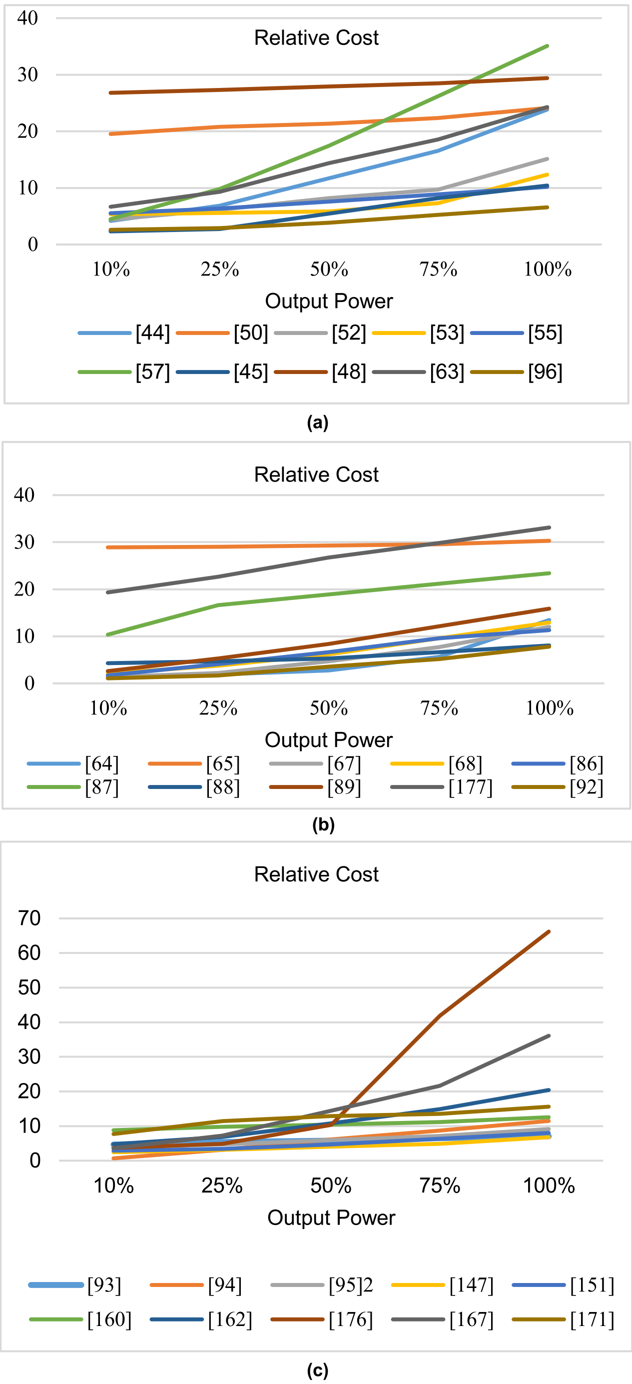

FIGURE 15. Relative cost comaprision of some converters.

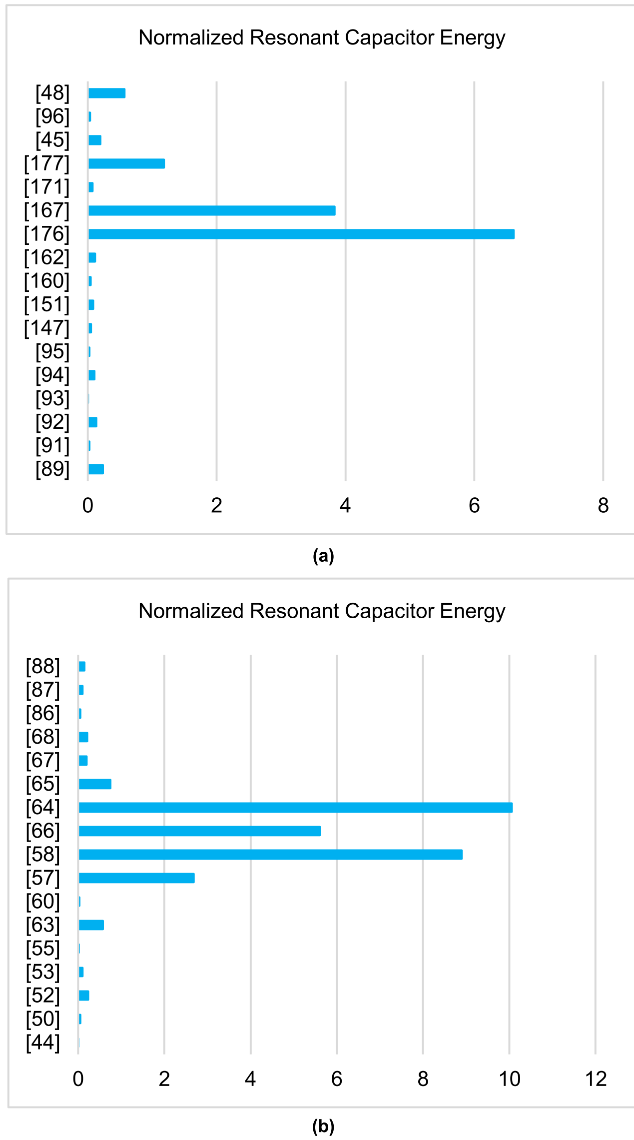

FIGURE 16. Comparison of some converters resonant capacitor normalized energy.

results in lower EMI noise. The PWAM approach operates at a fixed switching frequency, but has complexity and lower efficiency at high and low amplitudes [185], [186]. In [185] and [187], a bidirectional three-level converter has been proposed with Pulse Width and Amplitude Modulation (PWAM) control approaches for a wide range of voltage gain curve. The converter features a three- and two-level switching network, as well as different operational modes for different load situations. The PWAM approach can be applied to the converter due to the combination of PSM and PWM techniques.

The proposed converter offers better light-load operation, as compared to the conventional converters. However, it has some drawbacks such as numerous switches and gate drives, as well as high complexity and cost. The given converter in [187] has a two-level structure in the backward conduction mode, which shares similar issues with [185].

In addition, some approaches, including PFM and PWM, PFM and PSM, PFM and PWAM, PSM and Asymmetrical PWM (APWM), and so forth, have been combined to enhance performance and operation of the LLC resonant converters. For instance, in [66], [188], [189], [190], [191], [192], [193], and [194], a combination of PWM and PFM has been used, which limits the switching frequency range due to the hybrid control approach. Nevertheless, it inherits the advantages and disadvantages, as mentioned earlier for PFM and PWM control methods. In [172], [195], [196], [197], and [198], a combination of the PFM and APWM approaches has been

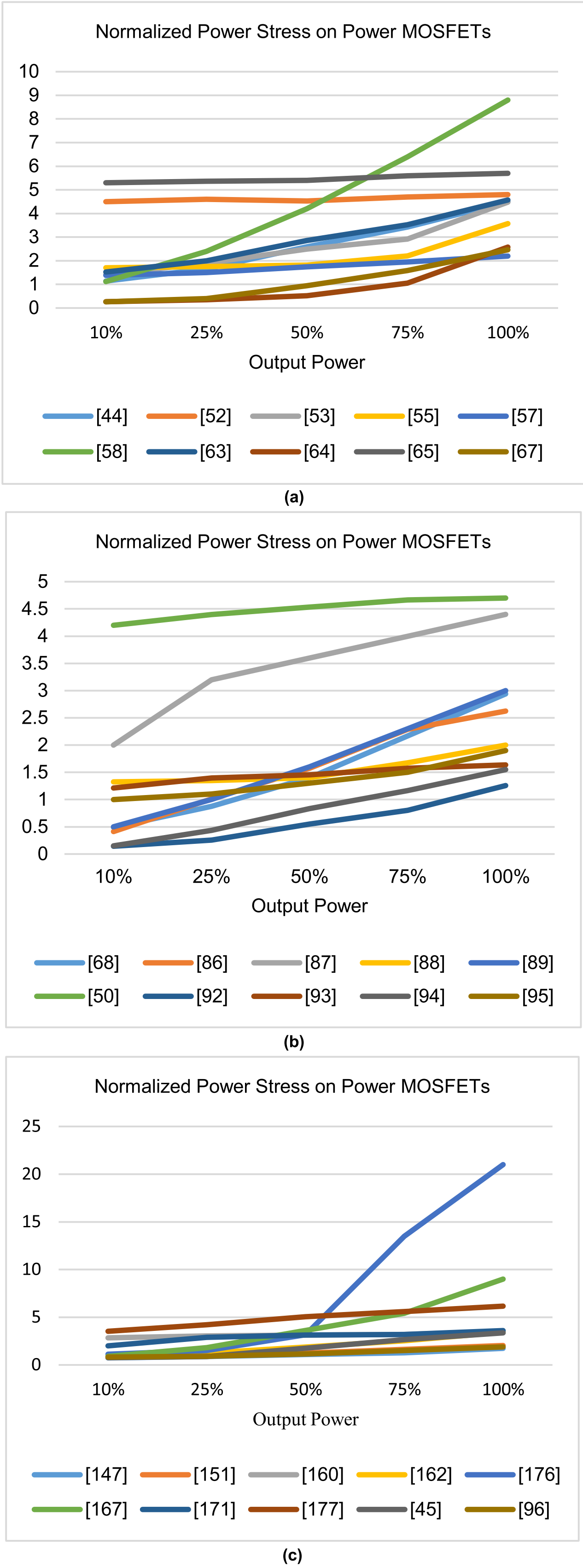

FIGURE 17. Switch comparison of some converters.

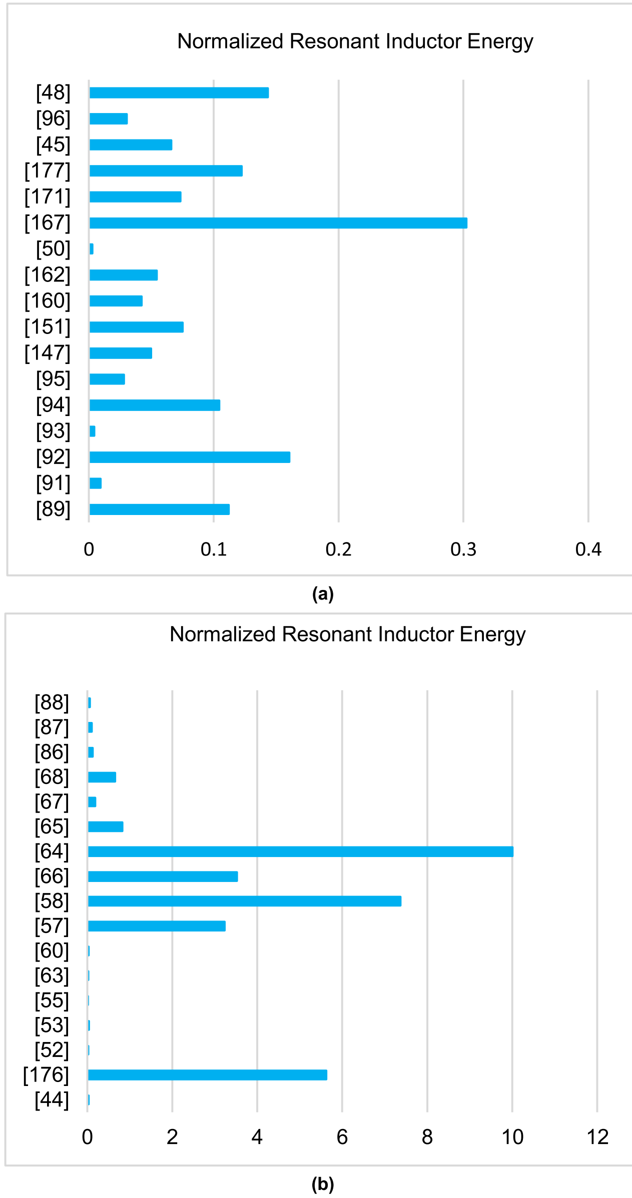

FIGURE 18. Comparison of some converters resonant inductor normalized energy.

employed, which shares the advantages and disadvantages of both PWM and PFM techniques, in practice.

Also, a combination of the PSM and PFM methods has been proposed in [199] and [200], which provides advantages of these two techniques, as well as their associated issues. In [201], a combination of the PWM, PFM, and PSM has been used, offering the same advantages and disadvantages of these approaches, along with a limited frequency range, as compared to the previous approaches. Additionally, this combined approach introduces more complexity and cost, too.

In addition to PFM control, another effective method to control the LLC resonant converter involves switching between full-bridge and half-bridge control approaches,

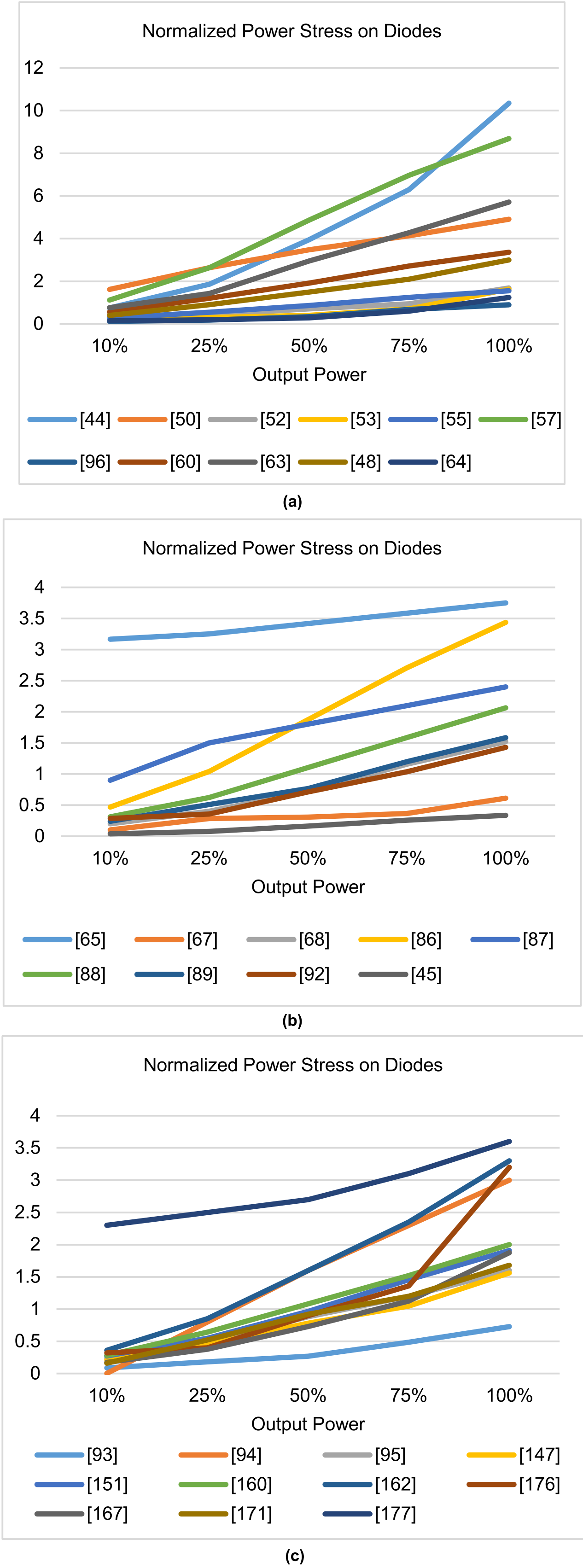

FIGURE 19. Comparison of diodes of some converters.

in combination with PFM. This strategy aims to reduce the voltage variation range, particularly useful in regulating output voltage while minimizing the frequency range. This approach has been successfully implemented in EV charging applications, as demonstrated in [202].

In summary, a wide range of applications, including HVDC, WPT, PV cells, fuel cells, and EV charging, can benefit from the implementation of combined control methods in LLC resonant converters. These methods offer the potential to increase efficiency and limit frequency variation range, addressing issues introduced by individual control approaches.

However, it is important to note that the use of combined control methods may increase the complexity of the converter system. This complexity could require a more sophisticated controller, potentially a digital one, to effectively manage the switching between control approaches and ensure optimal performance across a variety of operating conditions. Despite this challenge, the benefits of increased efficiency and improved performance make the implementation of combined control methods an attractive option for many applications.

IV. CIRCUIT ANALYSIS

A. LLC RESONANT CONVERTER BASIC CONFIGURATION

As shown in Fig. 20, the basic LLC resonant converter is essentially a resonant inverter composed of its three reactive components.

The LLC resonant converter offers several features that enable it to adapt to wide input and output voltage ranges, providing versatility and flexibility in various applications:

1) SOFT-SWITCHING OPERATION

LLC resonant converters operate with soft-switching techniques, which minimize switching losses and stress on power devices. This allows the converter to efficiently handle a wide range of input and output voltage levels without experiencing excessive switching losses.

2) RESONANT TANK CIRCUIT

The LLC resonant converter utilizes a resonant tank circuit composed of inductors and capacitors. This resonant tank circuit enables the converter to achieve zero-voltage switching (ZVS) and/or zero-current switching (ZCS) during the switching transitions, regardless of the input and output voltage levels. As a result, the LLC converter can maintain high efficiency across a wide range of voltage levels.

3) ADAPTIVE CONTROL MECHANISMS

Many LLC resonant converters employ adaptive control techniques to adjust the operating frequency or duty cycle dynamically based on the input/output voltage levels. These control mechanisms optimize the converter's performance for different voltage ranges, ensuring efficient operation under varying load conditions.

4) MULTILEVEL TOPOLOGIES

Advanced LLC resonant converter topologies, such as multilevel or cascaded configurations, are capable of handling wider voltage ranges by distributing the voltage stress across multiple stages. By dividing the voltage conversion process into several stages, these topologies mitigate the challenges associated with high voltage differentials and enhance overall system reliability.

5) MODULAR DESIGN

In some applications, LLC resonant converters are designed with modular architectures that allow for easy scalability and adaptation to different voltage requirements. By combining multiple converter modules in parallel or series configurations, designers can accommodate a wide range of input and output voltage levels while maintaining high efficiency and reliability.

The dc input voltage undergoes square voltage waveform conversion through a switching network, which is applying to the resonant tank network, where its harmonics are filtering out. The resulting output voltage is approximately a sinusoidal waveform, which is generally feeding into a transformer to isolate the input and output ports and to change the voltage level, if it is necessary. Finally, the transformer output voltage is rectified and applied to a capacitive filter to supply the load.

Input/output isolation plays a crucial role in LLC resonant converters, particularly in industrial environments, due to several key reasons:

6) SAFETY

Isolation ensures the safety of operators and equipment by preventing electrical hazards such as electric shock. In industrial environments where high voltages and currents are common, maintaining isolation between input and output circuits is essential to prevent accidents and ensure compliance with safety standards.

7) GALVANIC ISOLATION

LLC resonant converters often operate in systems where the input and output circuits are electrically isolated from each other. Galvanic isolation provided by the converter ensures that there is no direct electrical connection between the input and output sides, preventing ground loops and minimizing the risk of interference and noise coupling between different parts of the system.

8) VOLTAGE REGULATION

Isolation helps maintain stable voltage regulation by preventing voltage fluctuations or transients from propagating between the input and output circuits. This is particularly important in industrial applications where sensitive equipment may be adversely affected by voltage variations.

9) NOISE IMMUNITY

Isolation helps in reducing the impact of electromagnetic interference (EMI) and radio-frequency interference (RFI) on the operation of the converter and the connected equipment. By isolating the input and output circuits, the converter can effectively filter out external noise and disturbances, ensuring reliable operation in noisy industrial environments.

10) PROTECTION OF SENSITIVE ELECTRONICS

In industrial environments, there may be sensitive electronic equipment connected to the output of the LLC resonant converter. Input/output isolation helps protect these devices from potential damage caused by electrical faults or disturbances originating from the input side of the converter.

11) COMPLIANCE WITH REGULATORY STANDARDS

Many industrial applications require compliance with regulatory standards and certifications related to electrical safety and electromagnetic compatibility (EMC). Input/output isolation ensures that the LLC resonant converter meets these standards by providing the necessary isolation barriers between different electrical circuits.

All power MOSFETs of the LLC resonant converter are turning on under the ZVS condition and the output stage diodes are turning off under the ZCS conditions in a wide input voltage and load variation range conditions, if it is properly designed in the converter inductive region. In addition, the power MOSFETs turning off switching losses can be well reduced by considering a short dead time in between the gate-drive signals and turning of them fast before their drain-source voltages are increased, significantly. Sometimes small capacitors are connecting in parallel to the MOSFETs drain-sources to reduce more these switching losses, too. The converter soft switching operation reduces both the generated EMI noise and switching power losses [203], [204]. Consequently, it is possible to increase the operation switching frequency and power density as high as possible, to reduce the passive components volumes including capacitor, inductor, and transformer, as well as the input and output filters, which leads to high power density [204], [205]. In addition, this converter can provide wide voltage gain values and it well operates under the wide input and load operation conditions, in practice.

B. DIFFERENT OPERATIONAL STATES OVER A SWITCHING PERIOD

The key waveforms of a half-bridge LLC resonant converter are shown in Fig. 21(a), which clearly show soft switching operation of its all switches. To simplify the analyses, the short dead times between the power MOSFETs gate-drive signals are ignored.

State I (a) ($t_0 \sim t_1$): by turning off the S_2 power switch by the control circuit the converter experiences a short dead time interval to prevent the short circuited problem. Then, the

S_1 body diode conducts the current, as depicted in Fig. 21(a). Next, the switch S_1 is turning on under the ZVS condition to conduct the current, while its body diode is still on during the first subinterval time. The output voltage is applying across the magnetizing inductor (L_m), and its current is increasing, linearly. The L_r and L_m inductors currents difference passes through the transformer to supplies the load through the diode D_1. This subinterval is finished when the resonant inductor current passes through zero. The converter equivalent circuit during this subinterval is given in Fig. 20(a).

State I (b) ($t_1 \sim t_2$): at the beginning of this subinterval, the S_1 body diode is turning off under the ZCS condition, as shown in Fig. 21(a). The L_m and L_r currents difference supplies the load through the transformer and D_1, until this current value reaches to zero. Then, this subinterval is finished and D_1 is turning off under the ZCS condition.

Both ($t_0 \sim t_1$) and ($t_1 \sim t_2$) subintervals are generally considered as a single state, because their equivalent circuits are the same, as shown in Fig. 20(a).

State II ($t_2 \sim t_3$): during this subinterval, as depicted in Fig. 21(a), both magnetizing and resonant inductors currents are the same. Consequently, no current is transferred to the secondary side. Therefore, the diode D_1 is turned off under the ZCS condition. At the end of this subinterval, switch S_1 is turned off under the hard switching condition, by the control circuit. Nevertheless, its drain-source paralleled parasitic or equivalent added capacitance effectively reduces its switching loss, if it is turned off fast before its drain-source voltage is significantly increased during the short dead time. The converter equivalent circuit during this subinterval is given in Fig. 20(b).

State III (a) ($t_3 \sim t_4$): considering Fig. 21(a), at the beginning of this subinterval the S_2 switch body diode is turned on to conduct the resonant inductor current. Then, S_2 is turned on under the ZVS condition by the control circuit, while its body diode is still on during this subinterval. The output voltage is reversely applying across the magnetizing inductor and its current amplitude is increasing, linearly. The L_r and L_m inductors currents difference passes through the transformer to supplies the load through the diode D_2. This subinterval is finished when the resonant inductor current reaches zero.

State III (b) ($t_4 \sim t_5$): at the beginning of this subinterval, the S_2 body diode is turning off under the ZCS condition, as shown in Fig. 21(a). The L_m and L_r currents difference supplies the load through the transformer and D_2, until this current value reaches zero. Then, this subinterval is finished and D_2 is turning off under the ZCS condition.

Both ($t_3 \sim t_4$) and ($t_4 \sim t_5$) subintervals are generally considered as a single state, because their equivalent circuits are the same, as shown in Fig. 20(c).

State IV ($t_5 \sim t_6$): this operational state is similar to the second state. During this subinterval, as depicted in Fig. 21(a), both magnetizing and resonant inductors currents are the same. Consequently, no current is transferred to the secondary side. Therefore, the diode D_2 is turned off under the ZCS condition. At the end of this subinterval, switch S_2 is turned off under the hard switching condition, by the control circuit. Then the converter experiences a short dead time interval to prevent the short circuited problem. When the S_1 body diode conducts the current, then the switching period is finished. The converter equivalent circuit during this subinterval is given in Fig. 20(d). After this state, the switching period is finished and these operational states are repeated, in sequence [107].

Despite its desirable operation, the LLC resonant converter encounters complexity and various issues under certain operational conditions, particularly when operating far from its resonant frequency. This situation commonly occurs during light-load operation, where the switching frequency increases within the zero voltage switching (ZVS) region to regulate the output voltage. However, this approach results in the generation of increased harmonics and triangular current waveforms, as depicted in Fig. 21(b). These characteristics are evident in the Gain-Frequency curve, where frequencies far from the resonant frequency pose challenges. The resonant network becomes less effective in eliminating harmonics, which are responsible for these conditions.

C. LLC RESONANT CONVERTER DIFFERENT OPERATION MODES

Depending on whether the converter operates in the inductive or capacitive regions, it can provide zero-voltage switching (ZVS) or zero-current switching (ZCS) conditions for the power switches, respectively. In this section, different operational modes of the basic LLC resonant converter are discussed. For the MOSFET based converters, ZVS operation is preferred, because the main switching losses components of the MOSFETs are overcome, although diode reverse-recovery issues may lead to increased losses. However, by designing the converter in discontinuous conduction mode (DCM), these issues can be well mitigated, too [206]. Key waveforms of LLC resonant converter in two DCM and continuous conduction mode (CCM) mode are shown in Fig. 23. The LLC resonant converter can be controlled through pulse frequency modulation (PFM), which depends on factors such as the converter load and its inductors ratio values, which are essential parameters in the design process [207], [208], [209], [210], [211]. The normalized gain-frequency characteristics of the LLC resonant converter are shown in Fig. 22, which clearly show the converter has the ability to operate in both step-up and step-down operation modes. The LLC resonant converter exhibits two resonant frequencies, resulting in three distinct operation regions. The first region comprises frequencies lower than the first or smaller resonant frequency (f_{r1}), the second region includes frequencies between the two resonant frequencies (f_{r1}, f_{r2}), and the third region consists of frequencies higher than the second or larger resonant frequency (f_{r2}). Each region offers specific advantages, and the choice of region strongly depends on the intended application of the converter [212].

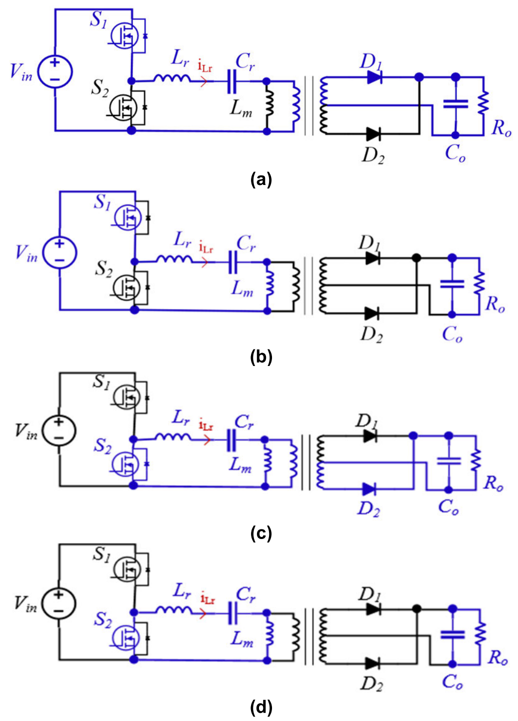

FIGURE 20. Half-bridge LLC resonant converter different operational states.

1) ***Operation in frequencies lower than*** $\mathbf{f_{r2}}$***:*** In this region, as mentioned earlier, the converter operates in the capacitive region and can realize ZCS condition for the power switches, but it is rarely studied in papers and it needs more investigations to analytically derive the converter exact characteristics, because the FHA approach is not enough accurate to predict the converter behavior under this operation region. However, it can be used for both step-up and step-down applications.
2) ***Operation in frequencies between the two resonant frequencies, i.e.*** $\mathbf{f_{r1} < f_s < f_{r2}}$**:** When the converter operates between its two resonant frequencies, it can operate in either the capacitive or the inductive region depending on the input impedance of the resonant tank. By setting the imaginary part of the input impedance of the resonant tank to zero, the boundary between these two regions can be identified, easily. If the load resistance exceeds the critical resistance value but with low or medium value, the converter operates in the discontinuous conduction mode (DCM) near the resonant frequency. On the other hand, if the load is high, the converter operates in DCM at frequencies lower than the resonant frequency. However, if the load resistance is less than the critical resistance, the converter operates in continuous conduction mode (CCM) [213]
3) ***Operation in frequencies higher than*** $\mathbf{f_{r1}}$***:*** When the converter operates in this operation region, the ZVS conditions are provided for the power switches, which is suitable for power MOSFET switches [215].

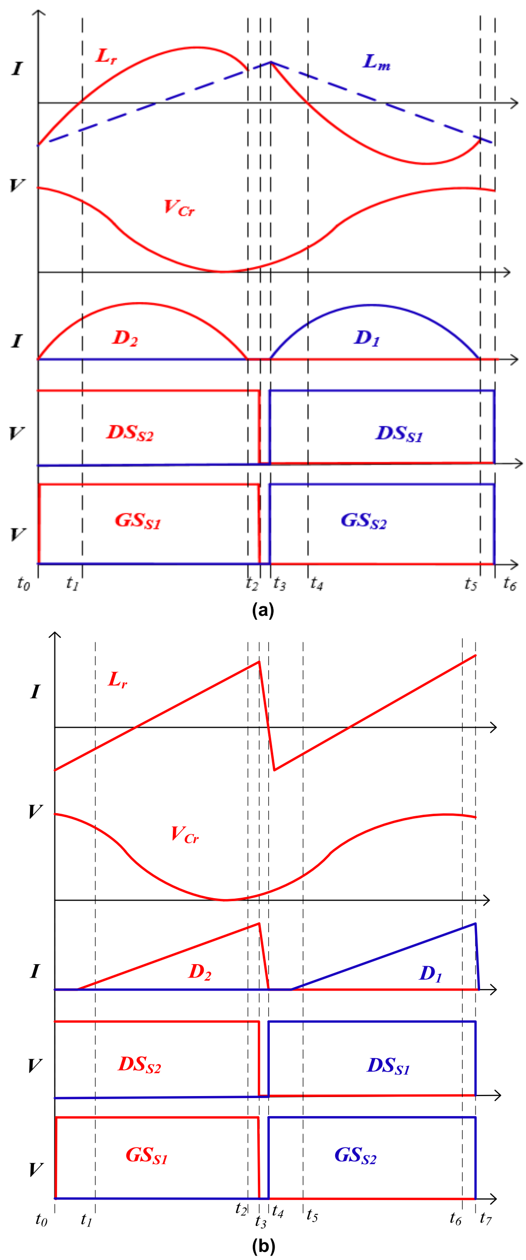

FIGURE 21. (A)Half-bridge LLC resonant converter key waveforms, (a) resonant tank inductors currents, (b) resonant capacitor voltage, (c) output stage diodes currents, (d) S_1 and S_2 drain-source voltages, and (e) S_1 and S_2 gate-source voltages waveforms. (B) Half-bridge LLC resonant converter key waveforms in resonant frequencies far from resonant frequency.

D. CALCULATING THE LLC CONVERTER POWER LOSSES

The LLC resonant converter, thanks to its soft-switching operation, experiences low power switching losses and exhibits high efficiency. However, various components in the converter still contribute to overall losses [216], [217], [218], [219], [220]. Numerous approaches have been proposed to optimize the LLC-based resonant converters' performance [221], [222], [223], [224], [225], [226], [227], and [228]. The power losses associated with different

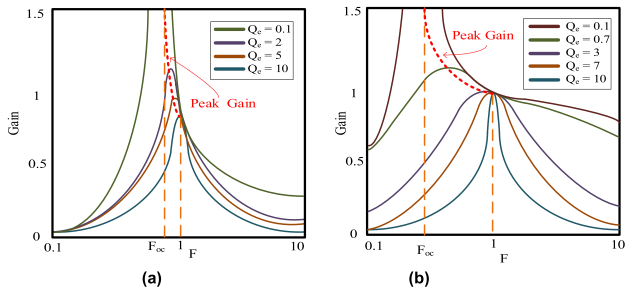

FIGURE 22. LLC resonant converter voltage gain versus normalized switching frequency at different quality factor values, (a) $L_n = 1$ and (b) $L_n = 20$.

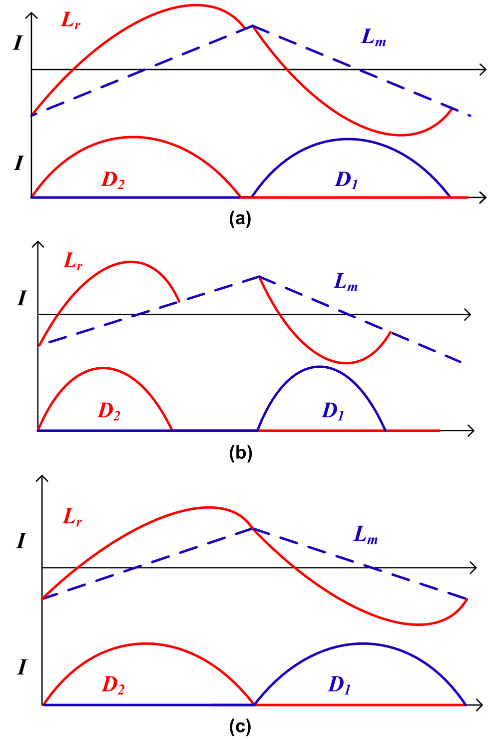

FIGURE 23. LLC resonant converter currents key waveforms under the different operation conditions in its inductive region, (a) DCM near the resonant frequency, (b) DCM far from the resonant frequency, and (c) CCM operation condition.

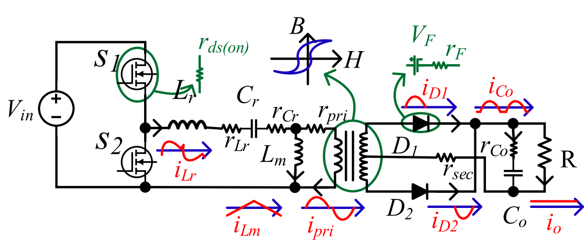

FIGURE 24. Power loss model of the LLC resonant converter and its different components currents waveforms.

components of the LLC resonant converter are illustrated in Fig. 24. The conduction losses are proportional to the currents passing through these components, which are depicted in

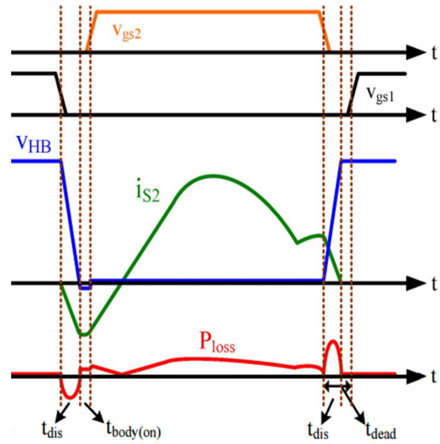

FIGURE 25. LLC resonant converter power switch different key switching waveforms [214].

Fig. 24 for the discontinuous conduction mode (DCM) [214]. In [214], it is assumed that for frequencies lower than the resonant frequency, the diodes conduction times are equal to half of the resonant period, and the waveforms resemble half of a full period of a sinusoidal waveform. Based on these assumptions, the different components power losses are given as follows, which are mainly derived from [12], [214], and [229]:

1) DIODE POWER LOSS

$$i_{D1}(t) = \begin{cases} nI_{Rm}\sin(\omega_o t) & 0 \le t < \frac{T_o}{2} \\ 0 & \frac{T_o}{2} \le t < T_s \end{cases} \tag{1}$$

$$i_{D2}(t) = \begin{cases} 0 & 0 \le t < \frac{T_s}{2} \\ nI_{Rm}\sin(\omega_o t) & \frac{T_s}{2} \le t < \frac{T_s + T_0}{2} \\ 0 & \frac{T_s + T_0}{2} \le t < T_s \end{cases} \tag{2}$$

where, ω_0 is equal to $2\pi f_o$ and

$$I_{Rm} = \frac{\pi I_o f_o}{2nf_s}. \tag{3}$$

Consequently, each diode RMS and average current values are respectively given as follows:

$$I_{D_{1,2}avg} = \frac{I_o}{2}. \tag{4}$$

$$I_{D_{1,2}rms} = \frac{\pi I_o}{4}\sqrt{\frac{f_o}{f_s}}. \tag{5}$$

Therefore, the conduction losses due to V_f and r_f of each diode, as well as the diodes total loss, are calculated as follows, respectively.

$$P_{Vf} = V_f I_{D1_{avg}} = \frac{1}{2}V_f I_o = \frac{1}{2}\frac{V_f}{V_o}P_o. \tag{6}$$

$$P_{rf} = I_{D1_{rms}}^2 r_f = \frac{\pi^2}{16}\frac{f_o}{f_s}\frac{r_f}{R_L}P_o. \tag{7}$$

$$P_D = P_{D1} + P_{D2} = \left(\frac{V_f}{V_o} + \frac{\pi^2}{8}\frac{f_o}{f_s}\frac{r_f}{R_L}\right)P_o. \quad (8)$$

2) OUTPUT CAPACITOR POWER LOSS

Output capacitor current value can be expressed as follows:

$$I_{Co}(t) = \begin{cases} nI_{Rm}\sin(2\omega_o t) - I_o, 0 \le t < \frac{T_0}{2} \\ -I_o. \frac{T_0}{2} \le t < T_s \end{cases} \quad (9)$$

$$I_{Co_{rms}} = I_o\sqrt{\frac{\pi^2}{8}\frac{f_o}{f_s} - 1}. \quad (10)$$

So, its power loss can be calculated as follows:

$$P_{r_{Co}} = I^2_{Co_{rms}} r_{Co} = \left(\frac{\pi^2}{8}\frac{f_o}{f_s} - 1\right) I_o^2 r_{Co} = \left(\frac{\pi^2}{8}\frac{f_o}{f_s} - 1\right)\frac{r_{Co}}{R_L}P_o. \quad (11)$$

3) TRANSFORMER POWER LOSS

The transformer magnetizing current can be approximated by a triangular current waveform. Therefore, the resonant inductor current waveform and its RMS value are simply derived as follows, respectively:

$$i_{Lr}(t) = \begin{cases} \frac{nV_o}{L_m}t - \frac{nV_o}{L_m}\frac{T_s}{4} + \frac{1}{n}i_{D1}(t)\, 0 \le t < \frac{T_s}{2} \\ -\frac{nV_o}{L_m}\left(t - \frac{T_s}{2}\right) + \frac{nV_o}{L_m}\frac{T_s}{4} - \frac{1}{n}i_{D2}(t)\, 0 \le t < \frac{T_s}{2} \end{cases} \quad (12)$$

$$I_{Lrms} = \sqrt{\frac{1}{48}\left(\frac{n}{f_s}\frac{V_o}{L_m}\right)^2 + \frac{\pi^2}{8}\left(\frac{I_o}{n}\sqrt{\frac{f_o}{f_s}}\right)^2 - \frac{V_o I_o}{2L_m}\left(\frac{1}{f_s} - \frac{1}{f_o}\right)} \quad (13)$$

Therefore, the transformer primary power loss can be expressed as follows:

$$P_{pri} = I^2_{Lr_{rms}} r_{pri} = \left[\frac{1}{48}\left(\frac{n}{f_s}\frac{V_o}{L_m}\right)^2 + \frac{\pi^2}{8}\left(\frac{I_o}{n}\sqrt{\frac{f_o}{f_s}}\right)^2 - \frac{I_o V_o}{2L_m}\left(\frac{1}{f_s} - \frac{1}{f_o}\right)\right] r_{pri} \quad (14)$$

In addition, its secondary side current could be calculated by considering the diode RMS current value, easily:

$$I_{\sec\ rms} = \sqrt{2}I_{D_{1rms}} = \frac{\sqrt{2}\pi}{4}\sqrt{\frac{f_o}{f_s}}I_o. \quad (15)$$

Therefore, transformer secondary side power loss is given:

$$P_{sec} = I^2_{\sec_{rms}} r_{sec} = \frac{\pi^2}{8}\frac{f_o}{f_s}I_o^2 r_{sec} = \frac{\pi^2}{8}\frac{f_o}{f_s}\frac{r_{sec}}{R_L}P_o. \quad (16)$$

In addition, the transformer copper loss is identified as follows:

$$P_{cu} = P_{pri} + P_{sec}. \quad (17)$$

Also, the transformer core loss, which is proportional to its B-H curve [230], is calculated as follows:

$$P_{tf} = K_h B^n_{ac} f_s^m M_{core}. \quad (18)$$

where, M_{core} is the core mass, and K_h, m, and n depend on the transformer core material types.

4) RESONANT TANK COMPONENTS POWER LOSSES

Power loss of each component of the resonant tank is calculated as follows:

$$P_{ESR_{Lr,Cr}} = ESR_{Lr,Cr} \times \left[\frac{1}{48}\left(\frac{n}{f_s}\frac{V_o}{L_m}\right)^2 + \frac{\pi^2}{8}\left(\frac{I_o}{n}\sqrt{\frac{f_o}{f_s}}\right)^2 - \frac{I_o V_o}{2L_m}\left(\frac{1}{f_s} - \frac{1}{f_o}\right)\right]. \quad (19)$$

where, $ESR_{Lr,Cr}$ refers to the equivalent resistances of the resonant capacitor and inductor, i.e., r_{Lr} and r_{Cr}.

5) POWER MOSFET DRIVING CIRCUIT LOSS AND ITS SWITCHING AND CONDUCTION LOSSES

There are conduction and switching power losses in each power MOSFET switch, as typically shown in Fig. 25.

t_{dis}:$2C_{dc}$ discharge time from input voltage to 0 V.
t_{dead}: dead time between gate-source signals.
$t_{delay(on)}$: power MOSFET switch delay for turning on.
$t_{body(on)}$: body diode conducting time.
V_{gs}: power MOSFET switches gate-source voltage.
V_{bF}: power MOSFET body diode forward voltage.
$t_{ds(on)}$: power MOSFET conducting time.

a: POWER MOSFET DRIVING CIRCUIT LOSS

This power loss component is mainly due to the employed gate drive circuit, which charges and discharges each MOSFET gate-source capacitor and it is simply calculated as follows for each MOSFET:

$$P_{drive} = \left(\frac{1}{2}C_{gs}V_{gs}^2\right)f_s \quad (20)$$

b: POWER MOSFET BODY DIODE LOSS

The power loss of the MOSFET body diode is given as follows:

$$P_{body} = 2V_{bF}\left[\left(\frac{nV_o}{L_m}\left(\frac{1}{4}\frac{1}{f_s} - t_{dis}\right)\right)\right]t_{body(on)}f_s. \quad (21)$$

where,

$$t_{dis} = 8\frac{L_m}{M_g}(C_{ds1} + C_{ds2})f_s. \quad (22)$$

$$t_{body(on)} = t_{dead} - t_{dis} + t_{delay(on)}. \quad (23)$$

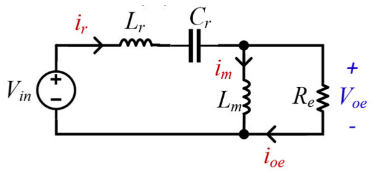

FIGURE 26. LLC resonant converter FHA equivalent circuit model.

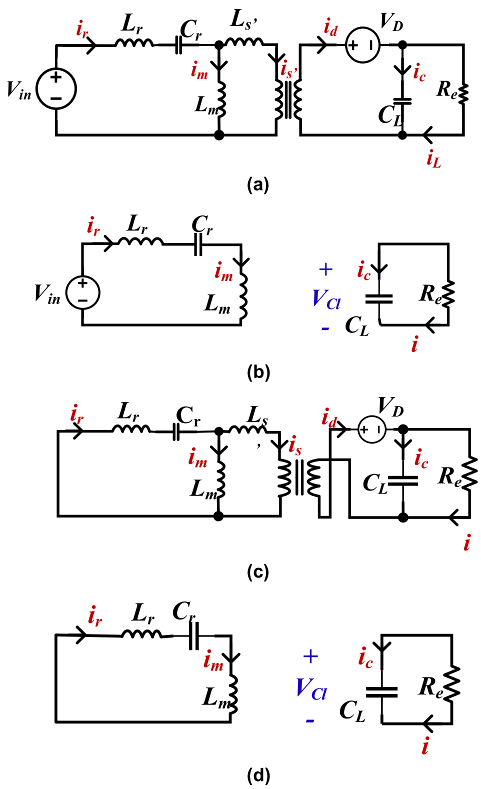

FIGURE 27. LLC resonant converter equivalent circuits under the DCM condition in different states [231], (a) t_0-t_1, (b) t_1-t_2, (c)t_2 -t_3, and (d) t_3-t_4.

c: POWER MOSFET SWITCHING LOSS

Due to the ZVS operation of the converter, the MOSFET turning on switching loss is effectively reduced and ignored, in practice. However, to calculate its turning off switching loss, two assumptions are made to simplify the analysis.

1) Meanwhile the power MOSFET is turning off, its current is near the magnetizing inductor current.

2) The drain-source voltage, as well as the magnetizing inductor current, rising is linear.

$$V_{ds}(\mathrm{t}) = V_{ds(on)} + \frac{V_{in} - V_{ds(on)}}{t_{dis}} t. \tag{24}$$

$$i_{ds}(t) = \frac{nV_o}{L_m}\frac{1}{4f_s}\left(1 - \frac{t}{t_{dis}}\right). \tag{25}$$

$$p_{tf} = 2f_s \int_0^{t_{dis}} v_{ds}(t)\, i_{ds}(t)\, dt = \frac{nV_o t_{dis}\left(V_{in} + 2V_{ds(on)}\right)}{12L_m}. \tag{26}$$

d: POWER MOSFET CONDUCTION LOSS

Each power MOSFET conduction loss is given as follows:

$$P_{r_{ds(on)}} = r_{ds_{on}} I^2_{ds_{rms}} \tag{27}$$

E. ANALYSIS OF THE LLC RESONANT CONVERTER

1) FIRST HARMONIC APPROXIMATION (FHA) ANALYSIS

The first harmonic approximation (FHA) approach is a simple method to analyze the LLC resonant converter, which is made based on the several simplifying assumptions as follows:

1) Only the fundamental harmonics of the input voltage and current waveforms are considered, while all other harmonics are ignored.

2) The output capacitor and all parasitic components of the transformer secondary side are neglected.

3) All components on the transformer secondary side are transferred to the primary side.

By considering these assumptions, the LLC resonant converter equivalent circuit, shown in Fig. 26, can be easily analyzed by using the FHA method [232] as follows [233]:

$$v_{ge}(t) = \frac{2V_{in}}{\pi} \sin(2\pi f_s t). \tag{28}$$

$$V_{ge} = \frac{2V_{in}}{\pi}. \tag{29}$$

$$v_{oe}(t) = \frac{4nV_o}{\pi} \sin(2\pi f_s t - \varphi_v). \tag{30}$$

where, φ_v is the difference phase between V_{oe} and V_{ge}.

$$V_{oe} = \frac{2\sqrt{2}\,n}{\pi} V_o. \tag{31}$$

$$i_{oe}(t) = \frac{\pi I_o}{2n} \sin(2\pi f_s t - \varphi_i). \tag{32}$$

where, φ_i is the difference phase between v_{oe} and i_{oe}.

$$I_{oe} = \frac{\pi}{2\sqrt{2}n} I_o. \tag{33}$$

$$R_e = \frac{V_{oe}}{I_{oe}} = \frac{8n^2}{\pi^2}\frac{V_O}{I_O} = \frac{8n^2}{\pi^2} R_L. \tag{34}$$

$$\omega_s = 2\pi f_s = \omega. \tag{35}$$

$$X_{C_r} = \frac{1}{\omega C_r}, X_{L_r} = \omega L_r, X_{L_m} = \omega L_m. \tag{36}$$

$$I_m = \frac{V_{oe}}{\omega L_m} = \frac{2\sqrt{2}\,n}{\pi \omega L_m} V_o. \tag{37}$$

$$I_r = \sqrt{I_m^2 + I_{oe}^2}. \tag{38}$$

Also, the converter voltage gain is calculated as follows:

$$M_{gDC} = \frac{nV_o}{V_{in}/2} = \frac{nV_o}{V_{DC}/2}. \tag{39}$$

To express the converter normalized voltage gain, some parameters are usually defined as follows:

$$L_n = \frac{L_m}{L_r}, Q = \frac{\sqrt{L_r/C_r}}{R_e}, F = \frac{f_s}{f_{r1}}, F_{oc} = \frac{f_{r2}}{f_{r1}}. \tag{40}$$

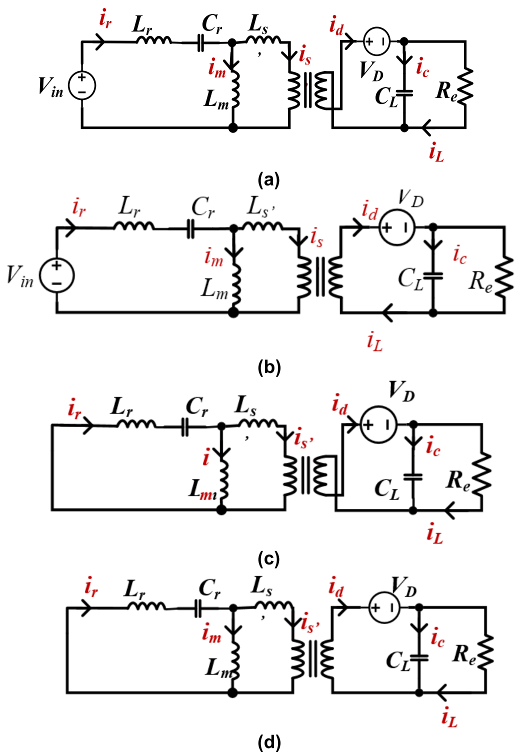

FIGURE 28. LLC resonant converter equivalent circuits under the CCM condition in different states [231], (a) t_0-t_1, (b) t_1-t_2, (c)t_2 -t_3, and (d) t_3-t_4.

$$f_{r1}=\frac{1}{2\pi\sqrt{L_rC_r}},f_{r2}=\frac{1}{2\pi\sqrt{(L_r+L_m)C_r}}. \tag{41}$$

$$M_g=\frac{F^2L_n}{\sqrt{\left[(L_n+1)\,F^2-1\right]^2+\left[F^2-1)FL_nQ\right]^2}}. \tag{42}$$

Here, Q, L_n, F, f_{r1}, f_{r2}, and f_s are the converter quality factor, the resonant inductances ratio, normalized switching frequency, short and open circuited resonant frequencies, and switching frequency, respectively. The resonant converter components are given as follows:

$$C_r=\frac{1}{2\pi f_sR_eQ},L_r=\frac{1}{(2\pi f_s)^2C_r},L_m=L_nL_r. \tag{43}$$

$$\begin{cases} E_{norm,L}=\dfrac{\sum\left(\frac{1}{2}LI^2\right)}{PT_s} \\ =\dfrac{1}{P_{max}}\sum\left(V_{\max S}I_{\max S}+V_{\max D}I_{\max D}\right) \end{cases} \tag{44}$$

F. SPACE STATE ANALYSIS

1) DCM ANALYSIS

The LLC resonant converter is analyzed here in both DCM and CCM operation modes respectively, based on the space state analysis, which is a relatively accurate technique. In this section some assumptions have been considered. $L_s'=n^2L_s$ is transformer secondary side leakage inductor which is transferred to primary side, k is voltage factor, k_i, k_p is integral and proportional factors respectively, V_{Co} is output capacitor voltage, V_{ref} reference voltage.

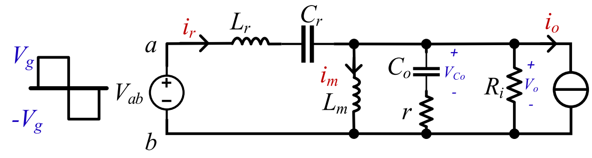

FIGURE 29. LLC resonant converter small-signal model from [236].

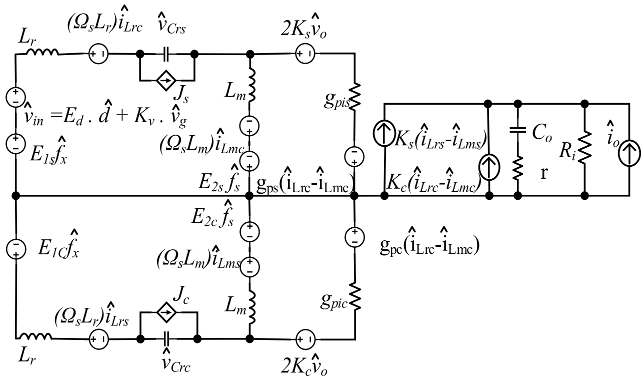

FIGURE 30. LLC resonant converter small-signal model [236].

f_{vco} is Voltage Controlled Oscillator (VCO) center frequency, V_{cr}, C_r voltage, V_D diode voltage drop, α feedback variable, x is state vector $x=[v_{cr}\ i_r i_m\ v_c\ \alpha]^T$ and u is input vector $u=[V_{in}\ V_{ref}]^T$. Therefore, the following equations are obtained [231], [234], [235]:

$$x'=A_nx+B_nu,\quad n=1,2,3,4. \tag{45}$$

$$x'=A_1x+B_1u. \tag{46}$$

There are four operational states, which are shown in Fig. 27. In the first state (t_0-t_1), the circuit equation set is given as follows:

$$A_1=\begin{bmatrix} 0 & 1/C_r & 0 & 0 & 0 \\ \frac{L_{s'}}{L_r^2k_3}-\frac{1}{L_r} & 0 & 0 & 0 & 0 \\ \frac{-L_{s'}}{L_rL_mk_3} & 0 & 0 & 0 & 0 \\ 0 & n/C_l & -n/C_l & 0 & 0 \\ 0 & 0 & 0 & kk_i & 0 \end{bmatrix}. \tag{47}$$

$$B_1=\begin{bmatrix} 0 & 0 \\ \frac{1}{L_r}-\frac{L_{s'}}{L_r^2k_3} & -k_1+\frac{k_1+k_2}{k_3}\frac{L_{s'}}{L_r} \\ \frac{L_{s'}}{L_rL_mk_3} & k_2-\frac{k_1+k_2}{k_3}\frac{L_{s'}}{L_m} \\ 0 & \frac{-1}{kC_lR_l} \\ 0 & -k_i \end{bmatrix}. \tag{48}$$

where,

$$\begin{cases} k_1=\dfrac{n}{L_r}\left(\dfrac{1}{k}+k_{di}\right),k_2=\dfrac{n}{L_m}\left(\dfrac{1}{k}+k_{di}\right), \\ k_3=1+\dfrac{L_{s'}}{L_m}+\dfrac{L_{s'}}{L_r},k_{di}=\dfrac{v_D}{V_{ref}}. \end{cases} \tag{49}$$

Output voltage ripple component is small. So, v_c in di_m/dt, di_r/dt, and dv_c/dt is replaced by V_{ref}/k to enormously reduce complexity of the model without decreasing its accuracy. In the second operational interval, $t_1 - t_2$, the following expressions are obtained, too:

$$x' = A_2x + B_2u. \tag{50}$$

$$A_2 = \begin{bmatrix} 0 & 1/C_r & 0 & 0 & 0 \\ -1/(L_r+L_m) & 0 & 0 & 0 & 0 \\ -1/(L_r+L_m) & 0 & 0 & 0 & 0 \\ 0 & 0 & 0 & 0 & 0 \\ 0 & 0 & 0 & kk_i & 0 \end{bmatrix}. \tag{51}$$

$$B_2 = \begin{bmatrix} 0 & 0 \\ 1/(L_r+L_m) & 0 \\ 1/(L_r+L_m) & 0 \\ 0 & -1/(kC_lR_l) \\ 0 & -k_i \end{bmatrix}. \tag{52}$$

Because of the symmetry, circuit operation in the $t_2 \sim t_4$ subinterval is similar to the $t_0 \sim t_2$ subinterval, but the relations between different states are as follows:

$$x_{t_1} = e^{A_1t_1}x_{t_0} + \int_0^{t_1} e^{A_1(t_1-\sigma)}d\sigma B_1u. \tag{53}$$

$$x_{t_2} = e^{A_2(t_2-t_1)}x_{t_1} + \int_{t_1}^{t_2} e^{A_2(t_2-\sigma)}d\sigma B_2u. \tag{54}$$

Because of the symmetry and linear relation between x_{t_2} and x_{t_0}, their relations could be expressed as follows.

$$x_{t_2} = W_1x_{t_0} + W_2. \tag{55}$$

$$W_1 = \begin{bmatrix} -1 & 0 & 0 & 0 & 0 \\ 0 & -1 & 0 & 0 & 0 \\ 0 & 0 & -1 & 0 & 0 \\ 0 & 0 & 0 & 1 & 0 \\ 0 & 0 & 0 & 0 & 1 \end{bmatrix}, W_2 = \begin{bmatrix} V_{in} \\ 0 \\ 0 \\ 0 \\ 0 \end{bmatrix}. \tag{56}$$

The conditions for the state switching between t_1 and t_2 is as follows:

$$W_3x_{t_1} = W_4x_{t_1}. \tag{57}$$

$$2t_2\left[f_{vco} + k_p\left(W_5x_{t_2} - V_{ref}\right) + W_6x_{t_2}\right] = 1. \tag{58}$$

$$W_3 = \left[0\ 1\ 0\ 0\ 0\right], W_4 = \left[0\ 0\ 1\ 0\ 0\right]. \tag{59}$$

$$W_5 = \left[0\ 0\ 0\ k\ 0\right], W_6 = \left[0\ 0\ 0\ 0\ 1\right]. \tag{60}$$

G. CCM ANALYSIS

Similar to the DCM operation mode, due to the converter symmetrical operation at $t_0 \sim t_2$ to $t_2 \sim t_4$, during these time subintervals the converter has similar space state analyses. Its equivalent circuits are shown in Fig. 28 during the different states. Because, the CCM and DCM analyses are similar, only the equivalent circuits are given and the analyses are ignored.

1) MALL-SIGNAL MODEL

In this section, the LLC resonant converter small-signal model is introducing based on the Extended Describing Functions (EDF). To obtain the small-signal model, certain assumptions are made as follows:

1) The added signal amplitude is very small, and its frequency is much smaller than the switching frequency.
2) All waveforms in the resonant tank are assumed sinusoidal.
3) All switches are considering ideal.

Based on these assumptions, the LLC resonant converter equivalent circuit is modeled as shown in Fig. 29. Here, C_o, r, R_i, and V_{ab} respectively represent the output capacitor and its Equivalent Series Resistance (ESR), load resistance, and the switching network output voltage waveform with an amplitude of V_g [211].

The following equations describe the converter behavior.

$$L_r\frac{di_{L_r}}{dt} + v_{C_r} + L_m\frac{di_{L_m}}{dt} = v_{ab}. \tag{61}$$

$$L_m\frac{di_{L_m}}{dt} = sgn\left(i_{L_r} - i_{L_m}\right)v_o. \tag{62}$$

$$C_r\frac{dv_{C_r}}{dt} = i_{L_r}. \tag{63}$$

$$\left(1 + \frac{r}{R}\right)C_o\frac{dv_{C_o}}{dt} + \frac{1}{R_i}v_{C_o} = \left|i_{L_r} - i_{L_m}\right| + i_o. \tag{64}$$

$$v_o = \frac{rR_i}{r+R_i}\left(\left|i_{L_r} - i_{L_m}\right| + i_o\right) + \frac{R_i}{R_i+r}v_{C_o}. \tag{65}$$

$$i_g = \frac{1}{T}\int_0^T i_{L_r}\frac{v_{ab}(t)}{v_g}dt. \tag{66}$$

Using the FHA simple analytical approach, the following equations describe the converter behavior.

$$i_{L_r} \approx i_{L_{rs}}(t)\sin(\omega_st) + i_{L_{rc}}(t)\cos(\omega_st). \tag{67}$$

$$i_{L_m} \approx i_{L_{ms}}(t)\sin(\omega_st) + i_{L_{mc}}(t)\cos(\omega_st). \tag{68}$$

$$v_{C_r} \approx v_{C_{rs}}(t)\sin(\omega_st) + v_{C_{rc}}(t)\cos(\omega_st). \tag{69}$$

$$\frac{di_{L_r}}{dt} \approx \left(\frac{di_{L_{rs}}}{dt} - \omega_si_{L_{rc}}\right)\sin(\omega_st) + \left(\frac{di_{L_{rc}}}{dt} + \omega_si_{L_{rs}}\right)\cos(\omega_st). \tag{70}$$

$$\frac{di_{L_m}}{dt} \approx \left(\frac{di_{L_{ms}}}{dt} - \omega_si_{L_{mc}}\right)\sin(\omega_st) + \left(\frac{di_{L_{mc}}}{dt} + \omega_si_{L_{ms}}\right)\cos(\omega_st). \tag{71}$$

$$\frac{dv_{C_r}}{dt} \approx \left(\frac{dv_{C_{rs}}}{dt} - \omega_sv_{C_{rc}}\right)\sin(\omega_st) + \left(\frac{dv_{C_{rc}}}{dt} + \omega_sv_{C_{rs}}\right)\cos(\omega_st). \tag{72}$$

Using the EDF approach, the following equations describe the converter behavior. Here, (v_{ab}, $\text{sgn}\left(i_{L_r} - i_{L_m}\right)$, $\left|i_{L_r} - i_{L_m}\right|$, i_g) nonlinear expressions are replaced to the dc components.

$$v_{ab} \approx f_1\left(v_g, d\right)\sin(\omega_st). \tag{73}$$

$$\text{sgn}\left(i_{L_r} - i_{L_m}\right)v_o \approx f_2\left(i_{L_{rs}} - i_{L_{ms}}, v_{co}\right)\sin(\omega_st) + f_3\left(i_{L_{rc}} - i_{L_{mc}}, v_{co}\right)\cos(\omega_st). \tag{74}$$

$$\left|i_{L_r} - i_{L_m}\right| \approx f_4\left(i_{L_{rs}} - i_{L_{ms}}, i_{L_{rc}} - i_{L_{mc}}\right). \tag{75}$$

$$i_g = f_5\left(i_{L_{rs}}, d\right). \tag{76}$$

Relations with f function, called EDF, are obtained by using Fourier transform [211]:

$$f_1\left(v_g, d\right) = \frac{4}{\pi}\sin(\pi d)\, v_g. \tag{77}$$

$$f_2\left(i_{Lrs} - i_{Lms}, v_{co}\right) = \frac{4}{\pi}\frac{i_{Lrs} - i_{Lms}}{i_p} v_{C_o}. \tag{78}$$

$$f_3\left(i_{Lrc} - i_{Lmc}, v_{co}\right) = \frac{4}{\pi}\frac{i_{Lrc} - i_{Lmc}}{i_p} v_{C_o}. \tag{79}$$

$$f_4\left(i_{Lrs} - i_{Lms}, i_{Lrc} - i_{Lmc}\right) = \frac{2}{\pi} i_p. \tag{80}$$

$$f_5\left(i_{Lrs}, d\right) = \frac{2}{\pi} i_{Lrs} \sin(\pi d). \tag{81}$$

$$i_p = \sqrt{(i_{Lrs} - i_{Lms})^2 + (i_{Lrc} - i_{Lmc})^2}. \tag{82}$$

By simplifying the described functions and linearization and approximation of $v_g = V_g + \hat{v}_g, i_o = 0 + \hat{i}_o, \mathrm{d} = \mathrm{D} + \hat{d}$, $\omega_s = \Omega_s + \hat{\omega}_s$, the following relations are achieving.

$$L_r\frac{d\hat{i}_{Lrs}}{dt} = \Omega_s L_r \hat{i}_{Lrs} + E_{1s}\hat{f}_s - \hat{v}_{Crs} - L_m\frac{d\hat{i}_{Lms}}{dt} + \Omega_s L_m \hat{i}_{Lmc} + E_{2s}\hat{f}_s + E_d\hat{d} + K_v\hat{v}_g. \tag{83}$$

$$L_r\frac{d\hat{i}_{Lrc}}{dt} = -\Omega_s L_r \hat{i}_{Lrs} + E_{1c}\hat{f}_s - \hat{v}_{Crs} - L_m\frac{d}{dt}\hat{i}_{Lms} - \Omega_s L_m \hat{i}_{Lmc} - E_{2c}\hat{f}_s. \tag{84}$$

$$L_m\frac{d\hat{i}_{Lms}}{dt} = \Omega_s L_r \hat{i}_{Lmc} + E_{2s}\hat{f}_s + 2K_s\hat{v}_o + g_{pis}\left(\hat{i}_{Lrs} - \hat{i}_{Lms}\right) - g_{ps}\left(\hat{i}_{Lrc} - \hat{i}_{Lmc}\right). \tag{85}$$

$$L_m\frac{d\hat{i}_{Lmc}}{dt} = \Omega_s L_r \hat{i}_{Lms} + E_{2c}\hat{f}_s + 2K_c\hat{v}_o + g_{pic}\left(\hat{i}_{Lrc} - \hat{i}_{Lmc}\right) - g_{pc}\left(\hat{i}_{Lrs} - \hat{i}_{Lms}\right). \tag{86}$$

$$C_r\frac{d\hat{v}_{Crs}}{dt} = \hat{i}_{Lrs} + G_s\hat{v}_{Crc} + J_{1s}\hat{f}_s = \hat{i}_{Lrs} + J_s. \tag{87}$$

$$C_r\frac{d\hat{v}_{Crc}}{dt} = \hat{i}_{Lrc} - G_s\hat{v}_{Crs} - J_{1c}\hat{f}_s = \hat{i}_{Lrc} - J_c. \tag{88}$$

$$C_o = \frac{d\hat{v}_{C_o}}{dt} = \frac{R_i}{R_i + r}\left[K_s\left(\hat{i}_{Lrs} - \hat{i}_{Lms}\right) + K_c\left(\hat{i}_{Lrc} - \hat{i}_{Lmc}\right) + \hat{i}_o\right]. \tag{89}$$

where, $\hat{v}_g, \hat{f}_s, \hat{d}$, and $\hat{i}_o$ are small signal variables. The rectifier network small signal model has been calculated as follows.

$$\hat{v}_o = \frac{rR_i}{R_i + r}\left[K_s\left(\hat{i}_{Lrs} - \hat{i}_{Lms}\right) + K_c\left(\hat{i}_{Lrc} - \hat{i}_{Lmc}\right) + \hat{i}_o\right] + \frac{R_i}{R_i + r}\hat{v}_{C_o}. \tag{90}$$

$$\hat{i}_g = \frac{2}{\pi}\hat{i}_{Lrs}\sin(\pi d). \tag{91}$$

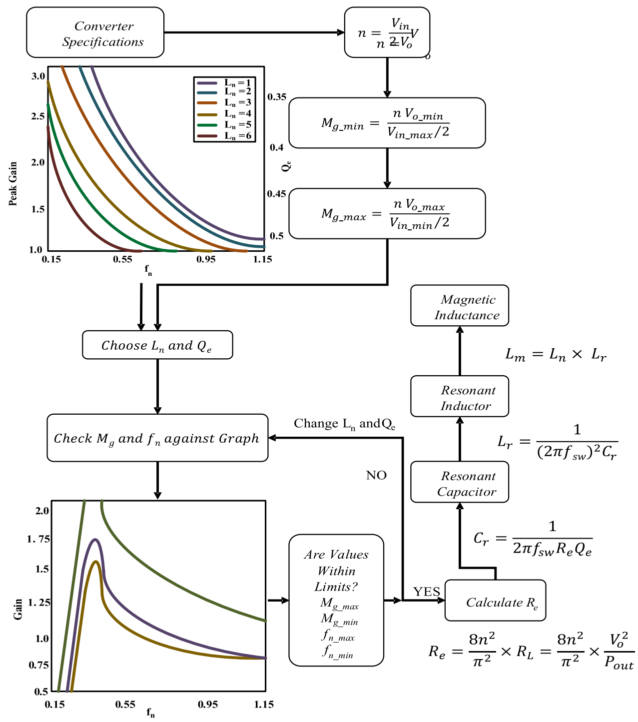

FIGURE 31. Design procedure of conventional LLC resonant converter.

So, the converter small-signal model can be constructed, as shown in Fig. 30.

$$\begin{cases} E_{LN} = \dfrac{(\frac{1}{2}L_r I_{L_r}^2)}{P_{max}T_s} \\ E_{CN} = \dfrac{\frac{1}{2}C_r V_{L_r}^2}{P_{max}T_s} \\ S_N = \dfrac{1}{P_{max}}(V_{MAXS}I_{MAXS} + V_{MAXD}I_{MAXD}) \end{cases}$$
$$C_{relativve} = \frac{n}{P_{max}}(3(V_{MAXS}I_{MAXS}) + V_{MAXD}I_{MAXD}) \tag{92}$$

$$\begin{cases} n = 1 \rightarrow LOW\ nomber\ of\ Components \\ n = 1.25 \rightarrow MEDIUM\ nomber\ of\ Components \\ n = 1.5 \rightarrow HIGH\ nomber\ of\ Components \end{cases} \tag{93}$$

H. LLC RESONANT CONVERTER DESIGN PROCEDURE

Improving the control and design of transformers and other active components in LLC resonant converters can significantly increase overall efficiency. Here are several ways to achieve this:

1) OPTIMIZED CORE DESIGN

Using high-quality magnetic materials and optimizing the core design can reduce core losses, leading to higher efficiency. Techniques such as using amorphous or nanocrystalline cores can help minimize hysteresis and eddy current losses.

2) HIGH-FREQUENCY OPERATION
Operating the converter at higher frequencies can reduce the size and weight of the transformer, as well as decrease the number of turns required, reducing copper losses and improving efficiency.

3) IMPROVED WINDING TECHNIQUES
Employing techniques such as interleaved windings or distributed windings can reduce leakage inductance and improve coupling between windings, leading to better performance and efficiency.

4) ENHANCED COOLING
Efficient cooling techniques, such as using high-thermal conductivity materials or incorporating liquid cooling, can help dissipate heat more effectively, reducing losses and improving efficiency.

5) ADVANCED CONTROL ALGORITHMS
Implementing advanced control algorithms can optimize the operation of the transformer and other active components, reducing losses and improving efficiency under varying load and operating conditions.

6) LOSS MINIMIZATION TECHNIQUES
Utilizing soft-switching techniques, such as zero-voltage switching (ZVS) or zero-current switching (ZCS), can reduce switching losses in active components like switches and diodes, improving overall efficiency.

7) INTEGRATED DESIGN
Integrating the transformer and other active components into a single, compact module can reduce parasitic elements, such as stray inductance and capacitance, improving efficiency and performance.

8) EFFICIENT ISOLATION
Using advanced isolation techniques, such as capacitive or inductive coupling, can improve isolation performance while minimizing losses, enhancing overall efficiency.

By implementing these improvements in the control and design of transformers and other active components, LLC resonant converters can achieve higher efficiency, making them more suitable for a wide range of applications.

Based on the given analyses, a design procedure is outlined as follows for the basic LLC resonant converter topology:

1) Determine the maximum and minimum values of the input and output voltages based on the design specifications.
2) Calculate the transformer turns- ratio, i.e., Np/Ns, using the input and output voltage values, obtained in the previous step.
3) Determine the boundaries for the minimum and maximum voltage gain values, based on the design requirements and constraints.
4) Calculate the required values of Q (quality factor) and L_n (inductances ratio), based on the gain-frequency characteristics of the LLC resonant converter.
5) Finally, calculate the values of the resonant tank components (L_r, L_m, and C_r) using the equations and formulas, derived from the design procedure.

A more detailed illustration of the LLC resonant converter design procedure is given in Fig. 31. This step-by-step process helps to select appropriate components values and to optimize the performance of the LLC resonant converter for the desired application [233].

V. CAMPARISION OF THE LLC RESONANT CONVERTER AND SOME OTHER BASIC POWER ELECTRONIC CONVERTER
Here, the LLC resonant converter and other basic power electronics converters are comparing, in summary. The LLC-based resonant converters offer several advantages, including high efficiency, low switching losses, high frequency operation, high power density, and improved electromagnetic compatibility performance.

The buck converter is a DC-DC step-down converter commonly used for voltage reduction and DC motor speed control. It employs an active switch and a low-pass filter for harmonic elimination [237], [238]. The Flyback converter is an AC-DC or DC-DC converter that shares similarities with a buck-boost converter and provides input-output isolation [239], [240]. The forward converter is a DC-DC converter with a structure similar to the Flyback converter but operates like a buck converter. Unlike the Flyback converter, the power is transferred to the secondary side when its switch is turned on and vice versa [241], [242]. The push-pull converter is a DC-DC converter with two switches that turn on and off in opposite phases, applying a square voltage waveform to the transformer, which supplies the load [243], [244].

The LC series resonant converter is a DC-DC converter, where the input voltage is connected to the switching network. The output square voltage waveform is applied to the LC resonant tank, which eliminates harmonics before passing through the transformer to supply the load. This resonant tank has a maximum voltage at its resonant frequency [245]. The parallel-LC resonant converter is another DC-DC converter similar to the series-LC resonant converter, but with a different resonant tank configuration, including a parallel component. Unlike the series resonant converter, the parallel resonant converter provides a voltage gain higher than unity [215]. The LCC resonant converter is another DC-DC converter similar to the LLC resonant converter, but it incorporates two capacitors in its resonant tank.

In summary, the LLC resonant converter stands out as a promising solution in modern power electronics. While it presents certain challenges and complexities in control and design, ongoing research and development efforts offer opportunities for further improvements. It has gained significant attention and it finds many applications in various domains. Continued advancements in this field will likely lead to enhanced performance, efficiency, and reliability of the LLC resonant converter technology.

As mentioned before, the LLC resonant converter is a powerful DC-DC converter with various advantages. Here, it is comparing to other basic power electronics converters, in summary:

1) ***Buck Converter:***
- **Application:** The buck converter is primarily used for voltage step-down applications, such as in DC-DC converters for powering electronic devices, controlling DC motor speeds, and low-power battery charging where soft switching is not critical.
- **Structure:** It consists of an active switch and a low-pass filter for harmonic elimination [237], [238].

2) ***Flyback Converter:***
- **Application:** The Flyback converter is commonly used in AC-DC and DC-DC converters that require input-output isolation. It is also suitable for low-power WPT systems and applications where high voltage and low current are involved.
- **Structure:**Similar to a buck-boost converter [239], [240].

3) ***Forward Converter:***
- **Application:** Similar to the buck converter but with the additional feature of input-output isolation, the forward converter is suitable for low-power applications requiring isolation, such as low-power battery charging and certain WPT applications, due to its hard-switching nature.
- **Structure:** Similar to the Flyback converter, but power is transferred to the secondary side when the switch is turned on and vice versa [241], [242].

4) ***Push-Pull Converter:***
- **Application:** The push-pull converter utilizes two switches that turn on and off in opposite phases, making it useful for battery charging and some fuel cell applications.
- **Structure:** Applies a square voltage waveform to the transformer, which supplies the load [243], [244].

5) ***Series-LC Resonant Converter:***
- **Application:** The series-LC resonant converter is used as a DC-DC converter with the input voltage connected to the switching network. It is beneficial for WPT and medium-power battery charging applications.
- **Structure:** The output square voltage waveform is applied to the series-LC resonant tank to eliminate harmonics. It has a resonant tank with a maximum unity voltage gain [245].

6) ***Parallel-LC Resonant Converter:***
- **Application:** Similar to the series-LC resonant converter, the parallel-LC resonant converter is advantageous for WPT and medium-power battery charging applications, as well as some medium-voltage direct current (MVDC) applications.

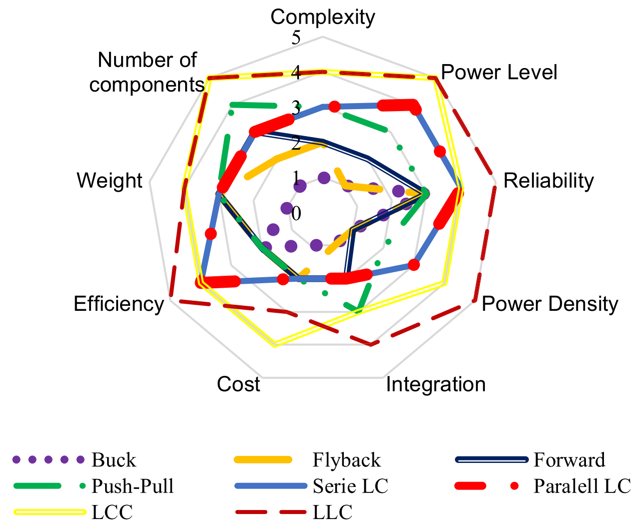

FIGURE 32. Comparsion of some basic and LLC resonant converters.

- **Structure:** Has a different resonant tank configuration with a parallel component, resulting in a voltage gain higher than unity [215].

7) ***LCC Resonant Converter:***
- **Application:** The LCC resonant converter is akin to the LLC resonant converter but is used in a narrower range of power applications, particularly for high voltage and low current applications.
- **Structure**: Similar to the LLC resonant converter but with two capacitors in its resonant tank. Its gain-frequency characteristic is the same as the LLC resonant converter but mirrored along the Y-axis [246], [247].

These different basic converters are comparing in Fig. 32 and Table 8, in detail.

VI. CHALENGES AND FUTURE OPPERTUNITIES

In this section, we delve into the challenges and future opportunities associated with the LLC resonant converter, aiming to provide insights into potential avenues for improvement and innovation in this field. While the LLC resonant converter offers numerous advantages, it also faces certain limitations that need to be addressed for further optimization and enhancement. Below, we outline some of these challenges along with potential pathways for improvement:

A. HIGH INPUT STRESS VOLTAGE

The LLC resonant converter may encounter high voltage stress at the input, leading to voltage spikes and potential reliability issues. To mitigate this challenge, advanced control algorithms and circuit designs can be implemented to regulate the input voltage and minimize stress on the converter components. Additionally, the integration of voltage clamping techniques and transient voltage suppressors can help to limit voltage spikes and ensure stable operation.

TABLE 8. Comparison of Some Basic Converters and LLC Resonant Converter.

Converters \ Features		Simplicity	Low component count	High voltage gain	Isolation	High power density	Low cost	Low EMI noise	Low design and control complexity	Soft Switching
PWM	BUCK	✓	✓	×	×	×	✓	×	✓	×
	FLYBACK	✓	✓	×	✓	×	✓	×	✓	×
	FORWARD	✓	✓	×	✓	×	✓	×	✓	×
	PUSH-PULL	✓	×	✓	✓	✓	×	×	×	×
Resonant	Series LC	✓	✓	×	✓	✓	✓	✓	✓	✓
	Parallel LC	✓	✓	✓	✓	×	✓	✓	✓	✓
	LCC	×	×	✓	✓	×	×	✓	×	✓
	LLC	×	×	✓	✓	✓	×	✓	×	✓

B. TRANSFORMER SECONDARY SIDE CURRENT STRESS

The current stress on the secondary side of the transformer poses a significant challenge and can impact the overall performance of the LLC resonant converter. To address this issue, innovative transformer designs, such as interleaved windings and advanced core materials, can be employed to reduce current stresses and improve efficiency. Moreover, optimizing the transformer design parameters and enhancing thermal management techniques can further alleviate current stress and enhance the converter's reliability.

C. COMPLEXITY OF MULTILEVEL STRUCTURE

LLC resonant converters with multilevel structures often exhibit increased complexity, requiring meticulous design and control methodologies. To simplify the design process and enhance efficiency, innovative topology optimization techniques and advanced control strategies can be employed. Moreover, the integration of modular and scalable architectures can streamline the implementation of multilevel converters, facilitating easier deployment and maintenance in practical applications.

D. LOW EFFICIENCY AT LIGHT LOADS

LLC resonant converters may experience reduced efficiency at light loads, presenting a challenge for applications requiring high efficiency across a wide load range. To improve efficiency under light load conditions, dynamic load adaptation techniques and adaptive control algorithms can be utilized to optimize the converter's operating parameters in real-time. Additionally, the integration of low-power mode operation and energy-saving features can help to minimize power losses and enhance efficiency at light loads.

E. CIRCULATING CURRENT DUE TO PFM CONTROL

The PFM control, while effective in regulating output voltage, can result in increased circulating currents and additional losses, particularly at low load conditions. To mitigate this challenge, innovative control strategies such as hybrid modulation techniques and predictive control algorithms can be employed to minimize circulating currents and optimize converter efficiency. Furthermore, the implementation of advanced current sensing and feedback mechanisms can help to accurately regulate circulating currents and improve overall converter performance.

F. LIMITED INPUT/OUTPUT VOLTAGE RANGE

The efficiency of the LLC resonant converter may decrease outside a certain input/output voltage range, limiting its applicability in diverse operating conditions. To expand the converter's voltage range and enhance versatility, novel voltage scaling techniques and adaptive control schemes can be utilized to optimize performance across a wider range of voltage levels. Additionally, the integration of voltage conversion stages and cascaded converter architectures can extend the operating range of the LLC resonant converter, enabling compatibility with a broader range of applications.

G. INCREASED SWITCHING HARMONICS

As the LLC resonant converter operates, increasing the switching harmonics, leading to potential electromagnetic interference (EMI) issues and performance degradation. To mitigate harmonics and reduce EMI, advanced filtering techniques such as passive LC filters and active power factor correction (PFC) circuits can be implemented. Moreover, innovative modulation schemes and interleaved converter topologies can help to minimize harmonic distortion and improve overall converter efficiency.

In conclusion, while the LLC resonant converter faces certain challenges, there are numerous opportunities for innovation and improvement to overcome these limitations and enhance its performance. By leveraging advanced control algorithms, innovative circuit designs, and optimized component technologies, the LLC resonant converter can achieve higher efficiency, wider voltage range, improved reliability, and enhanced compatibility with various applications. Through ongoing research and development efforts, the LLC resonant converter holds great promise for addressing the evolving needs of modern power electronics and driving advancements in energy conversion technology [13].

VII. CONCLUSION

In conclusion, the LLC resonant converter is a DC-DC power converter that offers numerous advantages, including input/output isolation, step-up and step-down operation, high efficiency and power density, soft-switching, low EMI noise, compatibility with various applications, and the ability to be connected in series or parallel configurations. These advantages have made the LLC resonant converter a popular choice for both home and industrial applications.

Throughout the review, different LLC structures have been examined, and it has been concluded that multilevel converters have the lowest voltage stress on switches and EMI noise. The interleaved boost and LLC resonant converter, on the other hand, demonstrate high efficiency in power factor correction (PFC) applications. Multi-phase converters excel in high voltage and current applications, while bidirectional converters are suitable for battery charging and electric vehicle (EV) industrial applications. Additionally, due to the presence of a transformer and resonant capacitor in the LLC structure, the converter can be modified for wireless power transfer (WPT) applications.

Comparison tables have been provided for each subsection, facilitating a better understanding of the different converters and their characteristics. It has been observed that the LLC resonant converter is strongly influenced by the quality factor, with lower quality factors resulting in higher voltage gain in the gain-frequency characteristic, and vice versa.

The review has covered various aspects of the LLC resonant converter, including its introduction, analysis of soft-switching operation, converter operation and switching, small signal model, FHA model, converter state space analysis, and analysis of component waste. Transformer and other active components have been identified as the most wasteful components, and improving their control can lead to increased efficiency.

Different control approaches have been presented, with pulse frequency modulation (PFM) being the most common. However, PFM control can result in circulating current issues at switching frequencies far from the resonant frequency. Combined control approaches offer better performance but come with their own challenges.

Lastly, the review has highlighted the wide range of applications for the LLC resonant converter, highlighting its versatility and widespread usages.

Overall, the LLC resonant converter is a highly advantageous power converter with significant potential for further improvement and development. Its favorable characteristics make it a favored choice in various industries, and ongoing research aims to enhance its performance and expand its applications.

REFERENCES

[1] M. M. Jovanovic, "Technology drivers and trends in power supplies for computer/telecom," in *Proc. APEC*, 2006.

[2] F. C. Lee, P. Barbosa, P. Xu, J. Zhang, B. Yang, and F. Canales, "Topologies and design considerations for distributed power system applications," *Proc. IEEE*, vol. 89, no. 6, pp. 939–950, Jun. 2001.

[3] R. Dufo-López, J. Krzywanski, and J. Singh, Eds., "Emerging developments in the power and energy industry," in *Proc. 11th Asia–Pacific Power Energy Eng. Conf. (APPEEC)*. Xiamen, China: CRC Press, Oct. 2019.

[4] J. Ma, X. Wei, L. Hu, and J. Zhang, "LED driver based on boost circuit and LLC converter," *IEEE Access*, vol. 6, pp. 49588–49600, 2018.

[5] R. L. Steigerwald, "A review of soft-switching techniques in high performance DC power supplies," in *Proc. 21st Annu. Conf. IEEE Ind. Electron. (IECON)*, Nov. 1995, pp. 1–7.

[6] H.-L. Cheng, Y.-C. Hsieh, and C.-S. Lin, "A novel single-stage high-power-factor AC/DC converter featuring high circuit efficiency," *IEEE Trans. Ind. Electron.*, vol. 58, no. 2, pp. 524–532, Feb. 2011.

[7] J.-W. Yang and H.-L. Do, "Bridgeless SEPIC converter with a ripple-free input current," *IEEE Trans. Power Electron.*, vol. 28, no. 7, pp. 3388–3394, Jul. 2013.

[8] N. S. Hasan, N. Rosmin, D. A. A. Osman, and A. H. Musta'amal, "Reviews on multilevel converter and modulation techniques," *Renew. Sustain. Energy Rev.*, vol. 80, pp. 163–174, Dec. 2017.

[9] W. Chen, F. C. Lee, M. M. Jovanovic, and J. A. Sabate, "A comparative study of a class of full bridge zero-voltage-switched PWM converters," in *Proc. IEEE Appl. Power Electron. Conf. Expo. (APEC)*, Mar. 1995, pp. 893–899.

[10] X. Ruan and Y. Yan, "Soft-switching techniques for PWM full bridge converters," in *Proc. IEEE 31st Annu. Power Electron. Specialists Conf.*, Jun. 2000, pp. 634–639.

[11] J.-G. Cho, J. A. Sabate, G. Hua, and F. C. Lee, "Zero-voltage and zero-current-switching full bridge PWM converter for high-power applications," *IEEE Trans. Power Electron.*, vol. 11, no. 4, pp. 622–628, Jul. 1996.

[12] R. Beiranvand, B. Rashidian, M. R. Zolghadri, and S. M. H. Alavi, "Using LLC resonant converter for designing wide-range voltage source," *IEEE Trans. Ind. Electron.*, vol. 58, no. 5, pp. 1746–1756, May 2011.

[13] J. Zeng, G. Zhang, S. S. Yu, B. Zhang, and Y. Zhang, "LLC resonant converter topologies and industrial applications—A review," *Chin. J. Electr. Eng.*, vol. 6, no. 3, pp. 73–84, Sep. 2020.

[14] G. Huang, A. Zhang, and Y. Gu, "LLC series resonant DC-to-DC converter," in *Proc. DPEC Seminar*, 2002.

[15] B. Yang, "Topology investigation for front end DC/DC power conversion for distributed power system," Ph.D. dissertation, Virginia Polytech. Inst. State Univ., 2003.

[16] T. Mohamed, A. Becetti, and S. Bayhan, "Design and analysis of full bridge LLC resonant converter for wireless power transfer applications," in *Proc. IEEE 12th Int. Conf. Compat., Power Electron. Power Eng. (CPE-POWERENG)*, Apr. 2018, pp. 1–5, doi: 10.1109/CPE.2018.8372606.

[17] K. Yi, "Capacitive coupling wireless power transfer with quasi-LLC resonant converter using electric vehicles' windows," *Electronics*, vol. 9, no. 4, p. 676, Apr. 2020.

[18] D. Rozario, N. A. Azeez, and S. S. Williamson, "A modified resonant converter for wireless capacitive power transfer systems used in battery charging applications," in *Proc. IEEE Transp. Electrific. Conf. Expo (ITEC)*, Jun. 2016, pp. 1–6, doi: 10.1109/ITEC.2016.7520272.

[19] B. Pakhaliuk, O. Husev, V. Shevchenko, J. Zakis, K. Maksym, and R. Strzelecki, "Modified inductive multicoil wireless power transfer approach based on Z-source network," *IEEE J. Emerg. Sel. Topics Power Electron.*, vol. 9, no. 4, pp. 4906–4917, Aug. 2021.

[20] K. Sirivennela and M. Sujith, "Wireless power transfer using resonant converters for defence application," in *Proc. 4th Int. Conf. Inventive Syst. Control (ICISC)*, Jan. 2020, pp. 353–358.

[21] Y.-C. Hsieh, C.-W. Chu, H.-W. Chang, and C.-Y. Lin, "Inductive power transfer converter with center-tapped pickup winding," *IEEE Trans. Power Electron.*, vol. 36, no. 11, pp. 12432–12439, Nov. 2021.

[22] Y. Yao, Y. Wang, X. Liu, H. Cheng, M. Liu, and D. Xu, "Analysis, design, and implementation of a wireless power and data transmission system using capacitive coupling and double-sided LCC compensation topology," *IEEE Trans. Ind. Appl.*, vol. 55, no. 1, pp. 541–551, Jan. 2019, doi: 10.1109/TIA.2018.2869120.

[23] J. Dai and D. C. Ludois, "Capacitive power transfer through a conformal bumper for electric vehicle charging," *IEEE J. Emerg. Sel. Topics Power Electron.*, vol. 4, no. 3, pp. 1015–1025, Sep. 2016.

[24] S. Sinha, B. Regensburger, K. Doubleday, A. Kumar, S. Pervaiz, and K. K. Afridi, "High-power-transfer-density capacitive wireless power transfer system for electric vehicle charging," in *Proc. IEEE Energy Convers. Congr. Expo. (ECCE)*, Oct. 2017, pp. 967–974.

[25] H. Zhang, F. Lu, H. Hofmann, W. Liu, and C. C. Mi, "A four-plate compact capacitive coupler design and LCL-compensated topology for capacitive power transfer in electric vehicle charging application," *IEEE Trans. Power Electron.*, vol. 31, no. 12, pp. 8541–8551, Dec. 2016.

[26] B. Regensburger, J. Estrada, A. Kumar, S. Sinha, Z. Popovic, and K. K. Afridi, "High-performance capacitive wireless power transfer system for electric vehicle charging with enhanced coupling plate design," in *Proc. IEEE Energy Convers. Congr. Expo. (ECCE)*, Sep. 2018, pp. 2472–2477.

[27] E. Abramov, I. Zeltser, and M. M. Peretz, "A network-based approach for modeling resonant capacitive wireless power transfer systems," *CPSS Trans. Power Electron. Appl.*, vol. 4, no. 1, pp. 19–29, Mar. 2019.

[28] F. Lu, H. Zhang, and C. Mi, "A two-plate capacitive wireless power transfer system for electric vehicle charging applications," *IEEE Trans. Power Electron.*, vol. 33, no. 2, pp. 964–969, Feb. 2018.

[29] M. P. Theodoridis, "Effective capacitive power transfer," *IEEE Trans. Power Electron.*, vol. 27, no. 12, pp. 4906–4913, Dec. 2012.

[30] F. Corti, A. Reatti, Y.-H. Wu, D. Czarkowski, and S. Musumeci, "Zero voltage switching condition in class-E inverter for capacitive wireless power transfer applications," *Energies*, vol. 14, no. 4, p. 911, Feb. 2021.

[31] Y. Bezawada and Y. Zhang, "A case study: Influence of circuit impedance on the performance of class-E2 resonant power converter for capacitive wireless power transfer," *Electronics*, vol. 10, no. 12, p. 1461, Jun. 2021.

[32] K.-W. Kim, Y. Jeong, J.-S. Kim, and G.-W. Moon, "Low common-mode noise LLC resonant converter with static-point-connected transformer," *IEEE Trans. Power Electron.*, vol. 36, no. 1, pp. 401–408, Jan. 2021.

[33] T. Yamamoto, Y. Konno, K. Sugimura, T. Sato, Y. Bu, and T. Mizuno, "Loss reduction of LLC resonant converter using magnetocoated wire," *IEEJ J. Ind. Appl.*, vol. 8, no. 1, pp. 51–56, 2019.

[34] S. Gao and Z. Zhao, "Magnetic integrated LLC resonant converter based on independent inductance winding," *IEEE Access*, vol. 9, pp. 660–672, 2021.

[35] M. Noah, T. Shirakawa, K. Umetani, J. Imaoka, M. Yamamoto, and E. Hiraki, "Effects of secondary leakage inductance on the LLC resonant converter," *IEEE Trans. Power Electron.*, vol. 35, no. 1, pp. 835–852, Jan. 2020.

[36] T. Yamamoto, Y. Bu, T. Mizuno, Y. Yamaguchi, and T. Kano, "Loss reduction of transformer for LLC resonant converter using a magnetoplated wire," *IEEJ J. Ind. Appl.*, vol. 7, no. 1, pp. 43–48, 2018.

[37] S. A. Ansari, J. N. Davidson, and M. P. Foster, "Analysis, design and modelling of two fully-integrated transformers with segmental magnetic shunt for LLC resonant converters," in *Proc. 46th Annu. Conf. IEEE Ind. Electron. Soc. (IECON)*, Oct. 2020, pp. 1273–1278.

[38] Z. Zhao, Q. Xu, Y. Dai, and H. Yin, "Analysis, design, and implementation of improved LLC resonant transformer for efficiency enhancement," *Energies*, vol. 11, no. 12, p. 3288, Nov. 2018.

[39] T. Ou, M. Noah, K. Morita, M. Tsuruya, S. Namiki, J. Imaoka, and M. Yamamoto, "A novel transformer structure used in a 1.4 MHz LLC resonant converter with GaNFETs," in *Proc. IEEE Int. Power Electron. Appl. Conf. Expo. (PEAC)*, Nov. 2018, pp. 1–5.

[40] M. Noah, S. Kimura, S. Endo, M. Yamamoto, J. Imaoka, K. Umetani, and W. Martinez, "A novel three-phase LLC resonant converter with integrated magnetics for lower turn-off losses and higher power density," in *Proc. IEEE Appl. Power Electron. Conf. Expo. (APEC)*, Mar. 2017, pp. 322–329.

[41] E.-S. Kim, S.-M. Lee, S. Phum, B.-G. Chung, and K.-H. Lee, "A novel planar transformer for low profile LLC resonant converter," in *Proc. 27th Annu. IEEE Appl. Power Electron. Conf. Expo. (APEC)*, Feb. 2012, pp. 2234–2239.

[42] S. Yang, S. Abe, and M. Shoyama, "Design consideration of flat transformer in LLC resonant converter for low core loss," in *Proc. Int. Power Electron. Conf. (ECCE ASIA)*, Jun. 2010, pp. 343–348.

[43] R. Chen, P. Brohlin, and D. Dapkus, "Design and magnetics optimization of LLC resonant converter with GaN," in *Proc. IEEE Appl. Power Electron. Conf. Expo. (APEC)*, Mar. 2017, pp. 94–98.

[44] H. G. Han, Y. J. Choi, S. Y. Choi, and R. Y. Kim, "A high efficiency LLC resonant converter with wide ranged output voltage using adaptive turn ratio scheme for a Li-ion battery charger," in *Proc. IEEE Vehicle Power Propulsion Conf. (VPPC)*, Oct. 2016, pp. 1–6, doi: 10.1109/VPPC.2016.7791570.

[45] B.-R. Lin and C.-X. Dai, "Wide voltage resonant converter using a variable winding turns ratio," *Electronics*, vol. 9, no. 2, p. 370, Feb. 2020.

[46] E. Rong, S. Li, R. Zhang, X. Du, Q. Min, and S. Lu, "A magnetic integration half-turn planar transformer for LLC resonant DC–DC converters," in *Proc. IEEE Appl. Power Electron. Conf. Expo. (APEC)*, Mar. 2018, pp. 484–488.

[47] D. Shu and H. Wang, "An ultrawide output range *LLC* resonant converter based on adjustable turns ratio transformer and reconfigurable bridge," *IEEE Trans. Ind. Electron.*, vol. 68, no. 8, pp. 7115–7124, Aug. 2021.

[48] H. Hu, X. Fang, F. Chen, Z. J. Shen, and I. Batarseh, "A modified high-efficiency LLC converter with two transformers for wide input-voltage range applications," *IEEE Trans. Power Electron.*, vol. 28, no. 4, pp. 1946–1960, Apr. 2013, doi: 10.1109/TPEL.2012.2201959.

[49] G. M. Leandro and I. Barbi, "DC–DC hybrid switched-capacitor LLC resonant converter: All switches with VDS = Vin/2," in *Proc. IEEE PES Innov. Smart Grid Technol. Conf.*, Sep. 2019, pp. 1–6, doi: 10.1109/ISGT-LA.2019.8895343.

[50] Z. Hu, Y. Qiu, L. Wang, and Y.-F. Liu, "An interleaved LLC resonant converter operating at constant switching frequency," *IEEE Trans. Power Electron.*, vol. 29, no. 6, pp. 2931–2943, Jun. 2014.

[51] R. Suryadevara and L. Parsa, "FB-ZCS DC–DC converter with dual-capacitor resonant circuit for renewable energy integration with MVDC grids," *IEEE Trans. Ind. Appl.*, vol. 56, no. 6, pp. 6792–6802, Nov. 2020.

[52] V. S. Costa, M. S. Perdigão, A. S. Mendes, and J. M. Alonso, "Evaluation of a variable-inductor-controlled LLC resonant converter for battery charging applications," in *Proc. 42nd Annu. Conf. IEEE Ind. Electron. Soc.*, Oct. 2020, pp. 5633–5638, doi: 10.1109/IECON.2016.7793916.

[53] Y. Wei, Q. Luo, Z. Wang, L. Wang, J. Wang, and J. Chen, "Design of LLC resonant converter with magnetic control for LEV application," in *Proc. IEEE 10th Int. Symp. Power Electron. Distrib. Gener. Syst. (PEDG)*, Jun. 2019, pp. 857–862.

[54] Y. Wei, Q. Luo, X. Du, N. Altin, J. M. Alonso, and H. A. Mantooth, "Analysis and design of the LLC resonant converter with variable inductor control based on time-domain analysis," *IEEE Trans. Ind. Electron.*, vol. 67, no. 7, pp. 5432–5443, Jul. 2020.

[55] C. Li, H. Wang, and M. Shang, "A five-switch bridge based reconfigurable LLC converter for deeply depleted PEV charging applications," *IEEE Trans. Power Electron.*, vol. 34, no. 5, pp. 4031–4035, May 2019, doi: 10.1109/TPEL.2018.2875058.

[56] L. F. Pacheco, K. C. M. Nascimento, and I. Barbi, "Isolated AC/AC converter with LLC resonant converter high-frequency link and four-quadrant switches in the output stage," *IEEE Access*, vol. 8, pp. 213104–213114, 2020.

[57] K. Colak, E. Asa, M. Bojarski, and D. Czarkowski, "A novel LLC resonant converter with semi bridgeless active rectifier," in *Proc. IEEE Transp. Electrific. Conf. Expo (ITEC)*, Jun. 2014, pp. 1–6.

[58] H. Wu, C. Wan, K. Sun, and Y. Xing, "A high step-down multiple output converter with wide input voltage range based on quasi two-stage architecture and dual-output LLC resonant converter," *IEEE Trans. Power Electron.*, vol. 30, no. 4, pp. 1793–1796, Apr. 2015, doi: 10.1109/TPEL.2014.2349917.

[59] K. Jin and X. Ruan, "Hybrid full-bridge three-level LLC resonant converter—A novel DC–DC converter suitable for fuel-cell power system," *IEEE Trans. Ind. Electron.*, vol. 53, no. 5, pp. 1492–1503, Oct. 2006, doi: 10.1109/TIE.2006.882020.

[60] X. Sun, Y. Shen, Y. Zhu, and X. Guo, "Interleaved boost-integrated LLC resonant converter with fixed-frequency PWM control for renewable energy generation applications," *IEEE Trans. Power Electron.*, vol. 30, no. 8, pp. 4312–4326, Aug. 2015.

[61] M. Feizi and R. Beiranvand, "A high-power high-frequency self-balanced battery charger for lithium-ion batteries energy storage systems," *J. Energy Storage*, vol. 41, Sep. 2021, Art. no. 102886.

[62] M. Feizi and R. Beiranvand, "Simulation of a high power self-equalized battery charger using voltage multiplier and phase-shifted full bridge converter for lithium-ion batteries," in *Proc. 11th Power Electron., Drive Syst., Technol. Conf. (PEDSTC)*, Feb. 2020, pp. 1–6.

[63] S.-H. Cho, C.-S. Kim, and S.-K. Han, "High-efficiency and low-cost tightly regulated dual-output *LLC* resonant converter," *IEEE Trans. Ind. Electron.*, vol. 59, no. 7, pp. 2982–2991, Jul. 2012.

[64] M. Shang and H. Wang, "LLC converter with reconfigurable voltage multiplier rectifier for high voltage and wide output range applications," in *Proc. 43rd Annu. Conf. IEEE Ind. Electron. Soc. (IECON)*, Oct. 2017, pp. 1279–1285.

[65] M. Shang, H. Wang, and Q. Cao, "Reconfigurable LLC topology with squeezed frequency span for high-voltage bus-based photovoltaic systems," *IEEE Trans. Power Electron.*, vol. 33, no. 5, pp. 3688–3692, May 2018.

[66] X. Sun, Y. Shen, W. Li, and H. Wu, "A PWM and PFM hybrid modulated three-port converter for a standalone PV/battery power system," *IEEE J. Emerg. Sel. Topics Power Electron.*, vol. 3, no. 4, pp. 984–1000, Dec. 2015.

[67] M. Abbasi, R. Emamalipour, M. A. M. Cheema, and J. Lam, "A constant-frequency high-voltage gain resonant converter module with semiactive phase-shifted voltage multiplier for MVDC distribution," *IEEE J. Emerg. Sel. Topics Power Electron.*, vol. 10, no. 4, pp. 3603–3616, Aug. 2022.

[68] J.-Y. Lee, Y.-S. Jeong, and B.-M. Han, "An isolated DC/DC converter using high-frequency unregulated *LLC* resonant converter for fuel cell applications," *IEEE Trans. Ind. Electron.*, vol. 58, no. 7, pp. 2926–2934, Jul. 2011.

[69] Y. Wei, Q. Luo, J. Chen, and H. Alan Mantooth, "Analysis and design of LLC resonant converter with variable magnetising inductance control," *IET Power Electron.*, vol. 13, no. 16, pp. 3528–3536, Dec. 2020.

[70] Y. Wei, Q. Luo, X. Du, N. Altin, A. Nasiri, and J. M. Alonso, "A dual half-bridge LLC resonant converter with magnetic control for battery charger application," *IEEE Trans. Power Electron.*, vol. 35, no. 2, pp. 2196–2207, Feb. 2020, doi: 10.1109/TPEL.2019.2922991.

[71] Y. Wei, Q. Luo, D. Woldegiorgis, and A. Mantooth, "Multiple-output LLC resonant converter with magnetic control," in *Proc. IEEE Energy Convers. Congr. Expo. (ECCE)*, Oct. 2020, pp. 1204–1209.

[72] E. Orietti, P. Mattavelli, G. Spiazzi, C. Adragna, and G. Gattavari, "Two-phase interleaved LLC resonant converter with current-controlled inductor," in *Proc. Brazilian Power Electron. Conf.*, Sep. 2009, pp. 298–304.

[73] I. Kolberg, D. Shmilovitz, and S. S. Ben-Yaakov, "Ceramic capacitor controlled resonant LLC converters," in *Proc. IEEE Appl. Power Electron. Conf. Expo. (APEC)*, Mar. 2018, pp. 2162–2167.

[74] D.-H. Kim, M.-S. Kim, S. Hussain Nengroo, C.-H. Kim, and H.-J. Kim, "LLC resonant converter for LEV (light electric vehicle) fast chargers," *Electronics*, vol. 8, no. 3, p. 362, Mar. 2019.

[75] Q. Zhou, Y. Liu, Z. Li, and Z. He, "A coupled-inductor interleaved LLC resonant converter for wide operation range," *Energies*, vol. 15, no. 1, p. 315, Jan. 2022.

[76] H. Jing, J. Wang, Z. Fang, and L. Xie, "LLC resonant converter with damping split inductor improving light-load regulation ability," *IEEE Trans. Veh. Technol.*, vol. 69, no. 2, pp. 1428–1439, Feb. 2020.

[77] Z. Chen, S. Liu, and L. Shi, "A soft switching full bridge converter with reduced parasitic oscillation in a wide load range," *IEEE Trans. Power Electron.*, vol. 29, no. 2, pp. 801–811, Feb. 2014.

[78] B.-Y. Choi, S.-R. Lee, J.-W. Kang, W.-S. Jeong, and C.-Y. Won, "A novel dual integrated LLC resonant converter using various switching patterns for a wide output voltage range battery charger," *Electronics*, vol. 8, no. 7, p. 759, Jul. 2019.

[79] E.-S. Kim, B.-G. Chung, S.-I. Kang, I.-S. Cha, and M.-H. Kye, "A novel topology of secondary LLC series resonant converter," in *Proc. 22nd Annu. IEEE Appl. Power Electron. Conf. Expo. (APEC)*, Mar. 2007, pp. 1625–1629.

[80] J. Oh, J. Lee, M. Kim, S. Yoo, E. Kim, Y. Jeon, and Y. Kook, "A 3-bridge LLC resonant converter operating with a wide output voltage control range using morphing control for mode transitions," in *Proc. IEEE Applied Power Electronics Conference and Exposition (APEC)*, Mar. 2019, pp. 2300–2304, doi: 10.1109/APEC.2019.8721889.

[81] F. Alaql and I. Batarseh, "LLC resonant converter with reconfigurable voltage rectifier for wide input voltage applications," in *Proc. IEEE Energy Convers. Congr. Expo. (ECCE)*, Oct. 2020, pp. 1191–1196, doi: 10.1109/ECCE44975.2020.9235896.

[82] F. Alaql, K. Alluhaybi, and I. Batarseh, "A wide input voltage range LLC converter with multi-mode operations," in *Proc. IEEE 9th Int. Power Electron. Motion Control Conf. (IPEMC-ECCE Asia)*, Nov. 2020, pp. 1710–1715.

[83] H.-D. Gui, Z. Zhang, X.-F. He, and Y.-F. Liu, "A high voltage-gain LLC micro-converter with high efficiency in wide input range for PV applications," in *Proc. IEEE Appl. Power Electron. Conf. Expo. (APEC)*, Mar. 2014, pp. 637–642.

[84] M. Shang and H. Wang, "A voltage quadrupler rectifier based pulsewidth modulated LLC converter with wide output range," *IEEE Trans. Ind. Appl.*, vol. 54, no. 6, pp. 6159–6168, Nov. 2018.

[85] N. A. Samsudin and D. Ishak, "Full-bridge LLC resonant high-voltage DC–DC converter with hybrid symmetrical voltage multiplier," *IETE J. Res.*, vol. 67, no. 5, pp. 687–698, Sep. 2021.

[86] X. Sun, X. Li, Y. Shen, B. Wang, and X. Guo, "Dual-bridge LLC resonant converter with fixed-frequency PWM control for wide input applications," *IEEE Trans. Power Electron.*, vol. 32, no. 1, pp. 69–80, Jan. 2017.

[87] T. Jiang, Q. Lin, J. Zhang, and Y. Wang, "A novel ZVS and ZCS three-port LLC resonant converter for renewable energy systems," in *Proc. IEEE Energy Convers. Congr. Expo. (ECCE)*, Sep. 2014, pp. 2296–2302.

[88] I.-O. Lee and G.-W. Moon, "Analysis and design of a three-level LLC series resonant converter for high- and wide-input-voltage applications," *IEEE Trans. Power Electron.*, vol. 27, no. 6, pp. 2966–2979, Jun. 2012, doi: 10.1109/TPEL.2011.2174381.

[89] I.-O. Lee, S.-Y. Cho, and G.-W. Moon, "Three-level resonant converter with double *LLC* resonant tanks for high-input-voltage applications," *IEEE Trans. Ind. Electron.*, vol. 59, no. 9, pp. 3450–3463, Sep. 2012, doi: 10.1109/TIE.2011.2170397.

[90] Y. Yuan and X. Mei, "Five-level LLC resonant converter suitable for wide output voltage range," *Electron. Lett.*, vol. 54, no. 20, pp. 1187–1189, Oct. 2018, doi: 10.1049/el.2018.6266.

[91] S. Alatai, M. Salem, D. Ishak, M. Kamarol, M. Jamil, and A. Bughneda, "Design and analysis of five-level cascaded LLC resonant converter," in *Proc. IEEE Int. Conf. Power Energy (PECon)*, Dec. 2020, pp. 66–70.

[92] M. Salem, V. K. Ramachandaramurthy, P. Sanjeevikumar, Z. Leonowicz, and V. Yaramasu, "Full bridge LLC resonant three-phase interleaved multi converter for HV applications," in *Proc. EEE Int. Conf. Environ. Elect. Eng.*, Jun. 2019, pp. 1–6, doi: 10.1109/EEEIC.2019.8783795.

[93] H.-N. Vu and W. Choi, "A novel dual full-bridge LLC resonant converter for CC and CV charges of batteries for electric vehicles," *IEEE Trans. Ind. Electron.*, vol. 65, no. 3, pp. 2212–2225, Mar. 2018.

[94] M. Abbasi, R. Emamalipour, M. A. M. Cheema, and J. Lam, "A new fully magnetically coupled SiC-based DC/DC step-up LLC resonant converter with inherent balanced voltage sharing for renewable energy systems with a medium voltage DC grid," in *Proc. IEEE Energy Convers. Congr. Expo. (ECCE)*, Sep. 2019, pp. 5542–5547.

[95] W. Sun, Y. Xing, H. Wu, and J. Ding, "Modified high-efficiency LLC converters with two split resonant branches for wide input-voltage range applications," *IEEE Trans. Power Electron.*, vol. 33, no. 9, pp. 7867–7879, Sep. 2018.

[96] Y. Shen, W. Zhao, Z. Chen, and C. Cai, "Full-bridge LLC resonant converter with series-parallel connected transformers for electric vehicle on-board charger," *IEEE Access*, vol. 6, pp. 13490–13500, 2018.

[97] Y. Dong, Y. Wang, F. Wang, and S. Wang, "Zero input current ripple LLC resonant converter with integrated interleaved boost converter," in *Proc. IEEE Int. Conf. Comput. Sci., Electron. Inf. Eng. Intell. Control Technol. (CEI)*, Sep. 2021, pp. 602–606.

[98] B.-R. Lin and K.-W. Wang, "Interleaved soft switching resonant converter with a small input ripple current," *Int. J. Electron.*, vol. 107, no. 4, pp. 644–658, Apr. 2020.

[99] B. Lin and Y. Lin, "Parallel current-fed resonant converter with balance current sharing and no input ripple current," *IET Power Electron.*, vol. 12, no. 2, pp. 212–219, Feb. 2019.

[100] P. Jia and Y. Mei, "Derivation and analysis of a secondary-side LLC resonant converter for the high step-up applications," *IEEE J. Emerg. Sel. Topics Power Electron.*, vol. 9, no. 5, pp. 5865–5882, Oct. 2021.

[101] D. Amani, R. Beiranvand, and M. Zolghadri, "A new high step-up interleaved LLC converter," in *Proc. 12th Power Electron., Drive Syst., Technol. Conf. (PEDSTC)*, Feb. 2021, pp. 1–6.

[102] D. Amani, R. Beiranvand, M. Zolghadri, and F. Blaabjerg, "A high step-up interleaved current-fed resonant converter for high-voltage applications," *IEEE Access*, vol. 10, pp. 105387–105403, 2022.

[103] J. Wu, D. Liu, Y. Wang, and Z. Chen, "Three-level LLC resonant converter with structure-reconfigurable control," in *Proc. IEEE 21st Workshop Control Model. Power Electron. (COMPEL)*, Nov. 2020, pp. 1–6.

[104] W. Chen, Y. Gu, and Z. Lu, "A novel three level full bridge resonant DC–DC converter suitable for high power wide range input applications," in *Proc. 22nd Annu. IEEE Appl. Power Electron. Conf. Expo. (APEC)*, Mar. 2007, pp. 373–379.

[105] J. Z. Liu, Y. Zhao, P. Hu, and T. T. Chen, "Analysis and design of three-level full-bridge LLC resonant converter based on pulse frequency modulation," *IOP Conf. Ser., Earth Environ. Sci.*, vol. 701, no. 1, Mar. 2021, Art. no. 012034.

[106] F. Canales, T. H. Li, and D. Aggeler, "Novel modulation method of a three-level isolated full-bridge LLC resonant DC–DC converter for wide-output voltage application," in *Proc. 15th Int. Power Electron. Motion Control Conf. (EPE/PEMC)*, Sep. 2012, pp. DS2b.11-1–DS2b.11-7.

[107] Y. Gu, Z. Lu, L. Hang, Z. Qian, and G. Huang, "Three-level LLC series resonant DC/DC converter," *IEEE Trans. Power Electron.*, vol. 20, no. 4, pp. 781–789, Jul. 2005, doi: 10.1109/TPEL.2005.850921.

[108] Y. Wei, Q. Luo, and A. Mantooth, "A hybrid half-bridge LLC resonant converter and phase shifted full-bridge converter for high step-up application," in *Proc. IEEE Workshop Wide Bandgap Power Devices Appl. Asia (WiPDA Asia)*, Sep. 2020, pp. 1–6.

[109] B.-C. Kim, K.-B. Park, and G.-W. Moon, "Analysis and design of two-phase interleaved LLC resonant converter considering load sharing," in *Proc. IEEE Energy Convers. Congr. Expo.*, Sep. 2009, pp. 1141–1144.

[110] M. Noah, K. Umetani, J. Imaoka, and M. Yamamoto, "Lagrangian dynamics model and practical implementation of an integrated transformer in multi-phase LLC resonant converter," *IET Power Electron.*, vol. 11, no. 2, pp. 339–347, Feb. 2018.

[111] Y. Yang, J. Yao, H. Li, and J. Zhao, "A novel current sharing method by grouping transformer's secondary windings for a multiphase LLC resonant converter," *IEEE Trans. Power Electron.*, vol. 35, no. 5, pp. 4877–4890, May 2020.

[112] T. Yu, X. Chen, and D. Wu, "A novel LLC resonant converter circuit-input parallel output series subside resonant LLC resonant converter," *J. Phys., Conf. Ser.*, vol. 1449, no. 1, Jan. 2020, Art. no. 012009.

[113] K.-H. Yi and G.-W. Moon, "Novel two-phase interleaved LLC series-resonant converter using a phase of the resonant capacitor," *IEEE Trans. Ind. Electron.*, vol. 56, no. 5, pp. 1815–1819, May 2009.

[114] C. Liu, H. Liu, G. Cai, S. Cui, H. Liu, and H. Yao, "Novel hybrid LLC resonant and DAB linear DC–DC converter: Average model and experimental verification," *IEEE Trans. Ind. Electron.*, vol. 64, no. 9, pp. 6970–6978, Sep. 2017.

[115] K. Yu, J. Du, and H. Ma, "A novel current sharing method for multi-module LLC resonant converters," in *Proc. IECON - 43rd Annu. Conf. IEEE Ind. Electron. Soc.*, Oct. 2017, pp. 613–618.

[116] K.-H. Yi, B.-C. Kim, and G.-W. Moon, "A simple and novel two phase interleaved LLC series resonant converter employing a phase of the resonant capacitor," in *Proc. IEEE Energy Convers. Congr. Expo.*, Sep. 2009, pp. 754–757.

[117] A. Mustafa and S. Mekhilef, "Dual phase LLC resonant converter with variable frequency zero circulating current phase-shift modulation for wide input voltage range applications," *IEEE Trans. Power Electron.*, vol. 36, no. 3, pp. 2793–2807, Mar. 2021.

[118] C. Li and H. Wang, "A wide gain range LLC resonant converter based on reconfigurable bridge and asymmetric resonant tanks," in *Proc. IEEE Appl. Power Electron. Conf. Expo. (APEC)*, Mar. 2019, pp. 3281–3286.

[119] H. Wang, Y. Chen, Y.-F. Liu, and P. C. Sen, "A general multi-phase coupled-resonant-tank resonant converter," in *Proc. IEEE Appl. Power Electron. Conf. Expo. (APEC)*, Mar. 2018, pp. 2183–2190.

[120] Y. Tada, M. Uno, and Y. Sato, "Three-phase interleaved LLC asymmetric resonant converter with capacitive current balancing and reduced switch voltage stress," *IEEE Access*, vol. 8, pp. 5688–5698, 2020.

[121] M. Sato, R. Takiguchi, J. Imaoka, and M. Shoyama, "A novel secondary PWM-controlled interleaved LLC resonant converter for load current sharing," in *Proc. IEEE 8th Int. Power Electron. Motion Control Conf. (IPEMC-ECCE Asia)*, May 2016, pp. 2276–2280.

[122] B. Xue, H. Wang, J. Liang, Q. Cao, and Z. Li, "Phase-shift modulated interleaved LLC converter with ultrawide output voltage range," *IEEE Trans. Power Electron.*, vol. 36, no. 1, pp. 493–503, Jan. 2021.

[123] H. Wu, X. Zhan, and Y. Xing, "Interleaved LLC resonant converter with hybrid rectifier and variable-frequency plus phase-shift control for wide output voltage range applications," *IEEE Trans. Power Electron.*, vol. 32, no. 6, pp. 4246–4257, Jun. 2017.

[124] Y. Wei, Q. Luo, and H. Alan Mantooth, "A novel LLC converter with topology morphing control for wide input voltage range application," *IEEE J. Emerg. Sel. Topics Power Electron.*, vol. 10, no. 2, pp. 1563–1574, Apr. 2022.

[125] Y. Wei, Q. Luo, and H. A. Mantooth, "An LLC converter with multiple operation modes for wide voltage gain range application," *IEEE Trans. Ind. Electron.*, vol. 68, no. 11, pp. 11111–11124, Nov. 2021.

[126] C.-E. Kim, J. Baek, and J.-B. Lee, "Three-switch LLC resonant converter for high-efficiency adapter with universal input voltage," *IEEE Trans. Power Electron.*, vol. 36, no. 1, pp. 630–638, Jan. 2021.

[127] L.-M. Wu and P.-S. Chen, "Interleaved three-level LLC resonant converter with fixed-frequency PWM control," in *Proc. IEEE 36th Int. Telecommun. Energy Conf. (INTELEC)*, Oct. 2014, pp. 1–8.

[128] C. Fei, R. Gadelrab, Q. Li, and F. C. Lee, "High-frequency three-phase interleaved LLC resonant converter with GaN devices and integrated planar magnetics," *IEEE J. Emerg. Sel. Topics Power Electron.*, vol. 7, no. 2, pp. 653–663, Jun. 2019.

[129] R. Gadelrab, F. C. Lee, and Q. Li, "Three-phase interleaved LLC resonant converter with integrated planar magnetics for telecom and server application," in *Proc. IEEE Appl. Power Electron. Conf. Expo. (APEC)*, Mar. 2020, pp. 512–519.

[130] M. Salem, V. K. Ramachandaramurthy, A. Jusoh, S. Padmanaban, M. Kamarol, J. Teh, and D. Ishak, "Three-phase series resonant DC–DC boost converter with double LLC resonant tanks and variable frequency control," *IEEE Access*, vol. 8, pp. 22386–22399, 2020.

[131] S. A. Arshadi, M. Ordonez, W. Eberle, M. A. Saket, M. Craciun, and C. Botting, "Unbalanced three-phase *LLC* resonant converters: Analysis and trigonometric current balancing," *IEEE Trans. Power Electron.*, vol. 34, no. 3, pp. 2025–2038, Mar. 2019.

[132] J. Cao, X. Zhang, P. Rao, S. Zhou, F. Zhou, and Q. Zhang, "Design of three-phase delta-delta LLC resonant converter," in *Proc. IEEE Vehicle Power Propuls. Conf. (VPPC)*, Nov. 2020, pp. 1–5.

[133] Z. Yu, H. Wu, W. Hua, J. Zhu, and Y. Xing, "A dual-transformer-based LLC resonant converter with phase-shift control for hold-up time compensation application," in *Proc. IEEE Energy Convers. Congr. Expo. (ECCE)*, Sep. 2018, pp. 5961–5966.

[134] J. Zhou and H. Ma, "Full-bridge LLC resonant converter with parallel-series transformer connection and voltage doubler rectifier," in *Proc. 10th Int. Conf. Power Electron. ECCE Asia (ICPE-ECCE Asia)*, May 2019, pp. 1–6.

[135] S. Wang, H. Wu, F. C. Lee, and Q. Li, "Integrated matrix transformer with optimized PCB winding for high-efficiency high-power-density LLC resonant converter," in *Proc. IEEE Energy Convers. Congr. Expo. (ECCE)*, Sep. 2019, pp. 6621–6627.

[136] J.-Y. Lin, H.-Y. Yueh, S.-Y. Lee, and P.-H. Liu, "A novel integrated transformer structure for high efficiency LLC converter," in *Proc. 4th Int. Conf. Intell. Green Building Smart Grid (IGBSG)*, Sep. 2019, pp. 61–66.

[137] L. A. D. Ta and D.-C. Lee, "A novel hybrid LLC converter topology of on-board battery chargers for electric vehicles," in *Proc. Korean Inst. Power Electron. (KIPE)*, 2018, pp. 197–198.

[138] S. Khan, D. Sha, X. Jia, and S. Wang, "Resonant LLC DC–DC converter employing fixed switching frequency based on dual-transformer with wide input-voltage range," *IEEE Trans. Power Electron.*, vol. 36, no. 1, pp. 607–616, Jan. 2021.

[139] D.-K. Kim, S. Moon, C.-O. Yeon, and G.-W. Moon, "High-efficiency LLC resonant converter with high voltage gain using an auxiliary LC resonant circuit," *IEEE Trans. Power Electron.*, vol. 31, no. 10, pp. 6901–6909, Oct. 2016.

[140] L. A. D. Ta, N. D. Dao, and D.-C. Lee, "High-efficiency hybrid LLC resonant converter for on-board chargers of plug-in electric vehicles," *IEEE Trans. Power Electron.*, vol. 35, no. 8, pp. 8324–8334, Aug. 2020.

[141] X. Tang, Y. Xing, H. Wu, and J. Zhao, "An improved LLC resonant converter with reconfigurable hybrid voltage multiplier and PWM-plus-PFM hybrid control for wide output range applications," *IEEE Trans. Power Electron.*, vol. 35, no. 1, pp. 185–197, Jan. 2020.

[142] B.-G. Chung, K.-H. Yoon, S. Phum, E.-S. Kim, and J.-S. Won, "A novel LLC resonant converter for wide input voltage and load range," in *Proc. 8th Int. Conf. Power Electron. (ECCE Asia)*, May 2011, pp. 2825–2830.

[143] C. Chien, Y. Wang, and B. Lin, "Analysis of a novel resonant converter with series connected transformers," *IET Power Electron.*, vol. 6, no. 3, pp. 611–623, Mar. 2013.

[144] D. Huang, S. Ji, and F. C. Lee, "LLC resonant converter with matrix transformer," *IEEE Trans. Power Electron.*, vol. 29, no. 8, pp. 4339–4347, Aug. 2014.

[145] D. Huang, S. Ji, and Fred. C. Lee, "Matrix transformer for LLC resonant converters," in *Proc. Twenty-Eighth Annu. IEEE Appl. Power Electron. Conf. Expo. (APEC)*, Mar. 2013, pp. 2078–2083.

[146] Z. U. Zahid, Z. M. Dalala, R. Chen, B. Chen, and J.-S. Lai, "Design of bidirectional DC–DC resonant converter for vehicle-to-grid (V2G) applications," *IEEE Trans. Transport. Electrific.*, vol. 1, no. 3, pp. 232–244, Oct. 2015.

[147] J.-H. Jung, H.-S. Kim, J.-H. Kim, M.-H. Ryu, and J.-W. Baek, "High efficiency bidirectional LLC resonant converter for 380 V DC power distribution system using digital control scheme," in *Proc. 27th Annu. IEEE Appl. Power Electron. Conf. Expo. (APEC)*, Feb. 2012, pp. 532–538.

[148] J. Lu, X. Tong, J. Zeng, M. Shen, and J. Yin, "Efficiency optimization design of L-LLC resonant bidirectional DC–DC converter," *Energies*, vol. 14, no. 11, p. 3123, May 2021.

[149] E. S. Kim, J. H. Park, J. S. Joo, S. M. Lee, K. Kim, and Y. S. Kong, "Bidirectional DC–DC converter using secondary LLC resonant tank," in *Proc. IEEE Appl. Power Electron. Conf. Expo. (APEC)*, Mar. 2015, no. May, pp. 2104–2108, doi: 10.1109/APEC.2015.7104639.

[150] B.-R. Lin and G.-Y. Wu, "Bidirectional resonant converter with half-bridge circuits: Analysis, design, and implementation," *Energies*, vol. 11, no. 5, p. 1259, May 2018.

[151] T. Jiang, X. Chen, J. Zhang, and Y. Wang, "Bidirectional LLC resonant converter for energy storage applications," in *Proc. 28th Annu. IEEE Appl. Power Electron. Conf. Expo. (APEC)*, Mar. 2013, pp. 1145–1151.

[152] G. Pledl, M. Tauer, and D. Buecherl, "Theory of operation, design procedure and simulation of a bidirectional LLC resonant converter for vehicular applications," in *Proc. IEEE Vehicle Power Propuls. Conf.*, Sep. 2010, pp. 1–5.

[153] J. Zhang, J. Liu, J. Yang, N. Zhao, Y. Wang, and T. Q. Zheng, "An LLC-LC type bidirectional control strategy for an LLC resonant converter in power electronic traction transformer," *IEEE Trans. Ind. Electron.*, vol. 65, no. 11, pp. 8595–8604, Nov. 2018.

[154] X. Ma, P. Wang, H. Bi, and Z. Wang, "A bidirectional LLCL resonant DC–DC converter with reduced resonant tank currents and reduced voltage stress of the resonant capacitor," *IEEE Access*, vol. 8, pp. 125549–125564, 2020.

[155] S. Hu, X. Li, and A. K. S. Bhat, "Operation of a bidirectional series-resonant converter with minimized tank current and wide ZVS range," *IEEE Trans. Power Electron.*, vol. 34, no. 1, pp. 904–915, Jan. 2019.

[156] C. Liu, J. Wang, K. Colombage, C. Gould, and B. Sen, "A CLLC resonant converter based bidirectional EV charger with maximum efficiency tracking," in *Proc. 8th IET Int. Conf. Power Electron., Mach. Drives (PEMD)*, Apr. 2016, pp. 1–6.

[157] Z. U. Zahid, Z. Dalala, and J. J. Lai, "Design and control of bidirectional resonant converter for vehicle-to-grid (V2G) applications," in *Proc. 40th Annu. Conf. IEEE Ind. Electron. Soc.*, Oct. 2014, pp. 1370–1376.

[158] J.-H. Jung, H.-S. Kim, M.-H. Ryu, and J.-W. Baek, "Design methodology of bidirectional CLLC resonant converter for high-frequency isolation of DC distribution systems," *IEEE Trans. Power Electron.*, vol. 28, no. 4, pp. 1741–1755, Apr. 2013.

[159] P. He, A. Mallik, A. Sankar, and A. Khaligh, "Design of a 1-MHz high-efficiency high-power-density bidirectional GaN-based CLLC converter for electric vehicles," *IEEE Trans. Veh. Technol.*, vol. 68, no. 1, pp. 213–223, Jan. 2019.

[160] J. Min and M. Ordonez, "Bidirectional resonant CLLC charger for wide battery voltage range: Asymmetric parameters methodology," *IEEE Trans. Power Electron.*, vol. 36, no. 6, pp. 6662–6673, Jun. 2021.

[161] A. N. Rahman, C.-Y. Lee, H.-J. Chiu, and Y.-C. Hsieh, "Bidirectional three-phase LLC resonant converter," in *Proc. IEEE Transp. Electrific. Conf. Expo, Asia–Pacific (ITEC Asia–Pacific)*, Jun. 2018, pp. 1–5.

[162] E.-S. Kim, S.-M. Lee, J.-H. Park, Y.-J. Noh, H. Xu, and Y.-S. Kong, "Resonant DC–DC converter for high efficiency bidirectional power conversion," in *Proc. Twenty-Eighth Annu. IEEE Appl. Power Electron. Conf. Expo. (APEC)*, Mar. 2013, pp. 2005–2011.

[163] E.-S. Kim, J.-S. Oh, M.-J. Kim, J.-H. Lee, J.-W. Woo, and Y.-S. Jeon, "Enhancing efficiency in bidirectional resonant DC–DC converter," in *Proc. IEEE Appl. Power Electron. Conf. Expo. (APEC)*, Mar. 2020, pp. 2230–2235.

[164] E.-S. Kim and J.-S. Oh, "High-efficiency bidirectional LLC resonant converter with primary auxiliary windings," *Energies*, vol. 12, no. 24, p. 4692, Dec. 2019.

[165] Y. Cai, C. Wang, F. Zhao, and R. Dong, "Design of a high-frequency isolated DTHB CLLC bidirectional resonant DC–DC converter," in *Proc. IEEE Conf. Expo Transp. Electrific. Asia–Pacific (ITEC Asia–Pacific)*, Aug. 2014, pp. 1–6.

[166] Y. Zuo, X. Pan, and C. Wang, "A reconfigurable bidirectional isolated LLC resonant converter for ultra-wide voltage-gain range applications," *IEEE Trans. Ind. Electron.*, vol. 69, no. 6, pp. 5713–5723, Jun. 2022.

[167] J. Ma, Y. Sun, and L. Hu, "A single-stage bridgeless LLC resonant converter with constant frequency control based LED driver," *IET Power Electron.*, vol. 14, no. 15, pp. 2507–2518, Nov. 2021.

[168] J. Yi, H. Ma, X. Li, S. Lu, and J. Xu, "A novel hybrid PFM/IAPWM control strategy and optimal design for single-stage interleaved boost-LLC AC–DC converter with quasi-constant bus voltage," *IEEE Trans. Ind. Electron.*, vol. 68, no. 9, pp. 8116–8127, Sep. 2021.

[169] R. Saasaa, W. Eberle, and M. Agamy, "A single-stage interleaved LLC PFC converter," in *Proc. IEEE Energy Convers. Congr. Expo. (ECCE)*, Sep. 2016, pp. 1–6.

[170] G. Li, J. Xia, K. Wang, Y. Deng, X. He, and Y. Wang, "A single-stage interleaved resonant bridgeless boost rectifier with high-frequency isolation," *IEEE J. Emerg. Sel. Topics Power Electron.*, vol. 8, no. 2, pp. 1767–1781, Jun. 2020.

[171] M. Ghasemi, R. Beiranvand, and M. Jami, "Analyzing a bridgeless single stage LLC resonant PFC converter controlled by frequency and pulse width modulations techniques," in *Proc. 6th Power Electron., Drive Syst. Technol. Conf. (PEDSTC)*, Feb. 2015, pp. 89–95.

[172] Z. Lu and L. Wei-Ming, "A single-stage LED driver using step-down Cuk/LLC with APWM-PFM hybird control," in *Proc. 15th China Int. Forum Solid State Lighting, Int. Forum Wide Bandgap Semiconductors China (SSLChina:IFWS)*, Oct. 2018, pp. 1–4.

[173] H.-S. Kim, J.-W. Baek, M.-H. Ryu, J.-H. Kim, and J.-H. Jung, "The high-efficiency isolated AC–DC converter using the three-phase interleaved LLC resonant converter employing the Y-connected rectifier," *IEEE Trans. Power Electron.*, vol. 29, no. 8, pp. 4017–4028, Aug. 2014.

[174] Y. Wei, Q. Luo, J. M. Alonso, and A. Mantooth, "A magnetically controlled single-stage AC–DC converter," *IEEE Trans. Power Electron.*, vol. 35, no. 9, pp. 8872–8877, Sep. 2020.

[175] Y. Wei, Q. Luo, D. Woldegiorgis, H. Mhiesan, and A. Mantooth, "Analysis of a magnetically controlled single stage LLC resonant converter," in *Proc. IEEE Appl. Power Electron. Conf. Expo. (APEC)*, Mar. 2020, pp. 1257–1263.

[176] A. K. Peter and J. Mathew, "A three-level half-bridge flying capacitor topology for single-stage AC–DC LLC resonant converter," in *Proc. IEEE Int. Conf. Power Electron., Drives Energy Syst. (PEDES)*, Dec. 2018, pp. 1–6, doi: 10.1109/PEDES.2018.8707458.

[177] A. K. Peter and J. Mathew, "A single phase, single stage AC–DC multilevel LLC resonant converter with power factor correction," *IEEE Access*, vol. 9, pp. 70884–70895, 2021.

[178] S. Esmailirad, R. Beiranvand, S. Salehirad, and S. Esmailirad, "Analysis of a bridgeless single stage PFC based on LLC resonant converter for regulating output voltage," in *Proc. IEEE 31st Int. Conf. Microelectron. (MIEL)*, Sep. 2019, pp. 353–356.

[179] T. Mishima, H. Mizutani, and M. Nakaoka, "A sensitivity-improved PFM LLC resonant full-bridge DC–DC converter with LC antiresonant circuitry," *IEEE Trans. Power Electron.*, vol. 32, no. 1, pp. 310–324, Jan. 2017.

[180] H. Wang and Z. Li, "A PWM LLC type resonant converter adapted to wide output range in PEV charging applications," *IEEE Trans. Power Electron.*, vol. 33, no. 5, pp. 3791–3801, May 2018.

[181] M. Shang and H. Wang, "A LLC type resonant converter based on PWM voltage quadrupler rectifier with wide output voltage," in *Proc. IEEE Appl. Power Electron. Conf. Expo. (APEC)*, Mar. 2017, pp. 1720–1726.

[182] K. Siri and C. Q. Lee, "Constant switching frequency LLC-type series resonant converter," in *Proc. 32nd Midwest Symp. Circuits Syst.*, Aug. 1989, pp. 513–516.

[183] J.-S. Lai, H. Miwa, W.-H. Lai, N.-H. Tseng, C.-S. Lee, C.-H. Lin, and Y.-W. Shih, "A high-efficiency on-board charger utilitzing a hybrid LLC and phase-shift DC–DC converter," in *Proc. Int. Conf. Intell. Green Building Smart Grid (IGBSG)*, Apr. 2014, pp. 1–8.

[184] O. Abdel-Rahim, N. Alamir, M. Abdelrahem, M. Orabi, R. Kennel, and M. A. Ismeil, "A phase-shift-modulated LLC-resonant micro-inverter based on fixed frequency predictive-MPPT," *Energies*, vol. 13, no. 6, p. 1460, Mar. 2020.

[185] T. Jiang, J. Zhang, X. Wu, K. Sheng, and Y. Wang, "A bidirectional three-level LLC resonant converter with PWAM control," *IEEE Trans. Power Electron.*, vol. 31, no. 3, pp. 2213–2225, Mar. 2016, doi: 10.1109/TPEL.2015.2438072.

[186] T. Jiang, J. Zhang, Y. Wang, Z. Qian, and K. Sheng, "PWAM control of bidirectional LLC resonant converter," in *Proc. 1st Int. Future Energy Electron. Conf. (IFEEC)*, Nov. 2013, pp. 827–832.

[187] S.-Y. Chen, Z. R. Li, and C.-L. Chen, "Analysis and design of single-stage AC/DC *LLC* resonant converter," *IEEE Trans. Ind. Electron.*, vol. 59, no. 3, pp. 1538–1544, Mar. 2012.

[188] S. Esmailirad, R. Beiranvand, and A. Y. Varjani, "Using the frequency and pulse width modulation techniques for regulating the LLC resonant converter output voltage," in *Proc. 9th Annu. Power Electron., Drives Syst. Technol. Conf. (PEDSTC)*, Feb. 2018, pp. 30–37.

[189] H.-P. Park and J.-H. Jung, "PWM and PFM hybrid control method for LLC resonant converters in high switching frequency operation," *IEEE Trans. Ind. Electron.*, vol. 64, no. 1, pp. 253–263, Jan. 2017.

[190] J. Yamamoto, T. Zaitsu, S. Abe, and T. Ninomiya, "PFM and PWM hybrid controlled LLC converter," in *Proc. Int. Power Electron. Conf. (IPEC-Hiroshima-ECCE ASIA)*, May 2014, pp. 177–182.

[191] X. Chen and I. Batarseh, "PWM and PFM hybrid modulation scheme for dual-input LLC resonant converter," in *Proc. IEEE Energy Convers. Congr. Expo. (ECCE)*, Oct. 2020, pp. 2569–2576.

[192] Y. Wei, Q. Luo, D. Woldegiorgis, H. Mhiesan, and A. Mantooth, "Hybrid PWM and PFM control strategy for LLC resonant converter with hold-up time operation requirement," in *Proc. IEEE Transp. Electrific. Conf. Expo (ITEC)*, Jun. 2020, pp. 291–295.

[193] J.-I. Cheon and C.-W. Ha, "PWM/PFM dual mode SMPS controller IC for active forward clamp and LLC resonant converters," *JSTS, J. Semiconductor Technol. Sci.*, vol. 7, no. 2, pp. 94–97, Jun. 2007.

[194] J. Gao, J. Zhang, Z. Zhu, and Q. Song, "Single-stage LLC AC/DC converter with wide input range and low bus voltage," *J. Power Electron.*, vol. 21, no. 1, pp. 1–12, Jan. 2021.

[195] H. Park, M. Kim, H. Kim, and J. Jung, "Design methodology of tightly regulated dual-output LLC resonant converter using PFM-APWM hybrid control method," *Energies*, vol. 12, no. 11, p. 2146, Jun. 2019.

[196] H. Park, M. Kim, and J. Jung, "Tightly regulated dual-output half-bridge converter using PFM-APWM hybrid control method," in *Proc. IEEE Appl. Power Electron. Conf. Expo. (APEC)*, Mar. 2017, pp. 2022–2026.

[197] H. Ma, G. Chen, J. H. Yi, Q. W. Meng, L. Zhang, and J. P. Xu, "A single-stage PFM-APWM hybrid modulated soft-switched converter with low bus voltage for high-power LED lighting applications," *IEEE Trans. Ind. Electron.*, vol. 64, no. 7, pp. 5777–5788, Jul. 2017.

[198] A. Awasthi, S. Bagawade, A. Kumar, and P. Jain, "Time-domain analysis of APWM-frequency modulated Low-Q LLC resonant converter for wide input and load range applications," in *Proc. IEEE Energy Convers. Congr. Expo. (ECCE)*, Sep. 2019, pp. 1334–1340.

[199] B. McDonald and F. Wang, "LLC performance enhancements with frequency and phase shift modulation control," in *Proc. IEEE Appl. Power Electron. Conf. Expo. (APEC)*, Mar. 2014, pp. 2036–2040.

[200] T. Mishima and Y. Koga, "Variable frequency phase-shift modulation symmetrical series-resonant bidirectional DC–DC converter—Analysis and verification of ZVS performance and reactive power minimization," *IEEJ J. Ind. Appl.*, vol. 10, no. 5, pp. 540–553, 2021.

[201] X. Yudi, M. Xingkui, Z. Zhe, and Y. Shi, "New hybrid control for wide input full-bridge LLC resonant DC/DC converter," in *Proc. 3rd Int. Conf. Intell. Green Building Smart Grid (IGBSG)*, Apr. 2018, pp. 1–4.

[202] J. Shahsevani and R. Beiranvand, "A bidirectional resonant converter for capacitive power transmission in electric vehicle and PowerWall applications," in *Proc. 31st Int. Conf. Electr. Eng. (ICEE)*, May 2023, pp. 264–270.

[203] T. Liu, Z. Zhou, A. Xiong, J. Zeng, and J. Ying, "A novel precise design method for LLC series resonant converter," in *Proc. 28th Int. Telecommun. Energy Conf.*, Sep. 2006, pp. 1–6.

[204] I. Barbi and F. Pöttker, *Soft Commutation Isolated DC–DC Converters*, vol. 1. Springer, 2019.

[205] J.-H. Jung and J.-G. Kwon, "Theoretical analysis and optimal design of LLC resonant converter," in *Proc. Eur. Conf. Power Electron. Appl.*, Sep. 2007, pp. 1–10.

[206] T. G. Grigorova, A. S. Vuchev, and I. P. Maradzhiev, "Output and control characteristics of an LLC resonant DC/DC converter," in *Proc. 10th Nat. Conf. Int. Participation (ELECTRONICA)*, May 2019, pp. 1–4.

[207] S. De Simone, C. Adragna, C. Spini, and G. Gattavari, "Design-oriented steady-state analysis of LLC resonant converters based on FHA," in *Proc. Int. Symp. Power Electron., Electr. Drives, Autom. Motion (SPEEDAM)*, May 2006, pp. 200–207.

[208] X. Li, "A LLC-type dual-bridge resonant converter: Analysis, design, simulation, and experimental results," *IEEE Trans. Power Electron.*, vol. 29, no. 8, pp. 4313–4321, Aug. 2014.

[209] Z. Zhao, Q. Xu, Y. Dai, and A. Luo, "Minimum resonant capacitor design of high-power LLC resonant converter for comprehensive efficiency improvement in battery charging application," *IET Power Electron.*, vol. 11, no. 11, pp. 1866–1874, Sep. 2018.

[210] N. Yildiran, "Design methodology and implementation of half-bridge LLC resonant converter," in *Proc. Int. Conf. Electr., Commun., Comput. Eng. (ICECCE)*, Jun. 2020, pp. 1–6.

[211] A. Awasthi, S. Bagawade, A. Kumar, and P. Jain, "Efficiency optimized design procedure of low-Q LLC resonant converter for wide input voltage and load range application," in *Proc. IEEE Appl. Power Electron. Conf. Expo. (APEC)*, Mar. 2020, pp. 3250–3256.

[212] B. Yang, F. C. Lee, A. J. Zhang, and G. Huang, "LLC resonant converter for front end DC/DC conversion," in *Proc. 17th Annu. IEEE Appl. Power Electron. Conf. Expo. (APEC)*, Mar. 2002, pp. 1108–1112.

[213] Z. Fang, T. Cai, S. Duan, and C. Chen, "Optimal design methodology for LLC resonant converter in battery charging applications based on time-weighted average efficiency," *IEEE Trans. Power Electron.*, vol. 30, no. 10, pp. 5469–5483, Oct. 2015.

[214] C.-H. Yang, T.-J. Liang, K.-H. Chen, J.-S. Li, and J.-S. Lee, "Loss analysis of half-bridge LLC resonant converter," in *Proc. 1st Int. Future Energy Electron. Conf. (IFEEC)*, Nov. 2013, pp. 155–160.

[215] B. Yang, "Topology investigation of front end DC/DC converter for distributed power system," 2003.

[216] E. S. Glitz and M. Ordonez, "MOSFET power loss estimation in LLC resonant converters: Time interval analysis," *IEEE Trans. Power Electron.*, vol. 34, no. 12, pp. 11964–11980, Dec. 2019.

[217] F. Li, R. Hao, H. Lei, X. Zhang, and X. You, "The influence of parasitic components on LLC resonant converter," *Energies*, vol. 12, no. 22, p. 4305, Nov. 2019.

[218] T. Jun, L. Facheng, L. Xiang, and Y. Xingchen, "Loss analysis and optimization design of half-bridge LLC resonant converter," *IOP Conf. Ser., Mater. Sci. Eng.*, vol. 533, no. 1, May 2019, Art. no. 012017.

[219] N. Wang, H. Jia, M. Tian, Z. Li, G. Xu, and X. Yang, "Impact of transformer stray capacitance on the conduction loss in a GaN-based LLC resonant converter," in *Proc. IEEE 3rd Int. Future Energy Electron. Conf. ECCE Asia (IFEEC-ECCE Asia)*, Jun. 2017, pp. 1334–1338.

[220] M. Escudero, M.-A. Kutschak, F. Pulsinelli, N. Rodriguez, and D. P. Morales, "On the practical evaluation of the switching loss in the secondary side rectifiers of LLC converters," *Energies*, vol. 14, no. 18, p. 5915, Sep. 2021.

[221] J. Zhang, S. Shao, Y. Li, J. Zhang, and K. Sheng, "A voltage balancing method for series-connected power devices in an LLC resonant converter," *IEEE Trans. Power Electron.*, vol. 36, no. 4, pp. 3628–3632, Apr. 2021.

[222] Y. Wei, Q. Luo, Z. Wang, and A. Mantooth, "Wide voltage gain range application for full-bridge LLC resonant converter with narrow switching frequency range," *IET Power Electron.*, vol. 13, no. 15, pp. 3283–3293, Nov. 2020.

[223] Z. Zhao, Q. Xu, Y. Dai, A. Luo, and Y. Chen, "Efficiency optimization design of LLC resonant converter for battery charging," in *Proc. 13th IEEE Conf. Ind. Electron. Appl. (ICIEA)*, May 2018, pp. 928–933.

[224] B. McDonald and Y. Li, "A novel LLC resonant controller with best-in-class transient performance and low standby power consumption," in *Proc. IEEE Appl. Power Electron. Conf. Expo. (APEC)*, Mar. 2018, pp. 489–493.

[225] J. Kucka and D. Dujic, "Equal loss distribution in duty-cycle controlled H-bridge LLC resonant converters," *IEEE Trans. Power Electron.*, vol. 36, no. 5, pp. 4937–4941, May 2021.

[226] W. Zhang, F. Wang, D. J. Costinett, L. M. Tolbert, and B. J. Blalock, "Investigation of gallium nitride devices in high-frequency LLC resonant converters," *IEEE Trans. Power Electron.*, vol. 32, no. 1, pp. 571–583, Jan. 2017.

[227] M. Jami, R. Beiranvand, M. Mohamadian, and M. Ghasemi, "Optimization the LLC resonant converter for achieving maximum efficiency at a predetermined load value," in *Proc. 6th Power Electron., Drive Syst. Technol. Conf. (PEDSTC)*, Feb. 2015, pp. 149–155.

[228] R.-L. Lin and L.-H. Huang, "Efficiency improvement on LLC resonant converter using integrated LCLC resonant transformer," *IEEE Trans. Ind. Appl.*, vol. 54, no. 2, pp. 1756–1764, Mar. 2018.

[229] R. Beiranvand, B. Rashidian, M. R. Zolghadri, and S. M. H. Alavi, "Optimizing the normalized dead-time and maximum switching frequency of a wide-adjustable-range LLC resonant converter," *IEEE Trans. Power Electron.*, vol. 26, no. 2, pp. 462–472, Feb. 2011.

[230] C. W. T. McLyman, *Transformer and Inductor Design Handbook*. Boca Raton, FL, USA: CRC Press, 2004.

[231] S. Li and B. Fahimi, "State-space modelling of LLC resonant half-bridge DC–DC converter," *IET Power Electron.*, vol. 13, no. 8, pp. 1583–1592, Jun. 2020.

[232] T. Duerbaum, "First harmonic approximation including design constraints," in *Proc. 20th Int. Telecommun. Energy Conf. (INTELEC)*, Oct. 1998, pp. 321–328.
[233] H. Huang, "Designing an LLC resonant half-bridge power converter," in *Proc. Texas Instrum. Power Supply Design Seminar (SEM)*, vol. 3, 2010, pp. 2010–2011.
[234] N. Madhanakkumar, T. Sivakumaran, G. Irusapparajan, and D. Sujitha, "Closed loop control of LLC resonant converter incorporating ZVS boost converter," *Int. J. Eng. Technol.*, vol. 6, no. 2, pp. 643–653, 2014.
[235] Z. U. Zahid, J. J. Lai, X. K. Huang, S. Madiwale, and J. Hou, "Damping impact on dynamic analysis of LLC resonant converter," in *Proc. IEEE Appl. Power Electron. Conf. Expo. (APEC)*, Mar. 2014, pp. 2834–2841.
[236] C.-H. Chang, E.-C. Chang, C.-A. Cheng, H.-L. Cheng, and S.-C. Lin, "Small signal modeling of LLC resonant converters based on extended describing function," in *Proc. Int. Symp. Comput., Consum. Control*, Jun. 2012, pp. 365–368.
[237] N. Mohan, T. M. Undeland, and W. P. Robbins, *Power Electronics: Converters, Applications, and Design*. Hoboken, NJ, USA: Wiley, 2003.
[238] J. Ejury, "Buck converter design," Infineon Technol. North Amer. (TFNA), Austin, TX, USA, Corn Desion Note 1, Jan. 2013.
[239] R. Erickson, *The Flyback Converter*, document ECEN4517, Lecture Notes, 2012.
[240] N. Coruh, S. Urgun, and T. Erfidan, "Design and implementation of flyback converters," in *Proc. 5th IEEE Conf. Ind. Electron. Appl.*, Jun. 2010, pp. 1189–1193.
[241] F. D. Tan, "The forward converter: From the classic to the contemporary," in *Proc. 17th Annu. IEEE Appl. Power Electron. Conf. Expo. (APEC)*, Mar. 2002, pp. 857–863.
[242] B.-R. Lin, K. Huang, and D. Wang, "Analysis, design, and implementation of an active clamp forward converter with synchronous rectifier," *IEEE Trans. Circuits Syst. I, Reg. Papers*, vol. 53, no. 6, pp. 1310–1319, Jun. 2006.
[243] R. W. Erickson and D. Maksimovic, *Fundamentals of Power Electronics*. Springer, May 2007.
[244] V. J. Thottuvelil, T. G. Wilson, and H. A. Owen, "Analysis and design of a push-pull current-fed converter," in *Proc. IEEE Power Electron. Specialists Conf.*, Jun. 1981, pp. 192–203.
[245] M. Salem, A. Jusoh, N. R. N. Idris, H. S. Das, and I. Alhamrouni, "Resonant power converters with respect to passive storage (LC) elements and control techniques—An overview," *Renew. Sustain. Energy Rev.*, vol. 91, pp. 504–520, Aug. 2018.
[246] A. Pawellek, C. Oeder, and T. Duerbaum, "Comparison of resonant LLC and LCC converters for low-profile applications," in *Proc. 14th Eur. Conf. Power Electron. Appl.*, Aug. 2011, pp. 1–10.
[247] S. Mao, J. Popovic, R. Ramabhadran, and J. A. Ferreira, "Comparative study of half-bridge LCC and LLC resonant DC–DC converters for ultra-wide output power range applications," in *Proc. 17th Eur. Conf. Power Electron. Appl. (EPE ECCE-Europe)*, Sep. 2015, pp. 1–10.

JASEM SHAHSEVANI (Student Member, IEEE) received the M.Sc. degree in power electronics engineering from Tarbiat Modares University, Tehran, Iran, in 2023.

His current research interests include dc/dc converter, LLC-based resonant converter, wireless power transfer, electric vehicle charging, soft-switching techniques, and PV-based renewable energy systems.

REZA BEIRANVAND (Senior Member, IEEE) received the M.Sc. and Ph.D. degrees in electrical engineering from the Sharif University of Technology, Tehran, Iran, in 1999 and 2010, respectively.

From 1999 to 2007, he was an Engineer with the Research and Development Centers of PARS-Electric and RADIO SHAHAB MFGs, Tehran, where he was engaged in designing the LCD and LED TVs based on the ST, LT, NXP, and Fairchild devices. From 2010 to 2012, he was a Postdoctoral Research Fellow with the Electrical Engineering College, Sharif University of Technology. He was an IEEE Consultant, from 2017 to 2019, and the Head of the Power Group, from 2018 to 2020, with Tarbiat Modares University. He is currently an Associate Professor with the Faculty of Electrical and Computer Engineering, Tarbiat Modares University, Tehran. His research interests include power electronics converters, soft-switching techniques, SCCs, SMPS, capacitive-coupling power transfer and inductive power transfer techniques, and PV-based renewable energy systems.

Dr. Beiranvand was between the top 2 % scientists of the world, based on Stanford University, Stanford, CA, USA, released lists, from 2020 to 2023.